PB92-177674

Publication No. FHWA-RD-91-012
January 1992

Effects on Safety of Pavement-Truck Tire Interaction

U.S. Department of Transportation
Federal Highway Administration

Research and Development
Turner-Fairbank Highway Research Center
6300 Georgetown Pike
McLean, Virginia 22101-2296

FOREWORD

This report (FHWA-RD-91-012) presents the findings of a research study to evaluate the frictional performance of truck and bus tires and its implications on highway safety, and to evaluate the effects of suspension characteristics on the braking and cornering performance of trucks. A new truck tire tester was built for the tire testing task, which enabled the measurement of the forces involved in braking and cornering under various speed, vertical load, and slip angle conditions on different pavement surfaces. Six types of radial and bias-ply tires were tested. A computer simulation study was conducted in the second task to investigate the effects of suspension type, tire type, roadway alignment, pavement roughness and surface wetness.

This report will be of interest to researchers and engineers concerned with the relative frictional performance of various types of truck tires in a series of controlled tests.

Sufficient copies of this report are being distributed by FHWA memorandum to provide two copies to each FHWA Region, and three copies to each FHWA Division and State highway agency. Direct distribution is being made to the division offices. Additional copies for the public are available from the National Technical Information Service (NTIS), Department of Commerce, 5285 Port Royal Road, Springfield, Virginia 22161.

Thomas J. Pasko, Jr., P.E.
Director, Office of Engineering
and Highway Operations
Research and Development

NOTICE

Technical Report Documentation Page

1. Report No.	2.	3. Recipient's Catalog No.
FHWA-RD-91-012	PB92-177674	

4. Title and Subtitle	5. Report Date
EFFECTS ON SAFETY OF PAVEMENT-TRUCK TIRE INTERACTION	January 1992
	6. Performing Organization Code
7. Author(s) B. T. Kulakowski, J. C. Wambold, D. W. Blue, R. R. Blackburn, D. W. Harwood	8. Performing Organization Report No. PTI 9112
9. Performing Organization Name and Address Pennsylvania Transportation Institute Research Building B The Pennsylvania State University University Park, PA 16802	10. Work Unit No. (TRAIS) NCP#3A5G0032 11. Contract or Grant No. DTFH61-85-C-00148
12. Sponsoring Agency Name and Address Federal Highway Administration Office of Engineering and Highway Operations, R&D 6300 Georgetown Pike McLean, VA 22101-2296	13. Type of Report and Period Covered Final Report October 1985 - December 1990 14. Sponsoring Agency Code

15. Supplementary Notes

Contracting Officer's Technical Representative: Stephen W. Forster, HNR-20

16. Abstract

A new truck tire tester was built to mesure tire forces in braking and cornering under various speed, vertical load, and slip angle conditions and on different pavement surfaces. Six of the most common truck and bus tires were tested. In general, rib tires performed better than lug tires and radial tires performed better than bias-ply tires. Overall, the radial rib tire performed best, both in braking and in cornering, among the six test tires. All of the independent test variables--pavement type, vehicle speed, axle load, and slip angle--have a significant effect on tire traction. The experimental data were processed to derive 48 regression models relating peak and sliding coefficients of braking and cornering friction and critical longitudinal slip to the independent variables. A computer simulation study using the T3DRS, Phase 4 program was also conducted to investigate the effects of suspension type, tire type, roadway alignment, pavement roughness, and surface wetness on truck braking distance. The simulation results showed that trucks may require considerably larger stopping distances than passenger cars.

17. Key Words	18. Distribution Statement
Tire traction, braking, cornering, braking distance	No restrictions. This document is available from the National Technical Information Service, Springfield, Virginia 22161

19. Security Classif. (of this report)	20. Security Classif. (of this page)	21. No. of Pages	22. Price
UNCLASSIFIED	UNCLASSIFIED	133	

Form DOT F 1700.7 (8-72) Reproduction of completed page authorized

SI* (MODERN METRIC) CONVERSION FACTORS

APPROXIMATE CONVERSIONS TO SI UNITS

Symbol	When You Know	Multiply By	To Find	Symbol
	LENGTH			
in	inches	25.4	millimetres	mm
ft	feet	0.305	metres	m
yd	yards	0.914	metres	m
mi	miles	1.61	kilometres	km
	AREA			
in^2	square inches	645.2	millimetres squared	mm^2
ft^2	square feet	0.093	metres squared	m^2
yd^2	square yards	0.836	metres squared	m^2
ac	acres	0.405	hectares	ha
mi^2	square miles	2.59	kilometres squared	km^2
	VOLUME			
fl oz	fluid ounces	29.57	millilitres	mL
gal	gallons	3.785	litres	L
ft^3	cubic feet	0.028	metres cubed	m^3
yd^3	cubic yards	0.765	metres cubed	m^3

NOTE: Volumes greater than 1000 L shall be shown in m^3.

Symbol	When You Know	Multiply By	To Find	Symbol
	MASS			
oz	ounces	28.35	grams	g
lb	pounds	0.454	kilograms	kg
T	short tons (2000 lb)	0.907	megagrams	Mg
	TEMPERATURE (exact)			
°F	Fahrenheit temperature	5(F-32)/9	Celcius temperature	°C

APPROXIMATE CONVERSIONS FROM SI UNITS

Symbol	When You Know	Multiply By	To Find	Symbol
	LENGTH			
mm	millimetres	0.039	inches	in
m	metres	3.28	feet	ft
m	metres	1.09	yards	yd
km	kilometres	0.621	miles	mi
	AREA			
mm^2	millimetres squared	0.0016	square inches	in^2
m^2	metres squared	10.764	square feet	ft^2
ha	hectares	2.47	acres	ac
km^2	kilometres squared	0.386	square miles	mi^2
	VOLUME			
mL	millilitres	0.034	fluid ounces	fl oz
L	litres	0.264	gallons	gal
m^3	metres cubed	35.315	cubic feet	ft^3
m^3	metres cubed	1.308	cubic yards	yd^3
	MASS			
g	grams	0.035	ounces	oz
kg	kilograms	2.205	pounds	lb
Mg	megagrams	1.102	short tons (2000 lb)	T
	TEMPERATURE (exact)			
°C	Celcius temperature	1.8C + 32	Fahrenheit temperature	°F

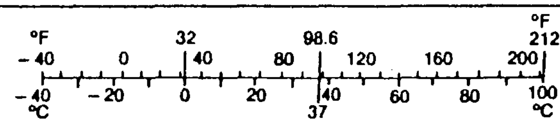

* SI is the symbol for the International System of Measurement

(Revised April 1989)

TABLE OF CONTENTS

TABLE OF CONTENTS (Continued).

LIST OF FIGURES

LIST OF FIGURES (Continued)

LIST OF FIGURES (Continued)

LIST OF TABLES

1. INTRODUCTION

Braking performance of trucks has become a critical element of highway safety in recent years for several reasons. First, the percentage of trucks in the highway traffic stream has increased dramatically, up to 30 percent on some roadways. Second, trucks are now equipped with very powerful engines that allow them to carry larger loads at higher speeds. The increase in speed and gross weight has not quite been offset by an increased efficiency of truck braking systems, including the use of antilock brakes. Furthermore, new developments in truck tire design that significantly reduced tire wear and rolling resistance have not always proved beneficial for truck braking and cornering performance. It has become obvious that acquiring more accurate data on truck braking performance and truck tire traction characteristics is crucial for determining the impact of trucks on highway safety. The main objective of this study was to collect and analyze such data.

The specific objectives were to:

- Collect experimental data on the frictional performance of typical truck and bus tires on a range of pavement surfaces.
- Determine effective friction forces under the effects of truck suspension reaction to imbalances and road roughness.
- Analyze the test results and determine performance limits and their effects on highway safety in braking and cornering.
- Develop recommendations for obtaining acceptable levels of safety for automobiles, buses, and trucks.

All work in this project was stopped on November 1, 1987, awaiting availability of wheel force transducers from another study. When, after a series of delays, it became clear that the wheel force transducers would not be available, the project was restarted on October 1, 1989, with a modified scope of work. As a result, the measurements of tire frictional characteristics were performed in the field testing program using a truck tire tester but tests involving full trucks were canceled. Truck braking and cornering maneuvers were simulated by computer instead of tested in the field. Also, the recommendations and conclusions that were formulated based on the results of computer simulation should be considered tentative until verified by experimental data obtained from field tests.

The remainder of this report is organized in five major sections. Chapter 2 describes a field testing program in which frictional characteristics of six of the most common truck and bus tires were measured. A new truck tire tester was built to measure braking, cornering, and vertical forces of truck and bus tires. Regression models for peak and sliding coefficients of tire braking and cornering friction were developed from the experimental data. The independent variables in these models are pavement skid number (SN_{40}), speed, tire vertical load, and slip angle.

Chapter 3 presents the testing plan for evaluating braking and cornering performance of trucks with different suspensions and tires and on pavement surfaces having different roughness levels. The effects of pavement, tire, and vehicle parameters on truck braking distance were investigated using the T3DRS, Phase 4 computer simulation model, and the results of the simulation are presented in chapter 4.

Chapter 5 contains discussion of the safety implications of the braking distance results presented in chapter 4. Chapter 6 of the report presents the final conclusions and recommendations.

2. FIELD MEASUREMENTS OF TIRE TRACTION CHARACTERISTICS

WORK PLAN

Tire traction characteristics are determined by forces generated at the tire-pavement interface as a result of driving, steering, and braking actions applied to the vehicle. Figure 1 shows the standard Society of Automotive Engineers (SAE) axis system illustrating all tire forces and moments. The three forces--longitudinal (or braking) force (F_x), lateral (or cornering) force (F_y), and normal force (F_z)--are the main dependent variables that were of interest in this study. The longitudinal force, or force along the x-axis, is generated when the rolling velocity of the tire (v_r) is different from the true longitudinal component (v_x) of the tire velocity. This occurs when an external torque is applied to the wheel due to braking or acceleration.[1] The tire longitudinal (or braking) coefficient of friction (f_x) is defined as the ratio of the braking force (F_x), generated at the tire-pavement interface, to the normal load (F_z) carried by the tire:

$$f_x = \frac{F_x}{F_z} \qquad (1)$$

The tire coefficient of braking friction varies with the difference between v_r and v_x, which is commonly expressed in terms of the longitudinal percent slip (s), defined by the following equation:

$$s = \left(\frac{v_x - v_r}{v_x}\right) \times 100 \qquad (2)$$

[1]The external torque that was of interest in this study will always be caused by braking; therefore, F_x will be referred to as the braking force in the remainder of this report.

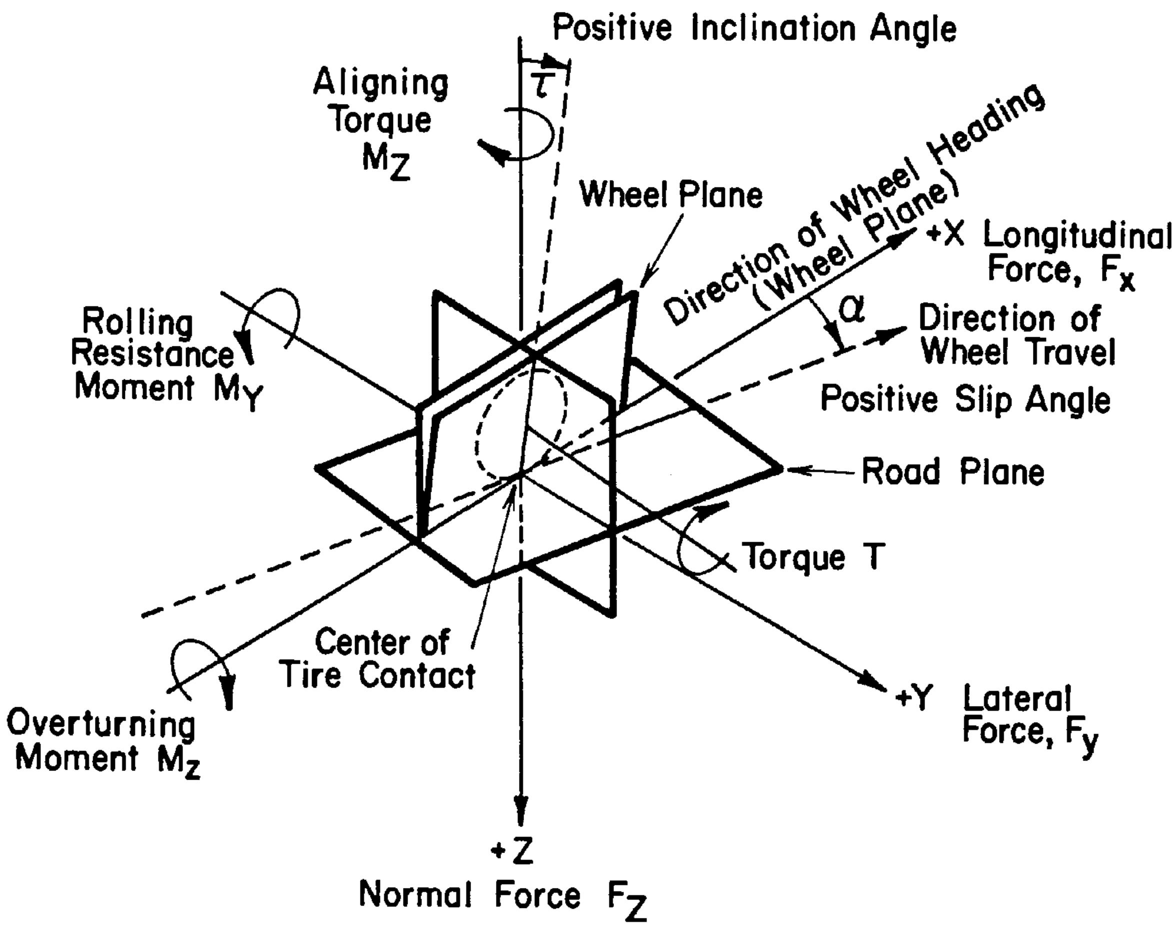

Figure 1. SAE tire axis system.

or, equally:

$$s = \left(1 - \frac{\Omega r_e}{V_x}\right) \times 100 \tag{3}$$

where Ω is the tire rotational velocity and r_e is an effective rolling radius of tire. Figure 2 shows a typical plot of the coefficient of braking friction versus longitudinal percent slip. The important parameters of this characteristic are peak braking coefficient of friction (f_{xp}), critical slip (s_{crit}), and sliding coefficient of friction (f_{xs}), representing friction between the pavement and a nonrotating (locked) tire.

The tire coefficient of cornering friction (f_y) is defined as the ratio of the lateral force (F_y) to the normal force (F_z):

$$f_y = \frac{F_y}{F_z} \tag{4}$$

The tire lateral force results from the tire deformation at the contact patch, which occurs when the plane of the wheel is not aligned with the wheel velocity vector. The angle between the direction of wheel heading and direction of wheel travel is the slip angle α (figure 1). A typical plot of the coefficient of cornering friction versus longitudinal slip is shown in figure 3. The coefficient of cornering friction has its maximum (f_{yp}) near zero longitudinal slip and decreases to a minimum (f_{ys}) at 100 percent slip. Typical plots of f_x and f_y as functions of slip angle α are shown in figure 4.

The main independent variables affecting tire braking and cornering friction are tire type, tire tread depth, tire inflation pressure, pavement type, wheel static load, vehicle speed, thickness of water film on pavement surface, longitudinal percent slip, and slip angle. A field testing program including all of these variables would require time and budgetary resources far exceeding those available in this study. A thorough literature survey was conducted to determine which of the independent variables could be eliminated from the testing program because they were less significant than other

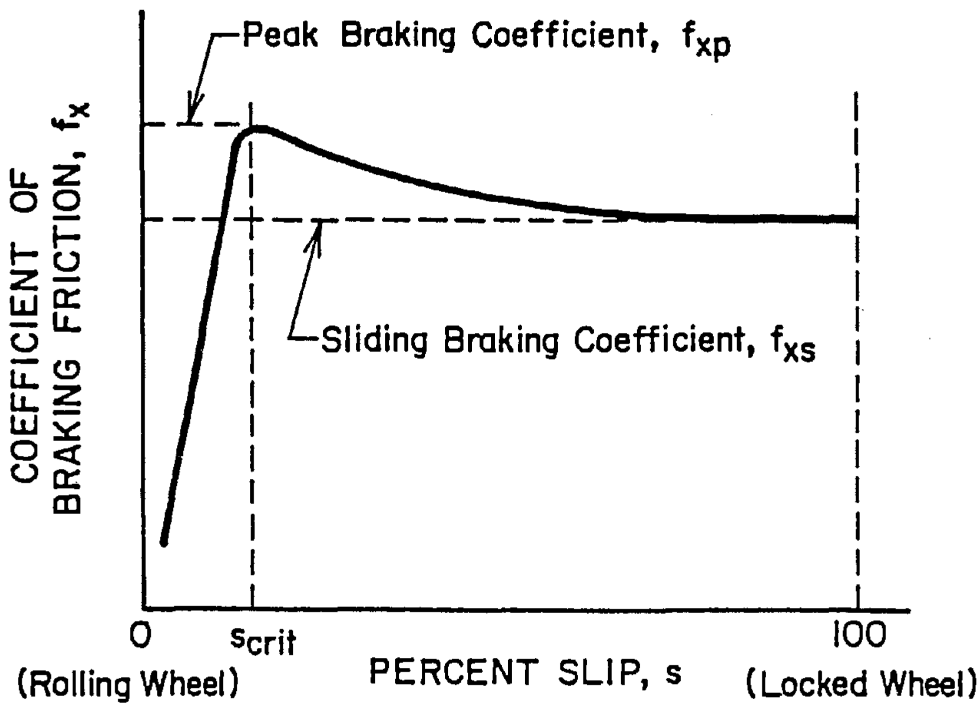

Figure 2. Typical plot of coefficient of braking friction versus longitudinal percent slip.

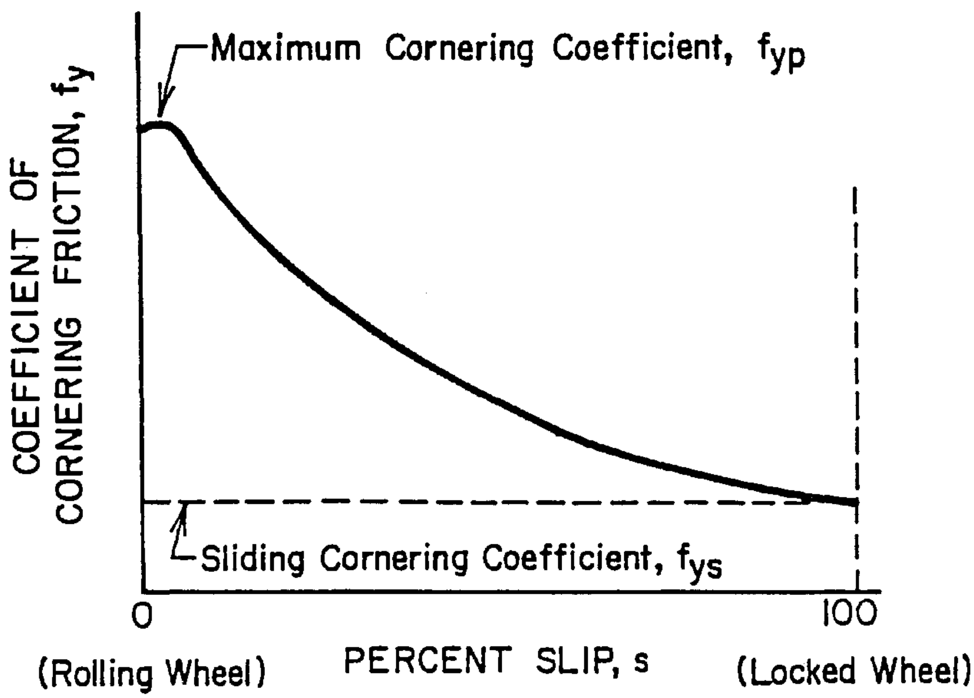

Figure 3. Typical plot of coefficient of cornering friction versus longitudinal percent slip.

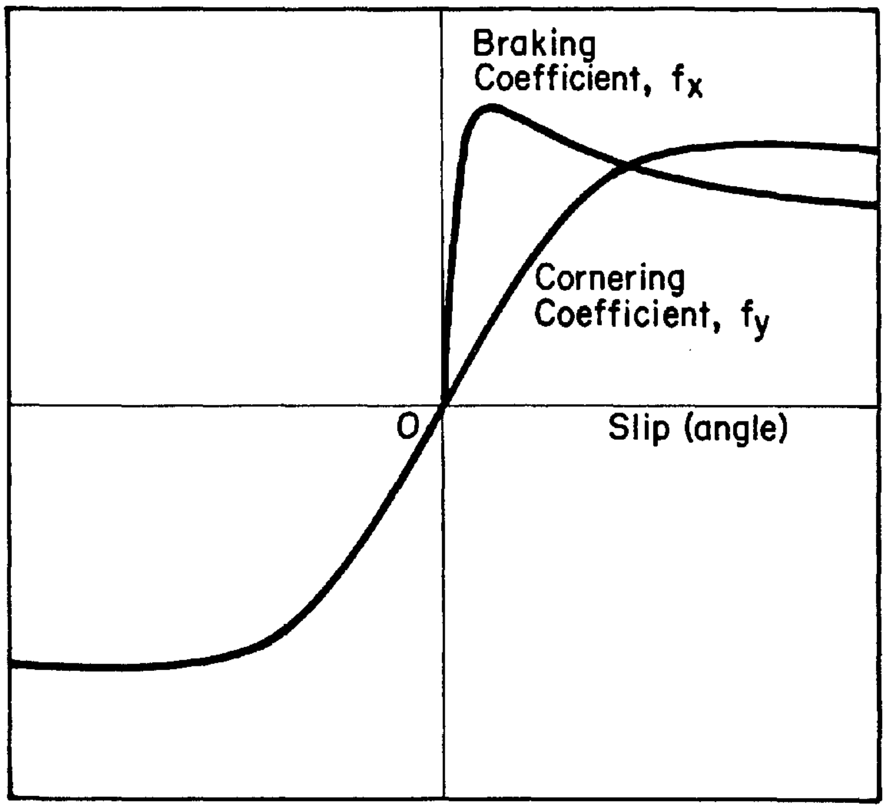

Figure 4. Typical plots of coefficients of braking and cornering friction versus slip angle.

variables or because their effects on tire-pavement friction were well documented.

Tire tread depth does not affect the coefficient of friction significantly until it becomes less than 0.1 in (2.5 mm).[1-4] Since all tires to be tested were new, and the tread depth was considerably larger than 0.1 in (2.5 mm), the tread depth was not included as a test variable. Tire inflation pressure was eliminated because it was found to have a negligible effect on the peak coefficient of friction and because it caused less than 10 percent change in the sliding coefficient of friction when varied from 68 to 102 psi for five different truck tires.[5] Axle load was eliminated as a potential test variable because its relationship with tire coefficient of friction is approximately linear and has been well documented in other studies.[5,6,7] Effects of water film thickness on tire-pavement friction were investigated extensively in another FHWA-sponsored study.[8]

After the literature review, the list of independent test variables was reduced to include the following variables: tire type, pavement type, longitudinal slip, speed, and slip angle.

Six tires were tested in the study:

- Radial rib tire, Goodyear 11R24.5.
- Bias-ply rib tire, Goodyear 10.00-20.
- Bias-ply lug tire, Kelley 11-22.5.
- Low-profile tire, Goodyear HT 285/75R24.5.
- Wide-base tire, Goodyear 16.5R22.5.
- Radial lug tire, Goodyear HT 285/75R24.5.

Six pavements were selected for the study, including four asphalt and two concrete pavements covering a range of micro- and macrotextures (listed in table 1). All pavements were located at University Park, Pennsylvania.

Tire longitudinal slip was varied from 0 to 100 percent during each braking test. The tests were conducted at three speeds: 25, 40, and approximately 50 mi/h (40, 64, and 80 km/h). Slip angle was set at four angles: 0, 4, 8, and 15 degrees.

Table 1. Texture characteristics of test surfaces.

Site Location	Material	Macrotexture	Microtexture	SN_{40}
Truck Lane	Asphalt	Poor	Poor	41
Skid Pad #4	Asphalt	Fair	Fair	41
Skid Pad #6	Asphalt	Poor	Good	48
Skid Pad #3	Asphalt	Good	Good	53
Skid Pad #5	PCC	Good	Good	60
Skid Pad #7	PCC	Poor	Good	69

The other independent variables, eliminated from the testing program, were to be kept constant in all tests at the following levels:

- Tire inflation pressure: manufacturer-recommended pressure.
- Vertical load: 3,500 lb (33 363 N).
- Water film thickness: 0.02 in (0.5 mm).

In the course of testing it became clear that the tire vertical load could not be kept constant. The vertical load varied in an uncontrolled manner and therefore became another independent variable.

TESTING EQUIPMENT

A new tester was designed to measure tire-pavement forces of commercial truck and bus tires on actual pavement surfaces. The two-wheel tester, shown in figure 5, is mounted under a host flatbed trailer. Three air cylinders are used to load the tires during testing and to lift the tires off the ground after the test is completed. The test tires, mounted on both sides of the instrumented axle, are braked by conventional air brakes, which are actuated by a pneumatic circuit. The tires' vertical loads are controlled by adjusting air pressure in two air cylinders. The tire slip angle (the same angle for both tires) is set to a selected constant value during each test using two turnbuckles. A water spraying system is installed on the trailer. The flow

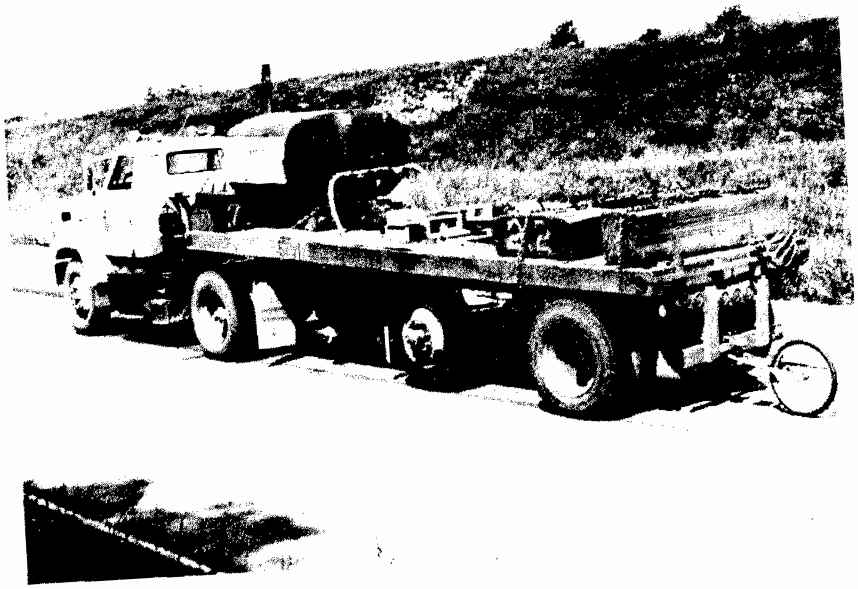

(a) Full View

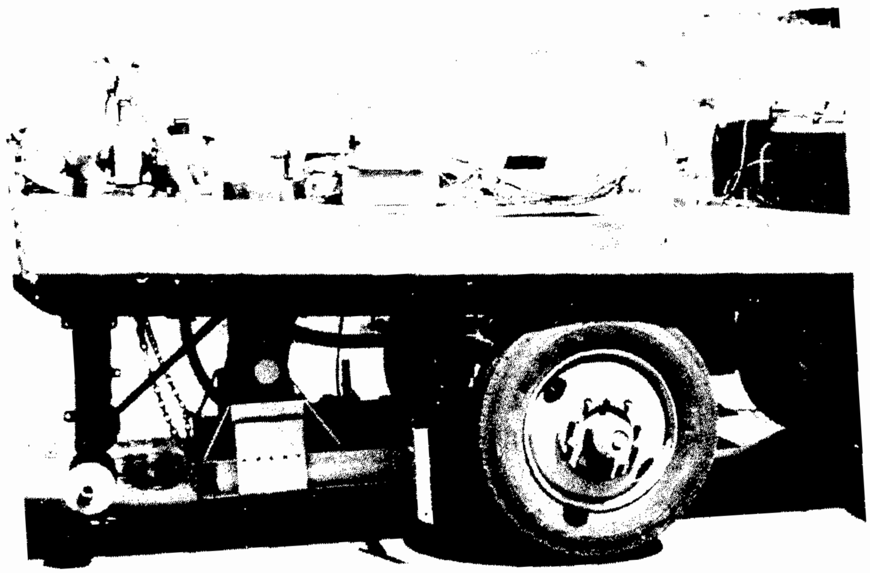

(b) Close-Up View

Figure 5. New truck tire tester--(a) full view and (b) close-up view.

rate of water through the nozzles mounted in front of the test tires is adjusted to produce a water film thickness of 0.02 in (0.5 mm) on the pavement surface. The test tire angular velocity is measured by a DC tachometer. The traveling speed of the tester is measured by a 26-in- (0.66-m-) diameter fifth wheel.

Measurements of tire vertical, braking, and lateral forces are obtained from strain gauges installed on the tester's axle. Three strain gauge assemblies, one for each force component, are located on each side of the axle. Because the signals representing forces are very small, the axle instrumentation was designed to measure moments rather than forces. The locations of the strain gauges on the axle and the bridge circuits for measuring three force components are shown in figure 6. The vertical and braking forces are proportional to the output voltages e_z and e_x:

$$F_z = k_1 e_z \tag{5}$$

$$F_x = k_2 e_x \tag{6}$$

Because the total bending moment acting on the axle has two components, vertical force moment and lateral force moment, the lateral force is calculated from the voltages e_z and e_y:

$$F_y = k_3 (e_y - k_4 e_z) \tag{7}$$

The calibration constants k_1, k_2, k_3, and k_4 were determined from the calibration tests performed with a force platform. Regression calibration models showed no apparent lack of linearity. The coefficient of correlation around a linear model was $R^2 = 0.99$ and a coefficient of variation of 2% was obtained for the three force components.

Researchers used an on-board personal computer data acquisition system to collect the test data. The system included an IBM-PC portable computer, a DT 2801A data acquisition board, and Honeywell signal amplifiers. A general interactive data acquisition program (GDA) was written. The sampling frequency for all test signals was 100 Hz. One thousand data points were

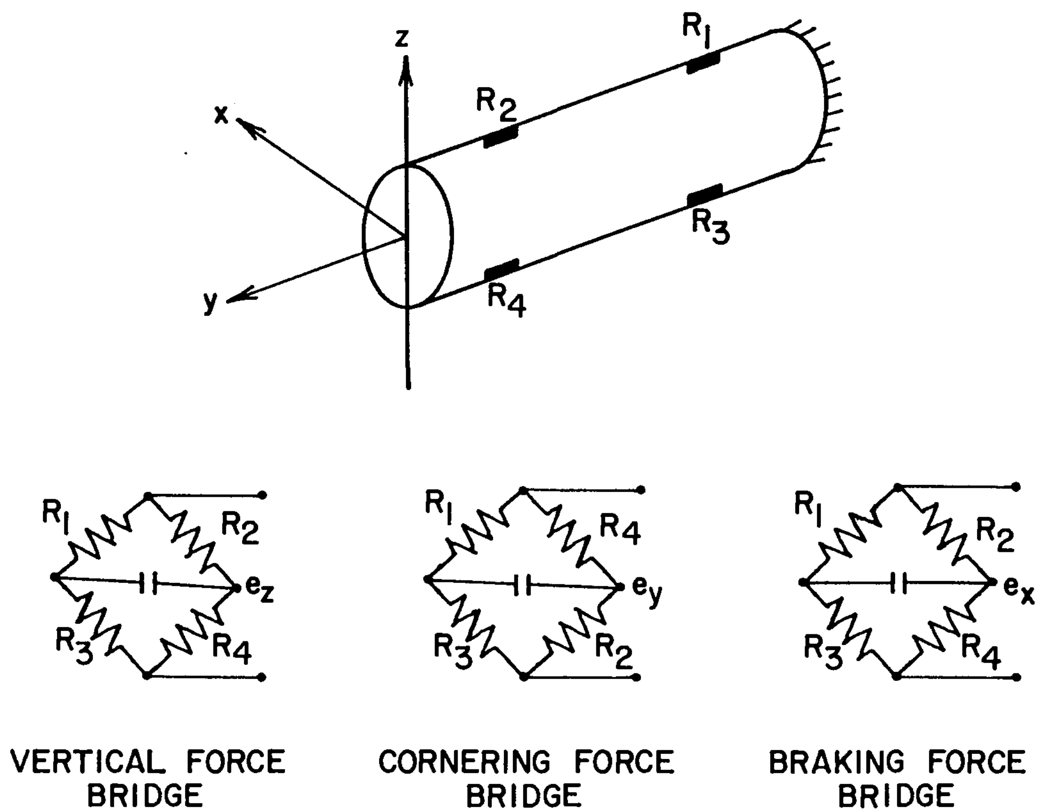

Figure 6. Locations of strain gauges and bridge circuits for measuring tire forces.

recorded in each channel during each test. A block diagram of the data acquisition system is shown in figure 7.

TEST PROCEDURE

Before each new series of tests, the test equipment was warmed up for 30 min, during which time the host truck was driven at 40 to 50 mi/h (64 to 80 km/h).

A typical test run was conducted in the following sequence. First, the truck driver brought the truck to the required speed with the tester lifted so that the test tire did not touch the pavement. As the truck approached the test section, the tester was lowered and a required vertical load was applied to the test tires through the air cylinders. The water spraying system was activated at that time if the test was to be conducted on a wet surface. When the tester entered the test section, the operator triggered the data acquisition system and the brakes were applied to the test wheels until the wheels were completely locked up. The test tires went through the transient longitudinal slip cycle from 0 to 100 percent. The duration of the transient lock-up process varied depending on pavement friction and vehicle speed, but it usually took about 2 s to lock up the tires. The lock-up stage was maintained for 1 s and then the brakes were released, the tester lifted, and the water flow shut off. The data acquisition cycle terminated automatically after 10 s. Sample plots of the three tire forces and the tire angular velocity recorded by the data acquisition system in a typical test run are shown in figures 8 through 11. Figure 10 shows that the average vertical load decreases in time, probably due to leaking valves of the air cylinders.

To provide reference friction data for the test pavements, American Society for Testing and Materials (ASTM) Standard E 274 skid resistance tests were conducted after the first truck tire test and then after every two truck tire tests.

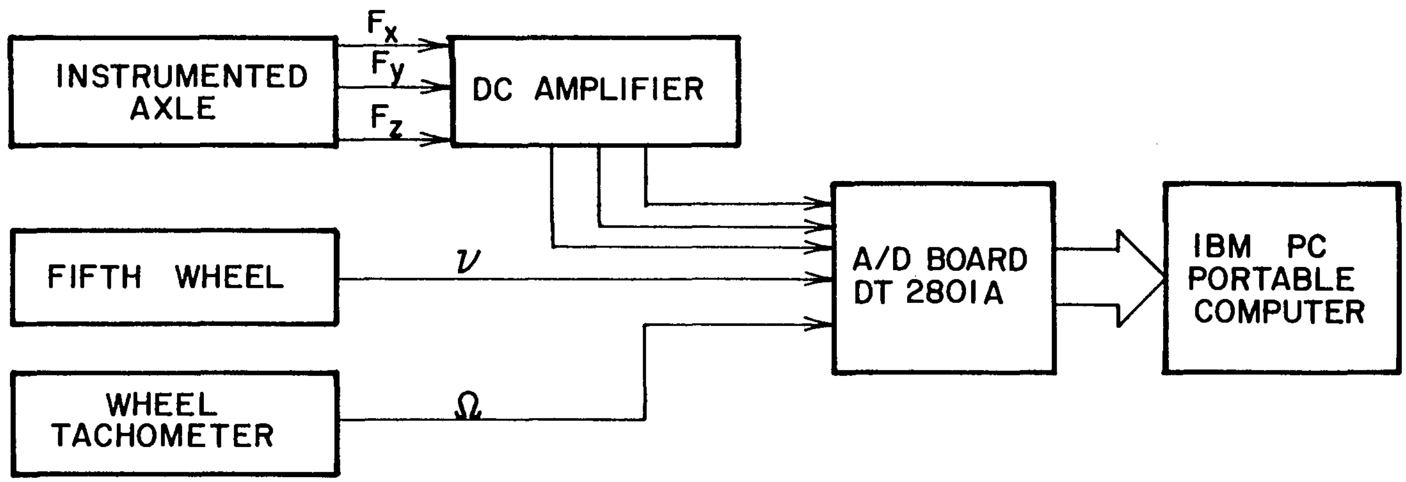

Figure 7. Personal computer data acquisition system.

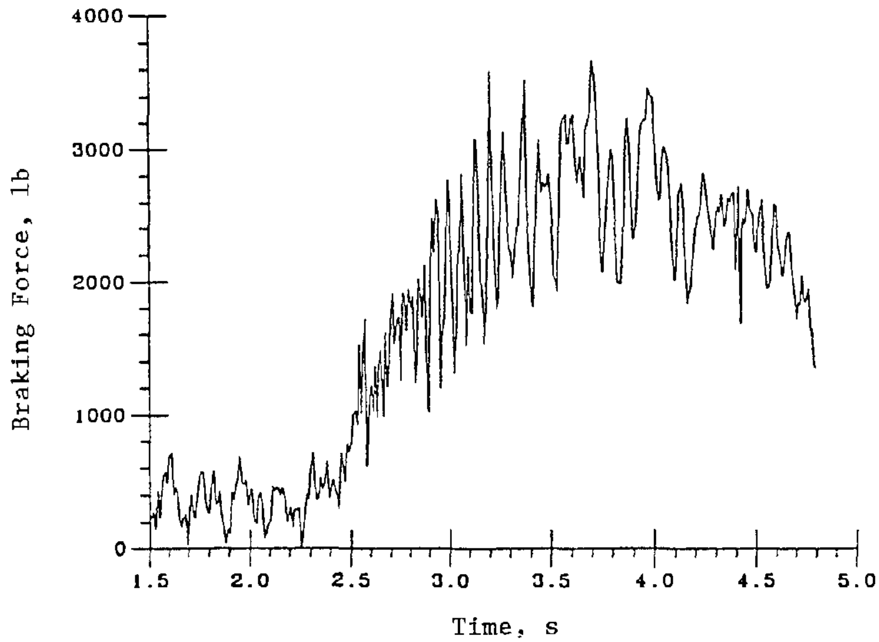

Figure 8. Tire braking force recorded in a typical test run.

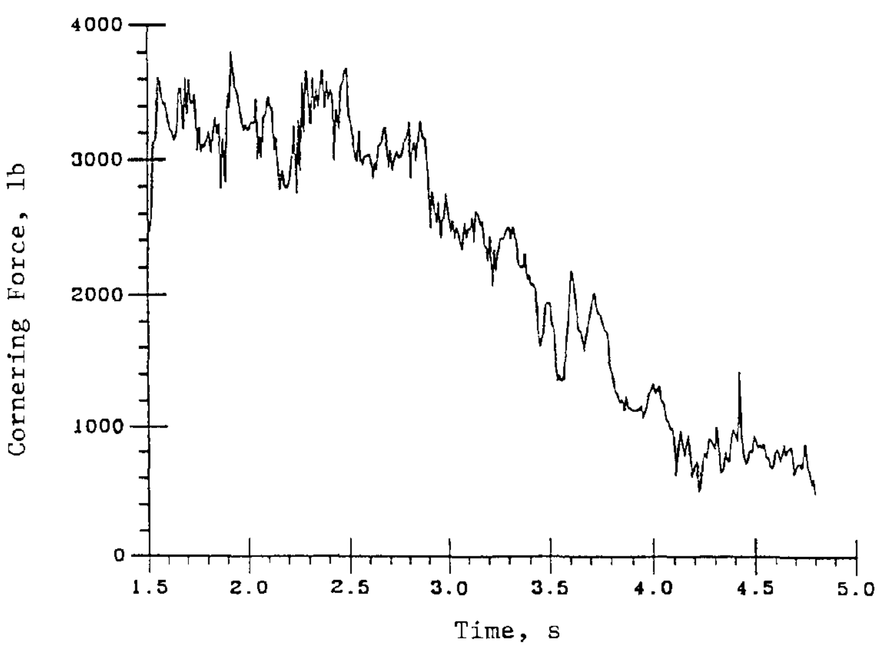

Figure 9. Tire cornering force recorded in a typical test run with slip angle $\alpha=4°$.

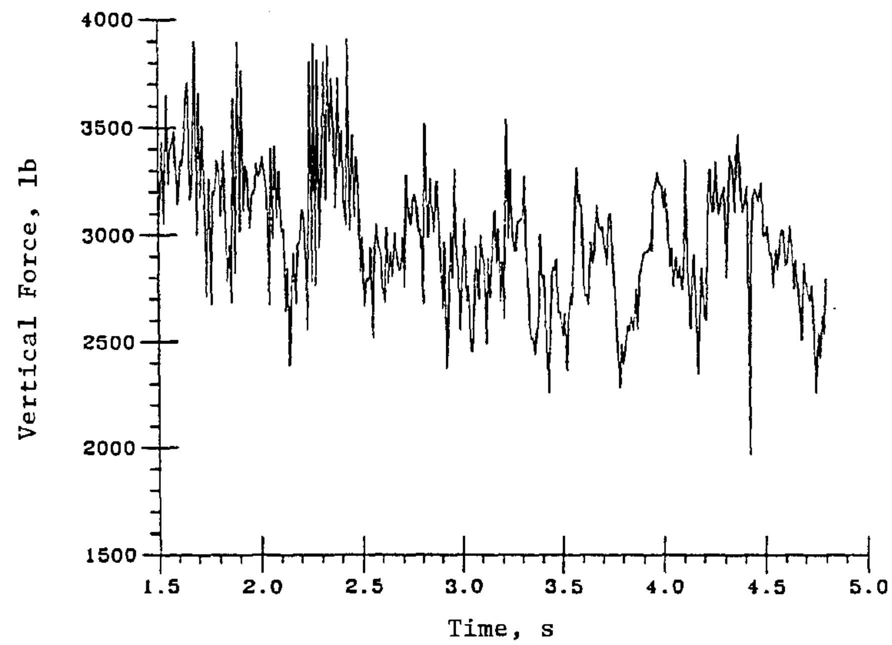

Figure 10. Tire vertical force recorded in a typical test run.

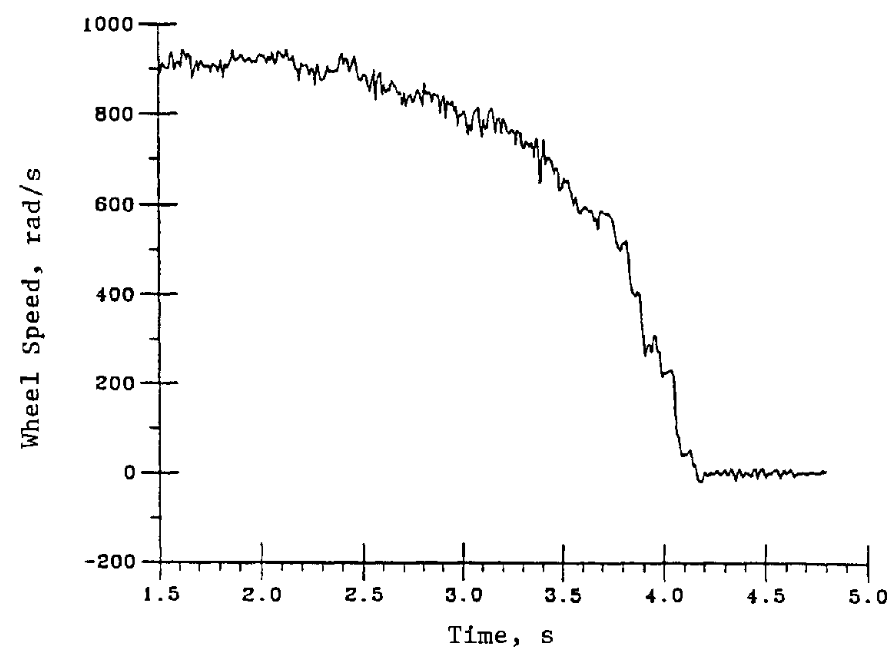

Figure 11. Wheel angular velocity recorded in a typical test run.

DATA REDUCTION

The raw data collected in all field tests were heavily contaminated by a high-frequency noise. The main sources of the noise were the on-board electric generator, the truck engine, vibration of the instrumented axle, and wheel bouncing. Fast Fourier Transform (FFT) analysis of the force data was performed to determine frequency spectra of the measuring signals. This analysis revealed that the dominant frequency range for the measurements was from 0 to 20 Hz. Therefore, a 20-Hz, low pass, digital filter program was written to eliminate the high-frequency noise. The filtering program was a 1,024-point finite impulse response (FIR) routine with adjustable pass and stop frequencies. Figures 12 through 15 show tire forces and longitudinal slip signals passed through the 20-Hz filter. The filtered data were used next to calculate tire breaking and cornering coefficients, f_x and f_y, defined by equations 1 and 4. The results are shown in figures 16 and 17. After FFT analysis of the filtered data, another low pass filter program was written to eliminate high-frequency noise in excess of 1 Hz from the braking coefficient, lateral coefficient, and slip data. The filtered signals are plotted in figures 18, 19, and 20.

TEST RESULTS

The tire coefficients of braking and cornering friction, f_x and f_y, are represented by the following five parameters:

- Peak coefficient of braking friction, $f_{xp} = \max\{ f_x \}$.
- Sliding coefficient of braking friction, $f_{xs} = f_x|_{s = 100\%}$.
- Critical longitudinal slip, s_{crit}, such that $f_x|_{s = s_{crit}} = f_{xp}$.
- Peak coefficient of cornering friction, $f_{yp} = \max\{ f_y \}$.
- Sliding coefficient of cornering friction, $f_{ys} = f_y|_{s = 100\%}$.

The test results are presented graphically in two sets of plots. In the first set (figures 21 through 25), the five parameters listed above are plotted in the form of envelopes of data collected on different types of pavements versus slip angle. In the second set (figures 26 through 30), the

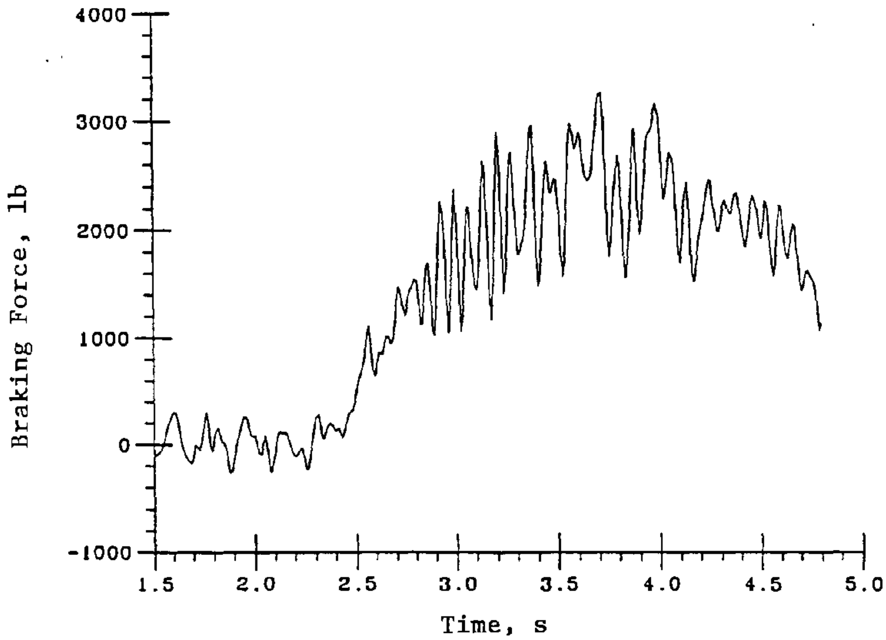

Figure 12. Tire braking force after 20-Hz filtering.

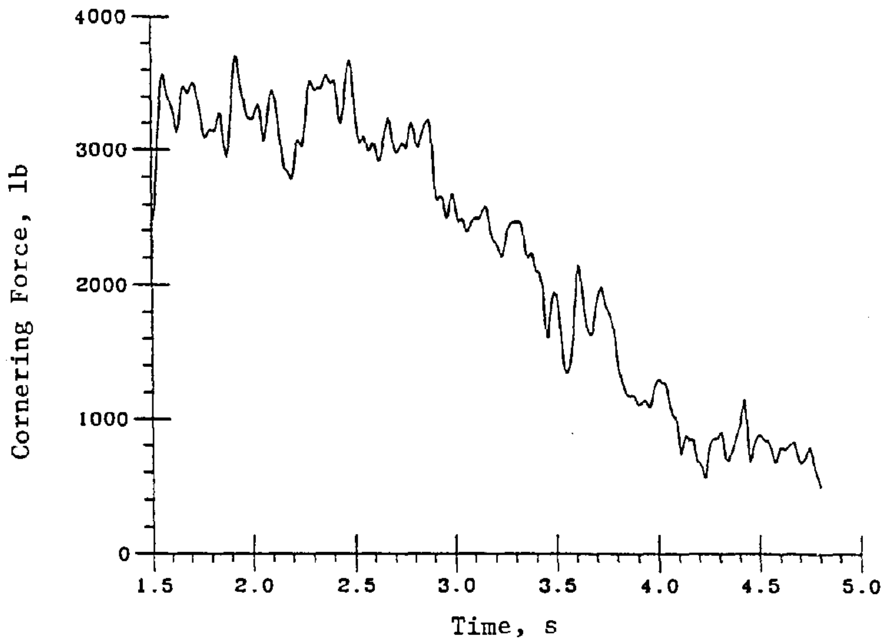

Figure 13. Tire cornering force after 20-Hz filtering.

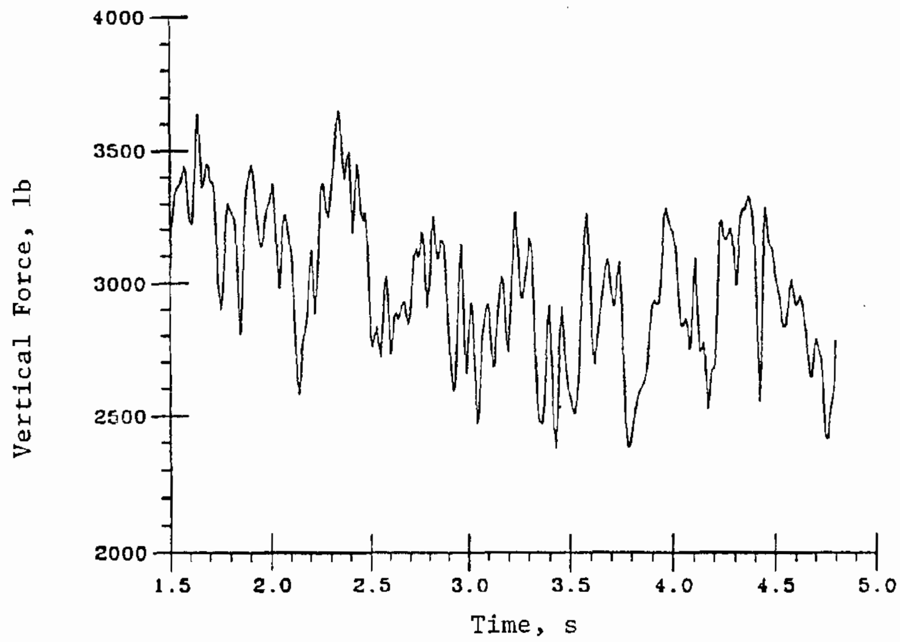

Figure 14. Tire vertical force after 20-Hz filtering.

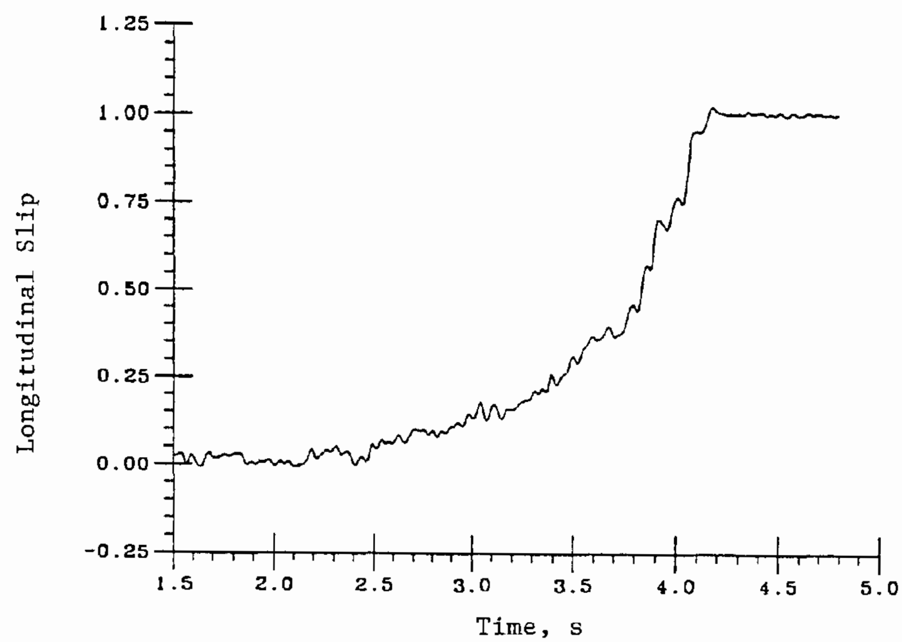

Figure 15. Longitudinal slip after 20-Hz filtering.

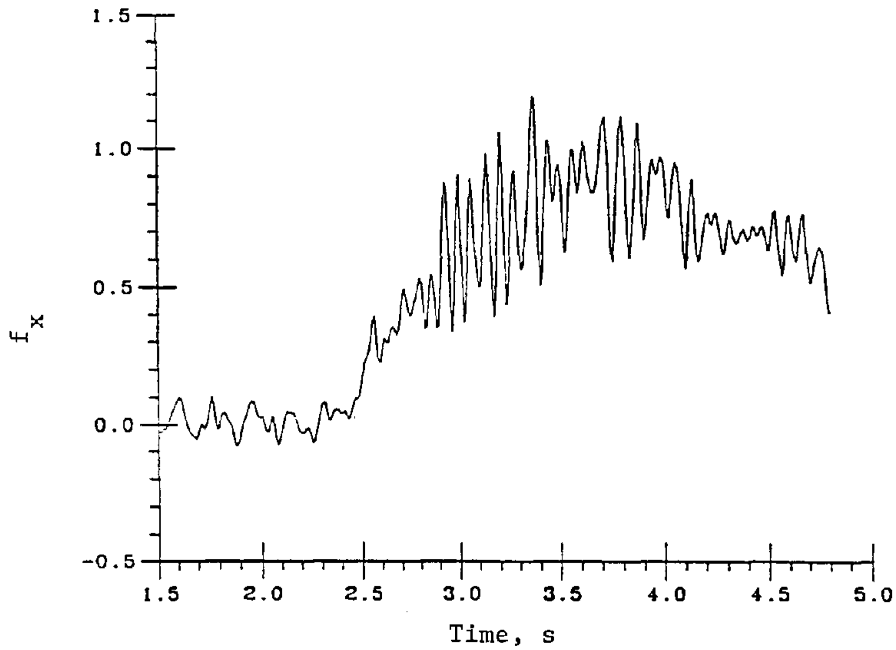

Figure 16. Tire coefficient of braking friction after 20-Hz filtering.

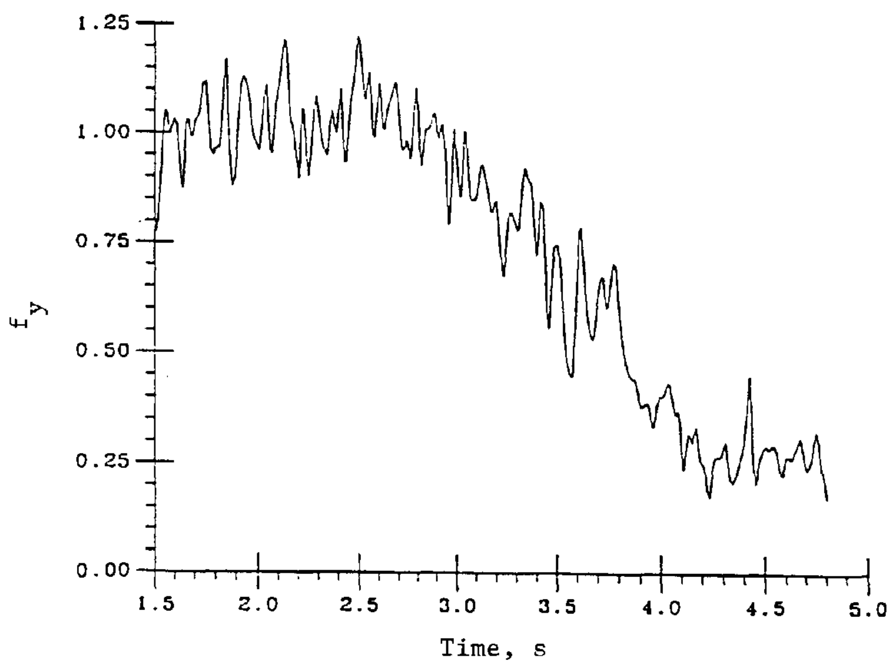

Figure 17. Tire coefficient of cornering friction after 20-Hz filtering.

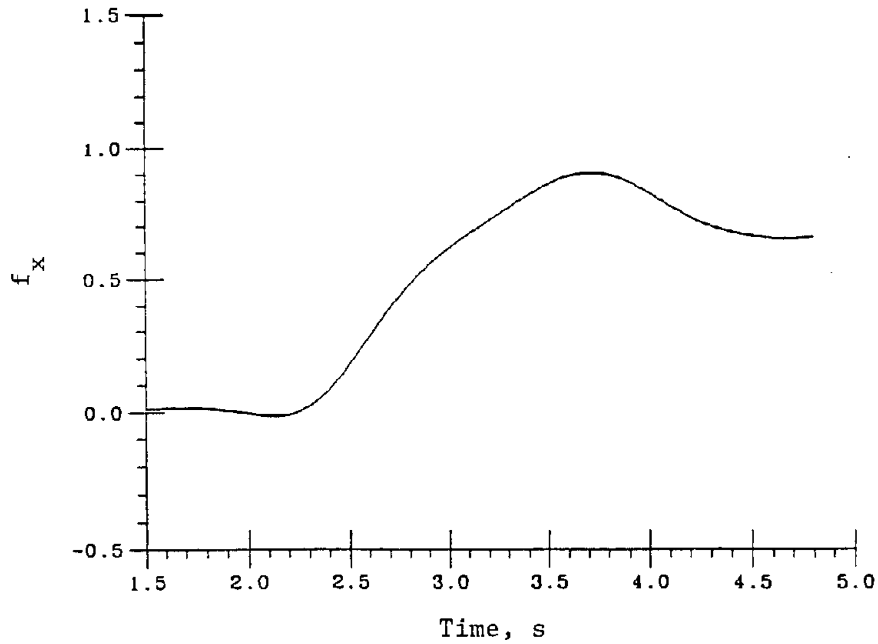

Figure 18. Tire coefficient of braking friction after 1-Hz filtering.

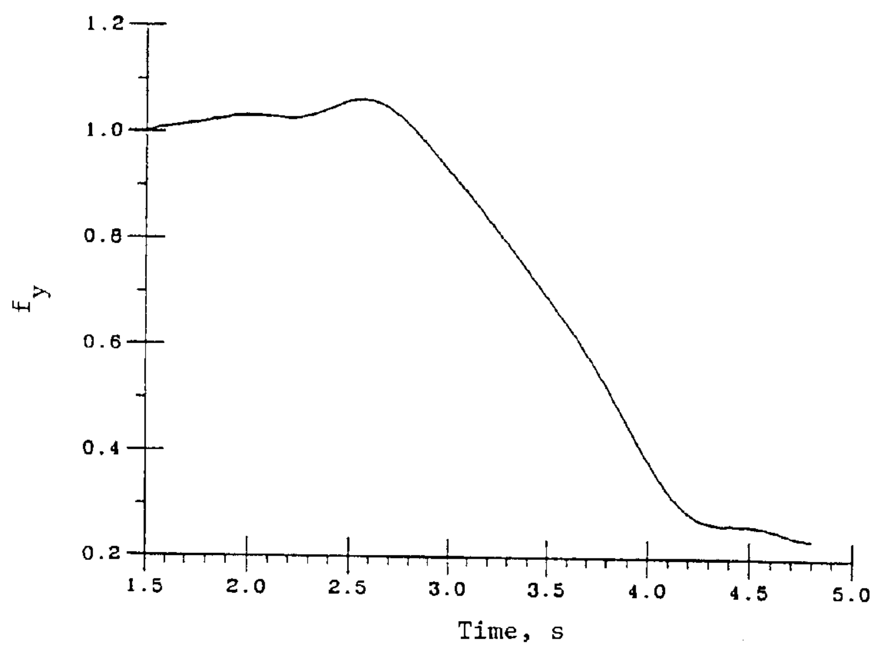

Figure 19. Tire coefficient of cornering friction after 1-Hz filtering.

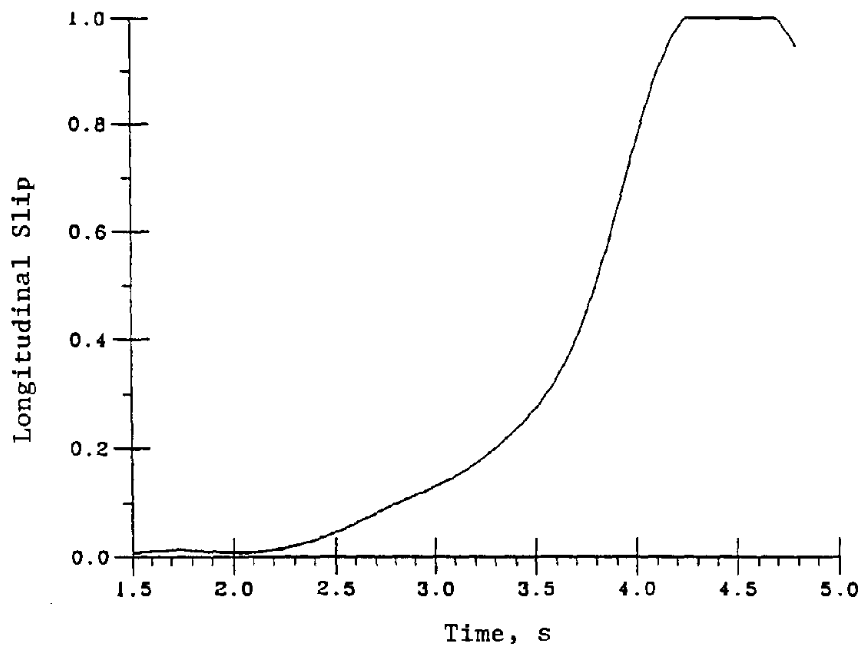

Figure 20. Longitudinal slip after 1-Hz filtering.

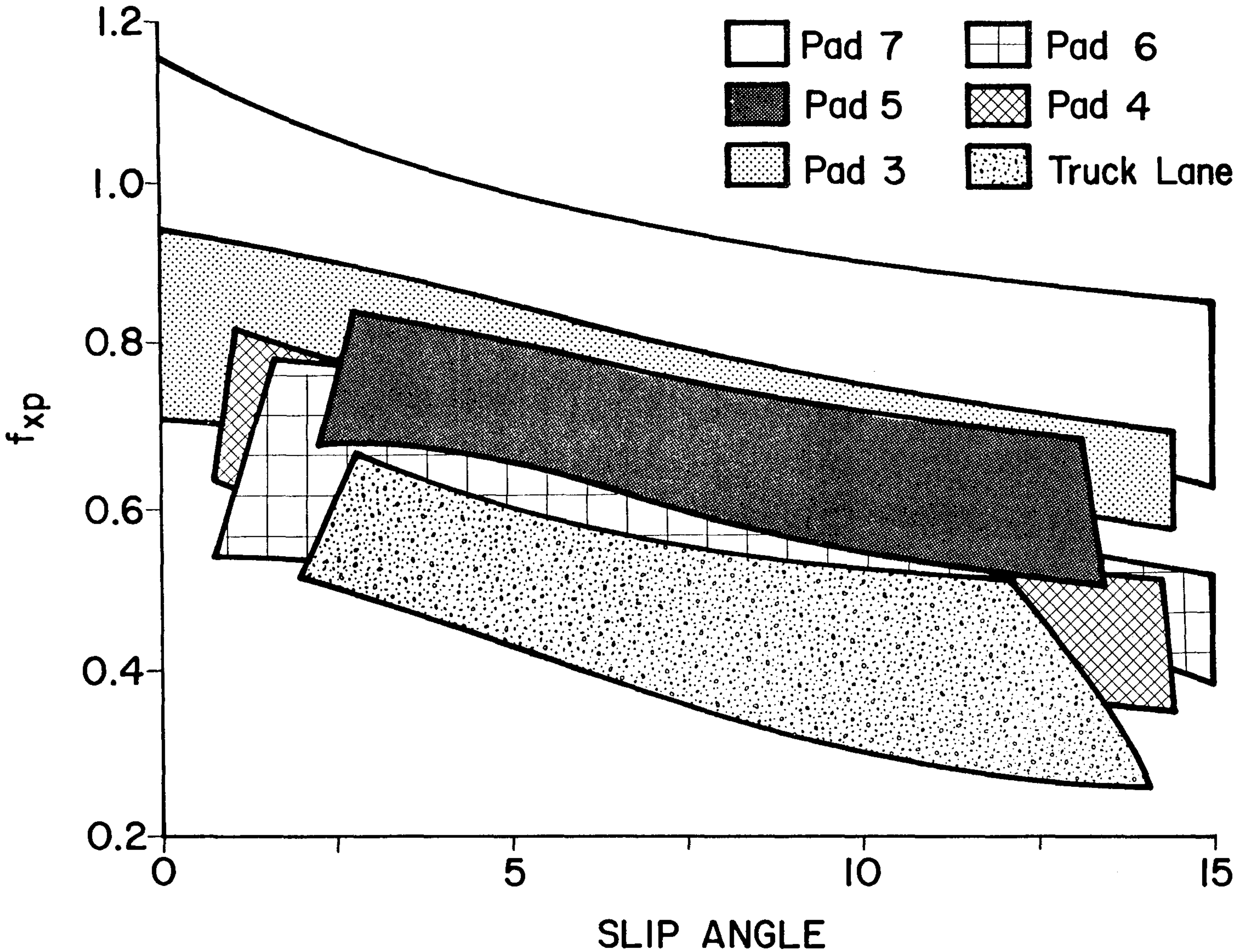

Figure 21. Envelopes of f_{xp} for six different pavements.

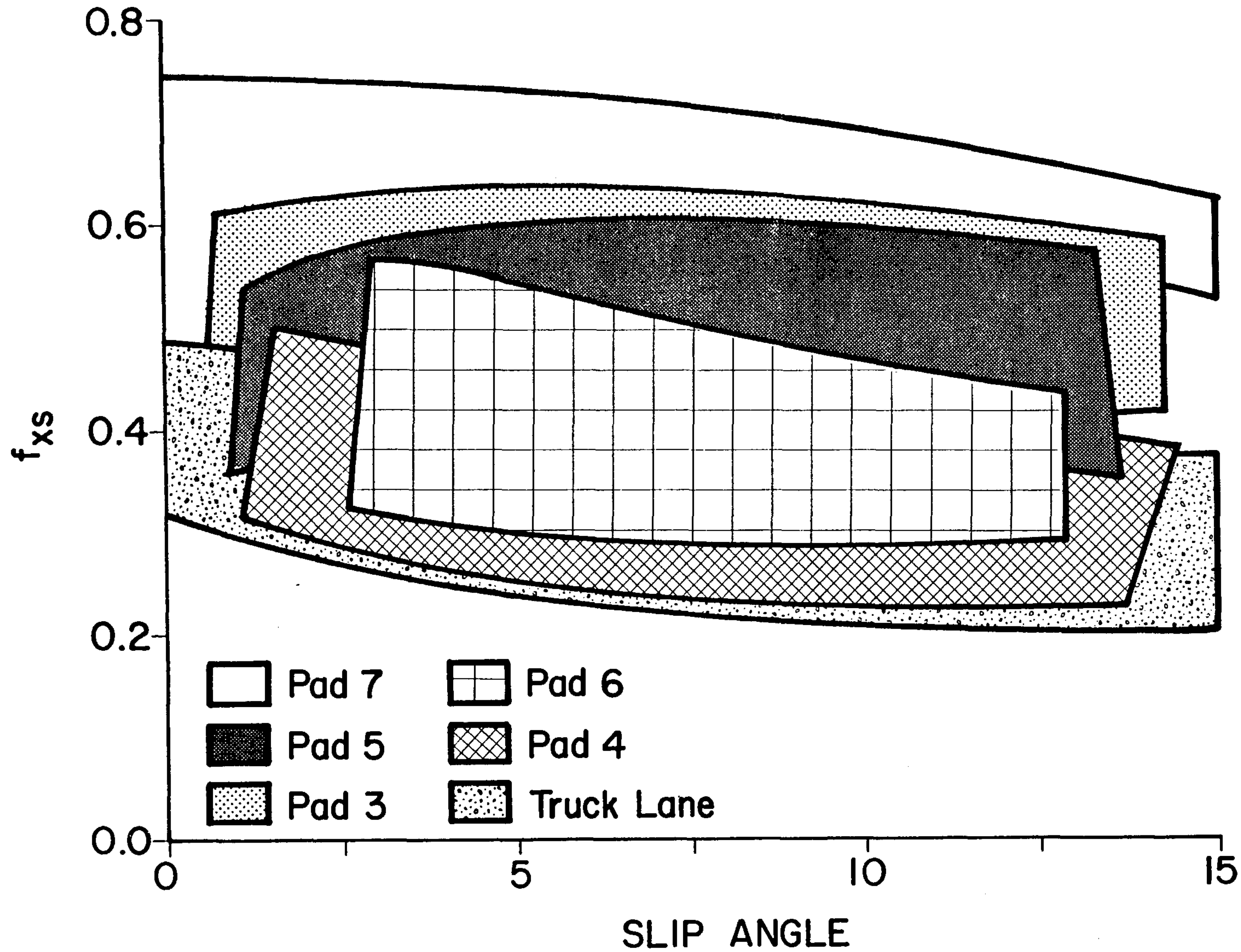

Figure 22. Envelopes of f_{xs} for six different pavements.

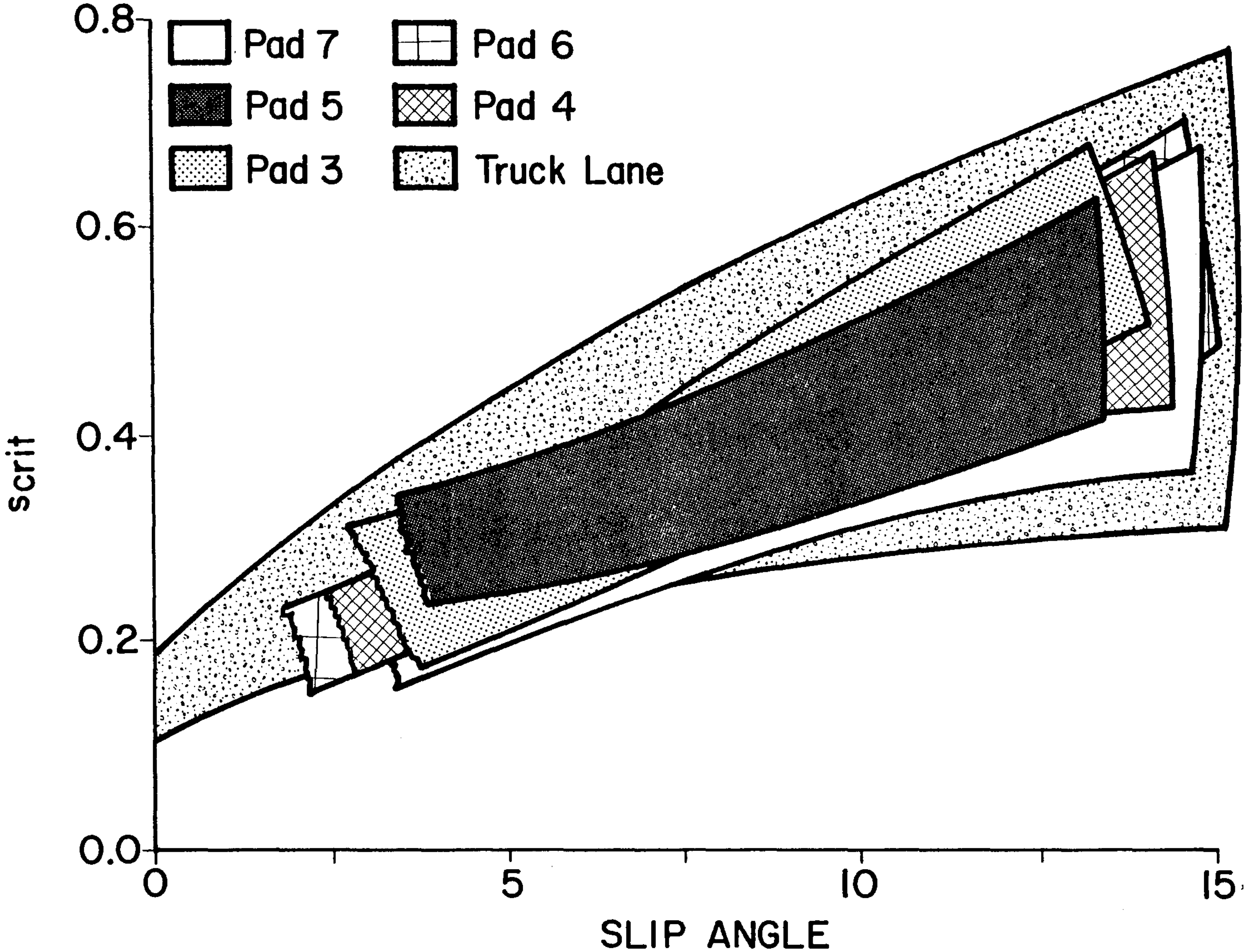

Figure 23. Envelopes of s_{crit} for six different pavements.

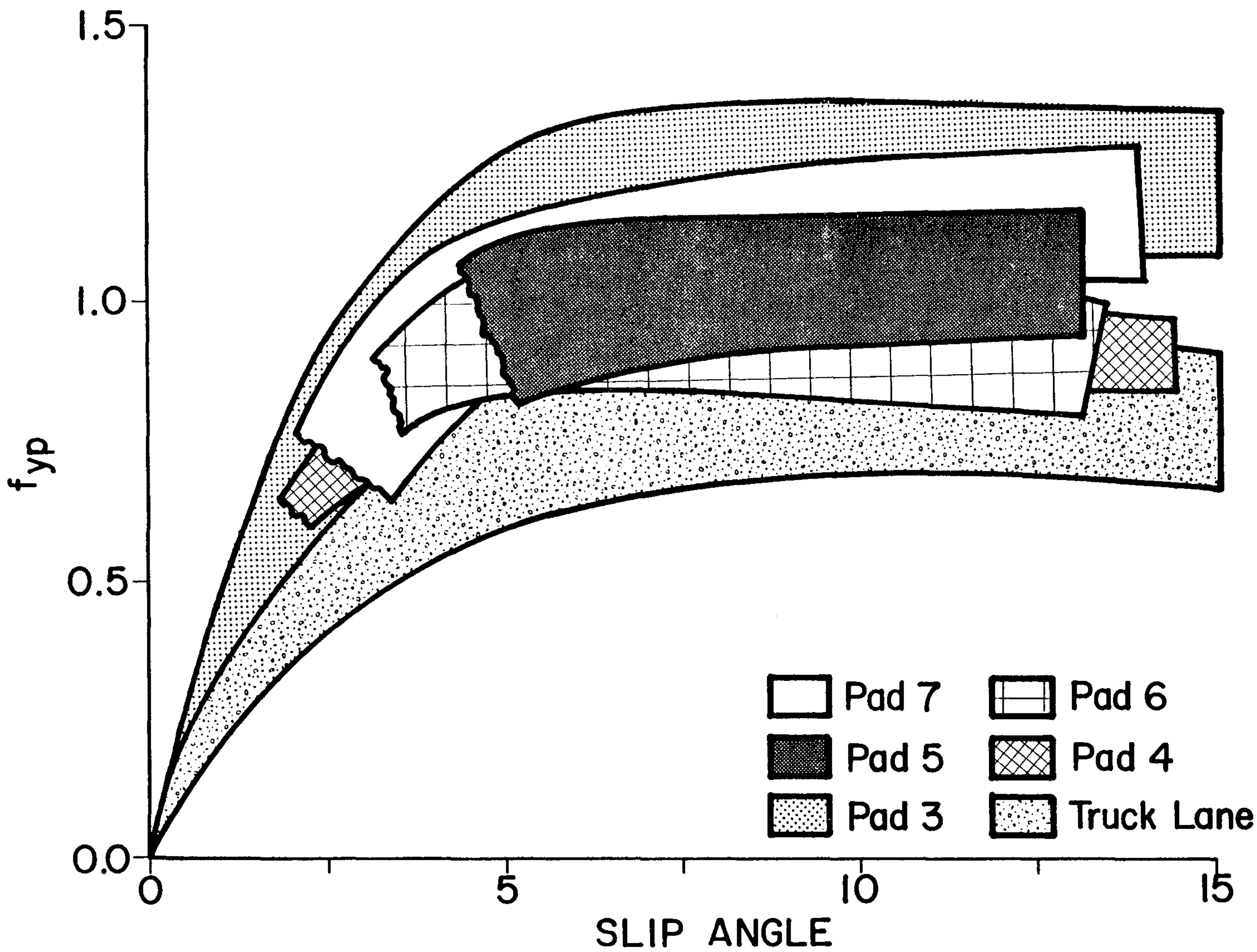

Figure 24. Envelopes of f_{yp} for six different pavements.

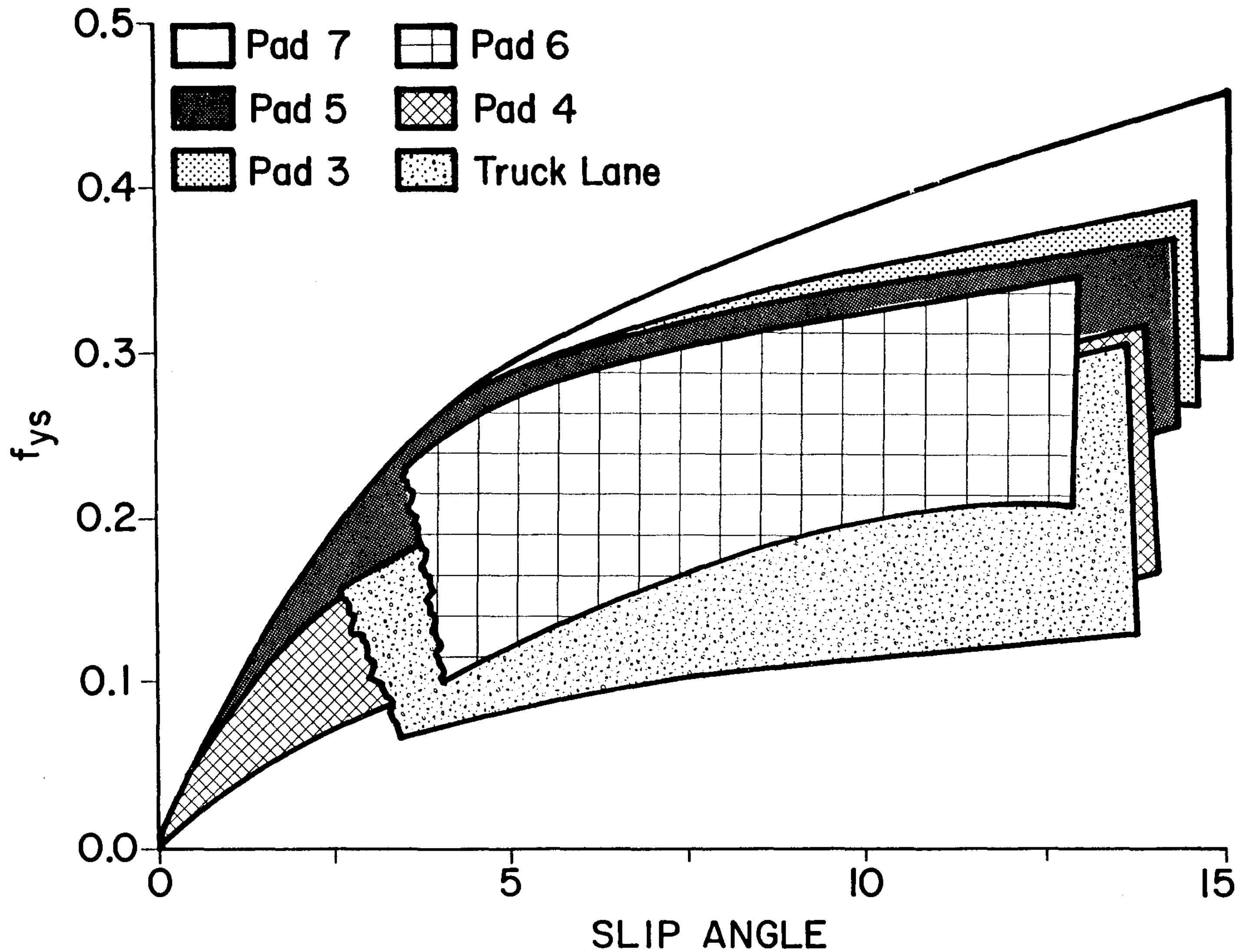

Figure 25. Envelopes of f_{ys} for six different pavements.

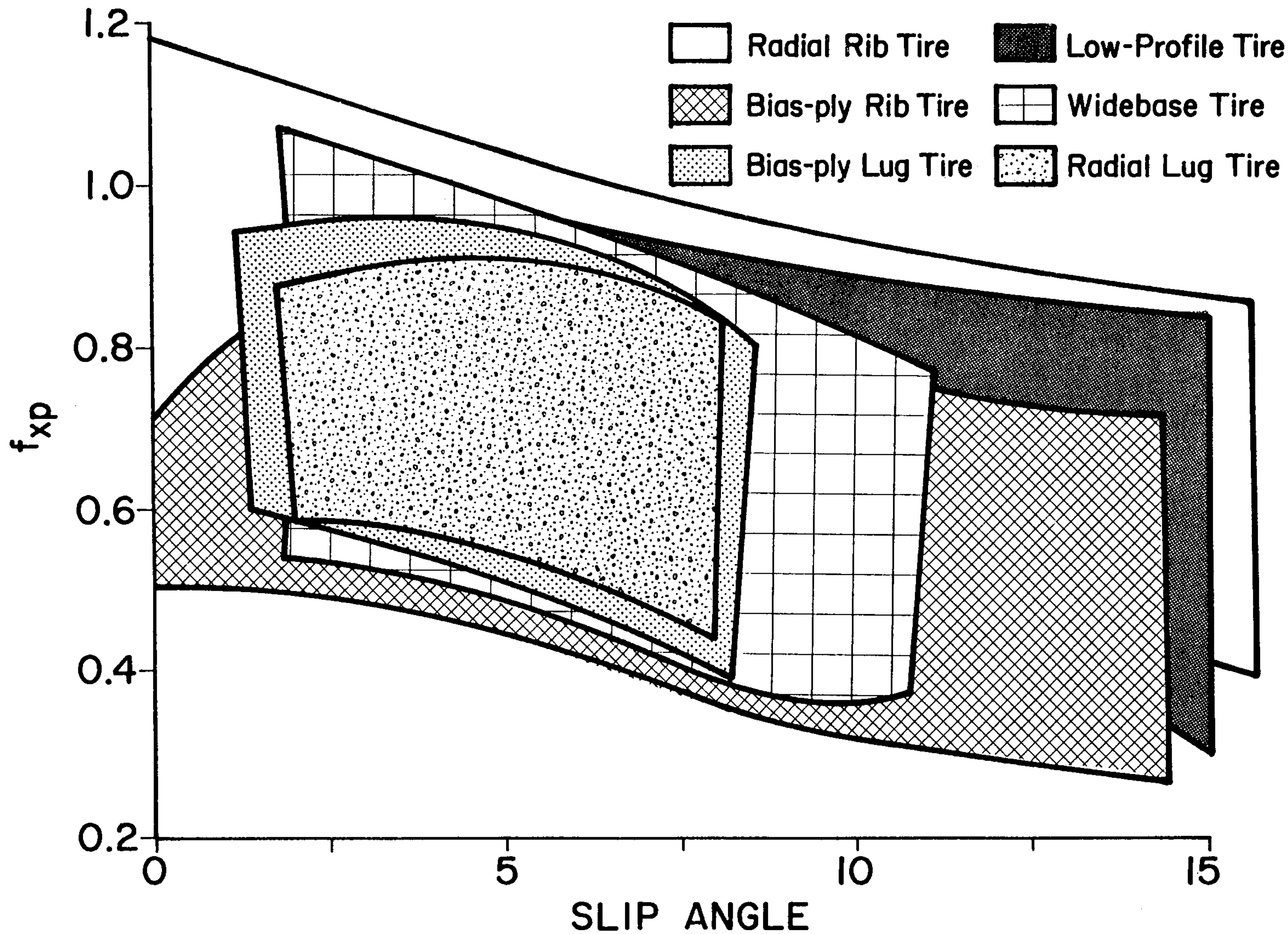

Figure 26. Envelopes of f_{xp} for six different tires.

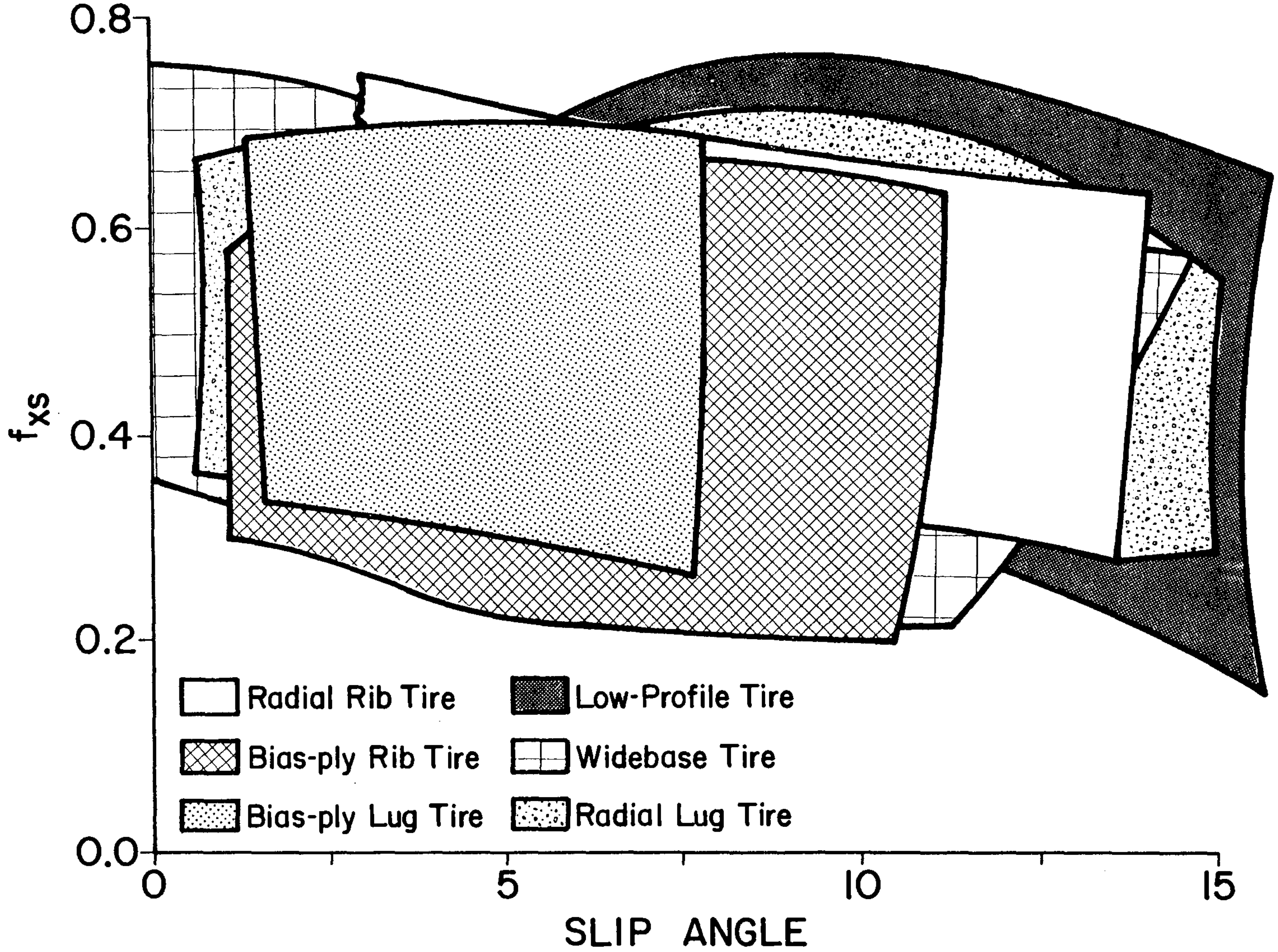

Figure 27. Envelopes of f_{xs} for six different tires.

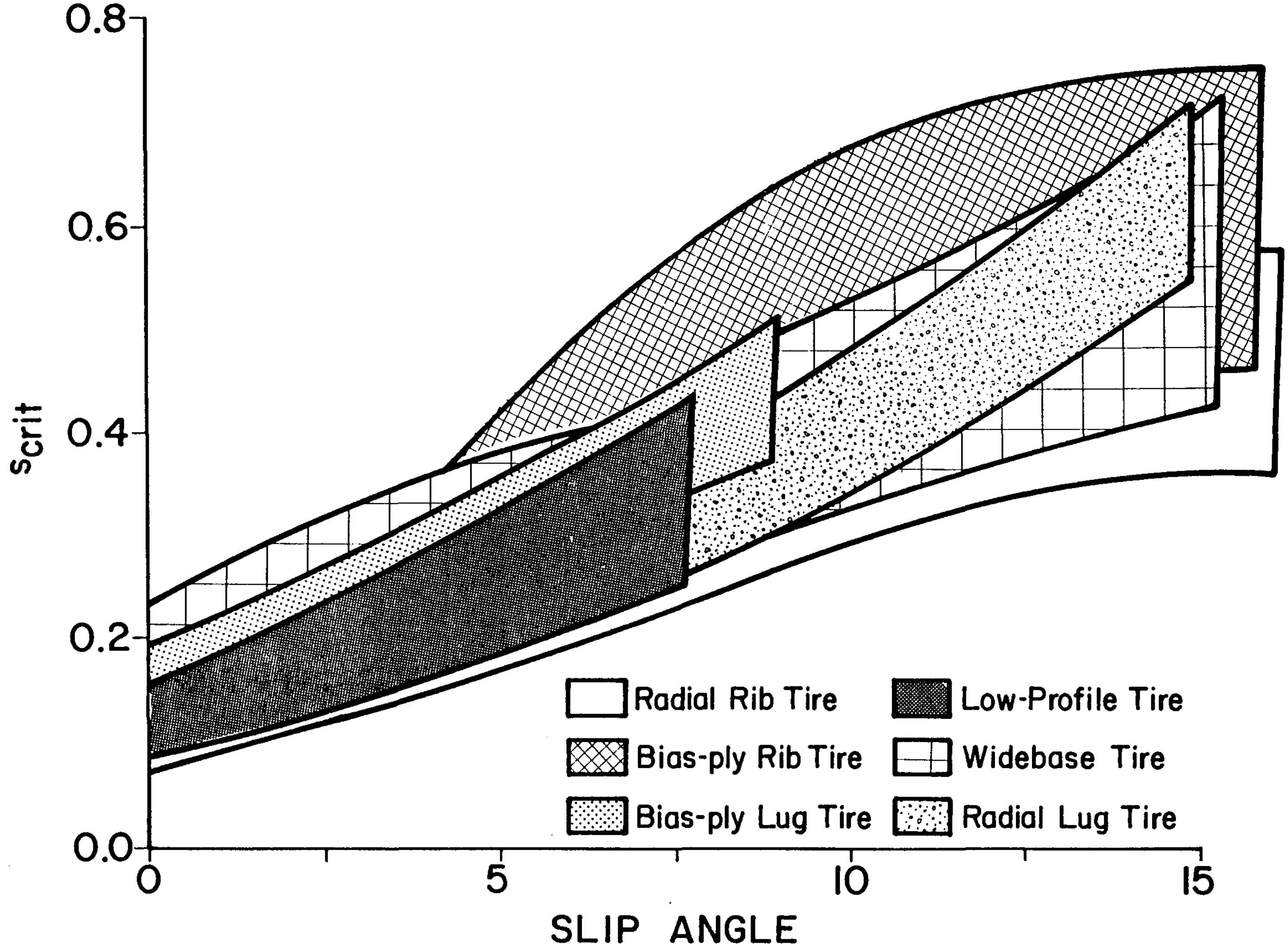

Figure 28. Envelopes of s_{crit} for six different tires.

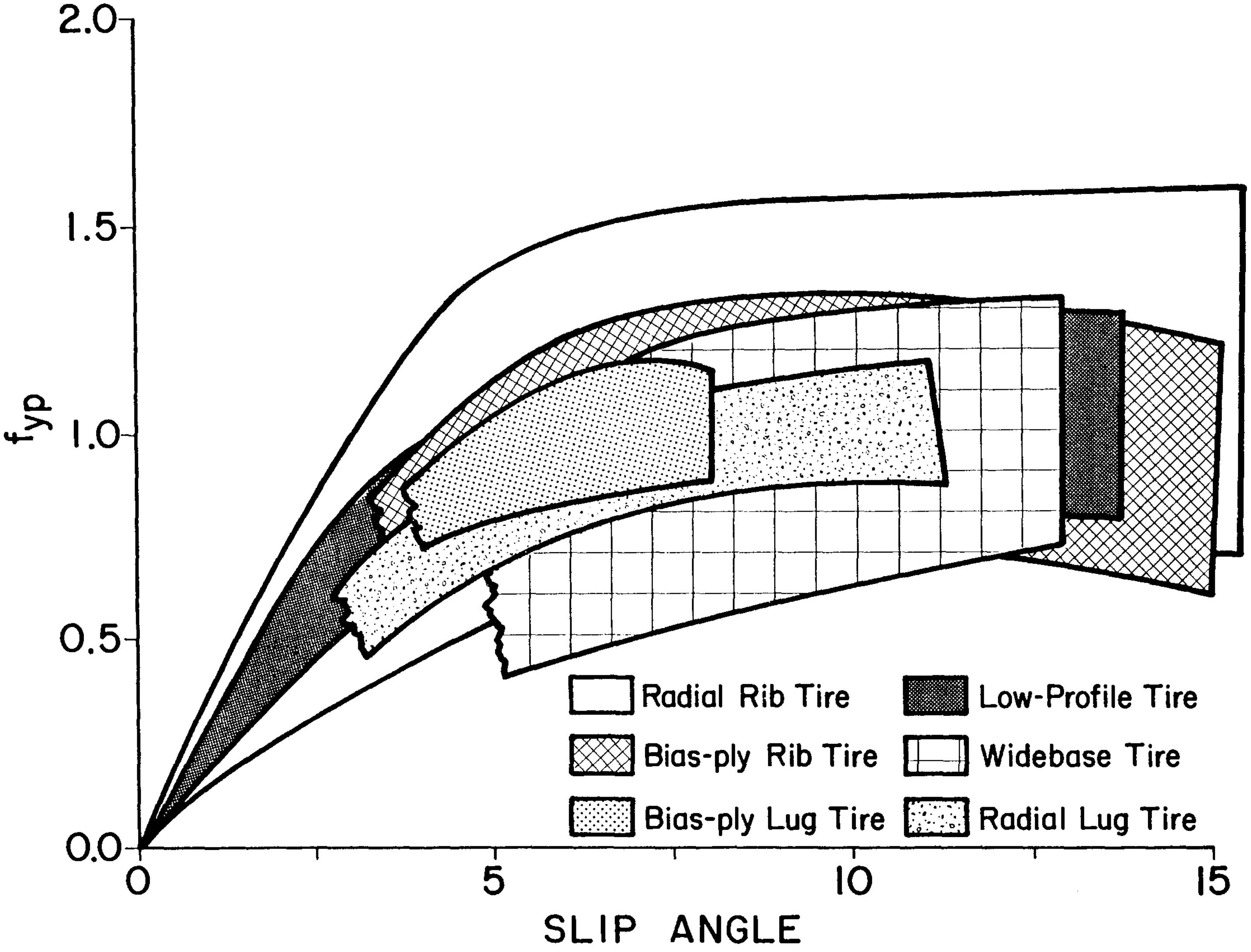

Figure 29. Envelopes of f_{yp} for six different tires.

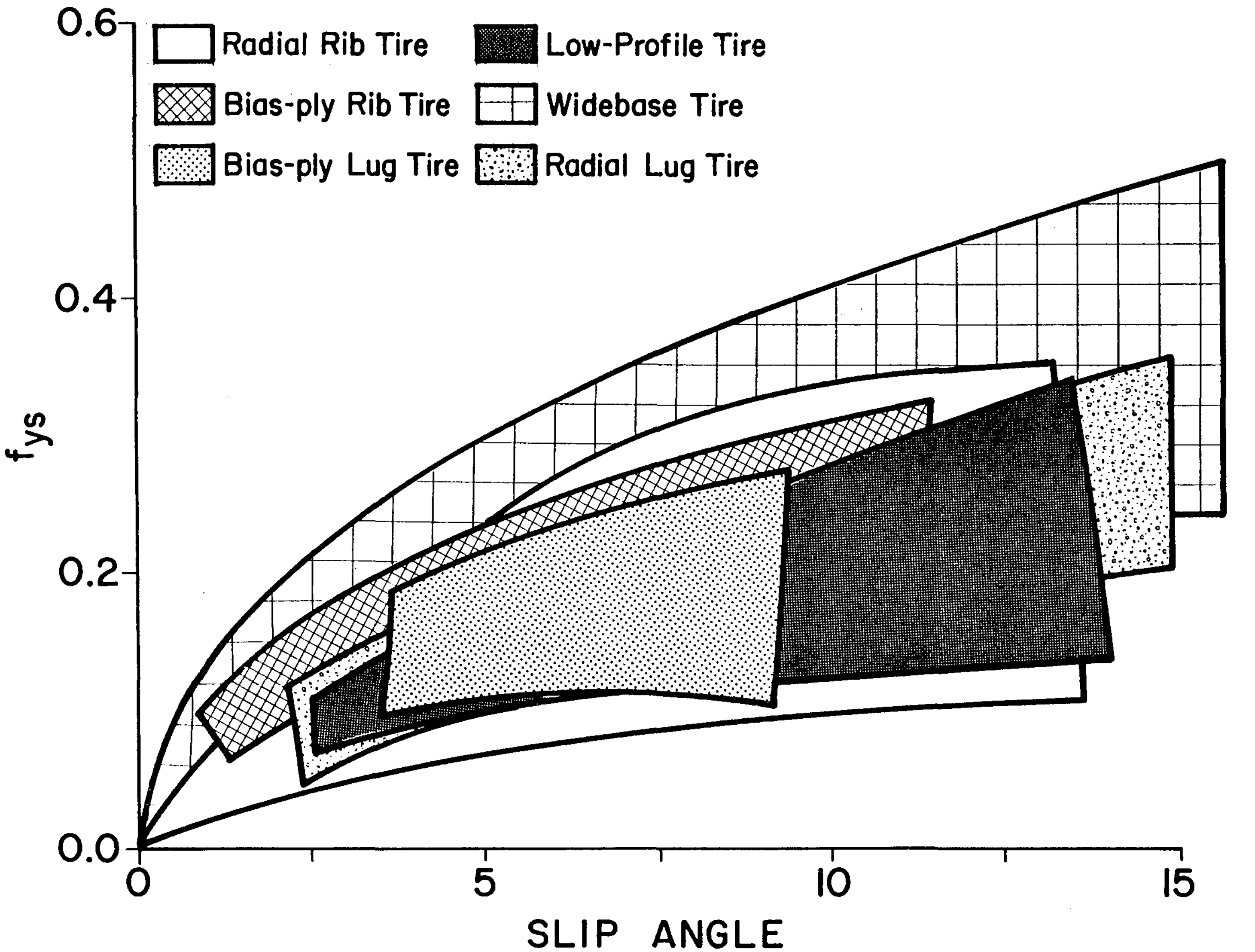

Figure 30. Envelopes of f_{ys} for six different tires.

tire friction parameters are plotted in the form of envelopes of data collected with different types of tires versus slip angle.

The first set of figures (figures 21 through 25) shows that the effects of pavement characteristics are, in most cases, proportional to that pavement's SN_{40} value. The skid pad no. 7, which had the highest SN_{40} of all pavements tested in this study, produced the highest values of f_{xp}, f_{xs}, and f_{yp} and the second highest value of f_{ys}. The truck lane and skid pad no. 4, which ranked lowest in terms of SN_{40}, also had the lowest values of f_{xp}, f_{xs}, f_{yp}, and f_{ys}. All truck tires tested in this study were new and thus had sufficient tread depth to expel water from the tire-pavement interface regardless of the surface macrotexture. Therefore, the truck tire traction parameters--f_{xp}, f_{xs}, f_{yp}, and f_{ys}--were primarily affected by the surface microtexture. Since SN_{40} is also sensitive to surface microtexture, its good correlation with truck tire coefficients of braking and cornering friction is well justified.

The critical longitudinal slip increased in an approximately linear fashion with increasing slip angle and was not strongly affected by pavement type.

The envelopes of the five traction parameters obtained for different tire types are very wide because each envelope includes data collected on six different pavements that produced a wide range of coefficients of braking and cornering friction for each tire type. However, several qualitative observations can be made from the plots shown in figures 26 through 30. The radial rib tire has about 20 percent higher peak coefficient of braking friction and slightly higher sliding coefficient of braking friction than the radial lug tire. Bias-ply rib and lug tires had similar values of coefficients of friction. Peak coefficient of braking friction is influenced more by tire type than the sliding coefficient of braking friction because tire construction has a significant effect on the performance of a rolling tire. The performance of a sliding tire is affected primarily by the tire tread pattern and pavement texture.

Peak coefficient of braking friction for all tire types decreases as slip angle increases. The sliding coefficient of braking friction has a maximum for slip angle between 4 and 8 degrees.

In general, the curves plotted in figures 21, 22, 24-27, 29, and 30 indicate an interaction between variations of longitudinal and lateral forces caused by changes in tire slip angle. At zero slip angle the tire longitudinal force has a maximum value whereas the tire lateral force is equal to zero. As the slip angle increases, the tire longitudinal force decreases and the lateral force increases. When slip angle is equal to 90 degrees, the longitudinal force reaches its minimum whereas the lateral force is at its maximum value. This interaction between tire longitudinal forces is illustrated by the friction ellipse shown in figure 31. It can be seen from figure 31 that for small values of slip angle, the changes in the coefficient of braking friction are much smaller than the changes in the coefficient of cornering friction, as the x-component of the resultant force decreases slightly from the half-length of the major axis and the y-component increases from zero to a significant portion of the minor axis of the ellipse. This is in good agreement with the experimental results shown in figures 21, 22, 24-27, 29, and 30.

Statistical analysis of the experimental tire traction data is presented in the following section.

STATISTICAL ANALYSIS OF TIRE TRACTION DATA

Regression models were developed for each of the five parameters, listed on page 17, describing a specified type of tire. Separate models were developed for braking only and for combined braking and cornering. In the "braking only" models, the independent variables were pavement skid number (SN_{40}), speed, and tire vertical load. The vertical load varied considerably from test to test due to uncontrolled variability of performance of the actuating air cylinders in the truck tire tester. The regression models obtained from the "braking only" data are summarized in table 2. Parameter p represents an actual probability that a hypothesis about a lack of statistical significance is true. In other words, the smaller the value of p, the more

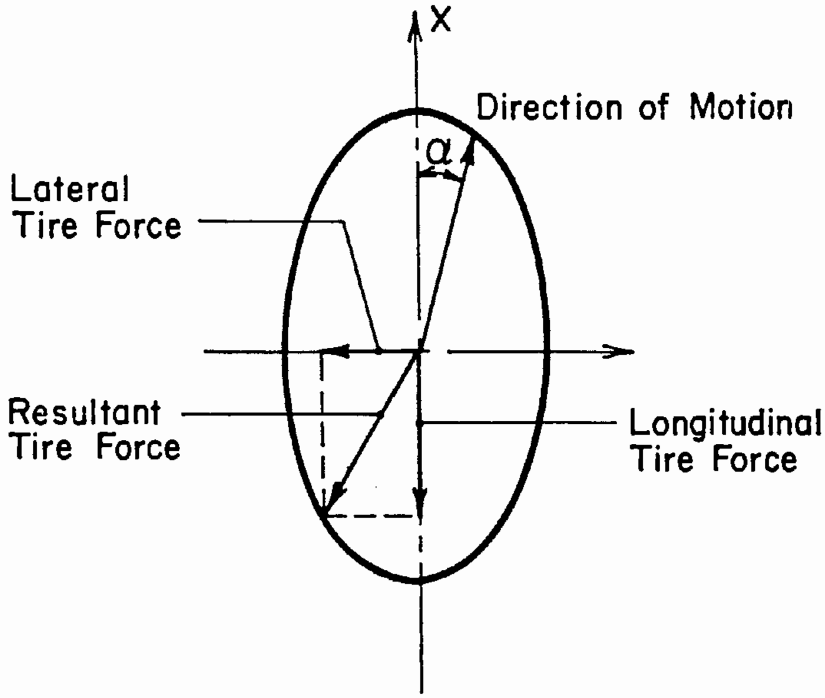

Figure 31. Friction ellipse.

Table 2. Summary of regression models for tire traction in braking (slip angle = 0).

Tire Type	Variable	Regression Coefficients: Intercept	SN_{40}	Speed	Load	R^2	St. Dev.	P
Radial rib	f_{xp}	0.659	0.0113	-0.00453	-0.000080	92.9	0.06	0.000
	f_{xs}	0.190	0.0093	-0.00518	-0.000028	95.0	0.03	0.000
	s_{crit}	0.118	0.0010	-0.00123	0.000001	52.4	0.02	0.099
Bias-ply rib	f_{xp}	1.090	-0.0027	-0.00677	-0.000015	26.7	0.10	0.243
	f_{xs}	0.519	0.0014	-0.00552	-0.000003	53.2	0.06	0.017
	s_{crit}	0.249	-0.0002	-0.00231	-0.000011	34.5	0.03	0.127
Bias-ply lug	f_{xp}	0.531	0.0075	-0.00354	-0.000036	71.4	0.06	0.237
	f_{xs}	0.422	0.0065	-0.00651	-0.000037	63.7	0.08	0.328
	s_{crit}	-0.017	0.0043	-0.00385	-0.000016	96.2	0.01	0.012
Low-profile rib	f_{xp}	1.040	0.0064	-0.00766	-0.000118	64.5	0.09	0.033
	f_{xs}	0.630	0.0058	-0.00759	-0.000073	66.9	0.06	0.025
	s_{crit}	0.198	-0.0001	-0.00232	-0.000004	25.6	0.03	0.475
Wide-base	f_{xp}	1.510	0.0083	-0.00916	-0.000259	75.6	0.13	0.001
	f_{xs}	0.363	0.0127	-0.00734	-0.000107	81.5	0.10	0.000
	s_{crit}	0.635	-0.00133	-0.00203	-0.000090	30.8	0.10	0.239
Radial lug	f_{xp}	0.918	0.0104	-0.00984	-0.000109	70.2	0.11	0.006
	f_{xs}	0.476	0.00582	-0.00951	-0.000016	93.1	0.04	0.000
	s_{crit}	0.418	0.00147	-0.00509	-0.000029	47.3	0.04	0.082

significant a regression model is. If a fixed significance level of 0.05 is selected, all models of critical slip are statistically insignificant except for the bias-ply lug tire model. Models of peak and sliding coefficients of friction are significant for radial rib, low-profile rib, wide-base, and radial lug tires. For bias-ply rib tires, only the model of sliding coefficient of friction is significant. Both models of f_{xp} and f_{xs} are insignificant for the bias-ply lug tire. Measurements obtained with this tire were very inconsistent in all aspects. Lack of significance of the critical slip models was caused by rather flat peaks of f_x versus slip curves, which, combined with measuring noise, resulted in large variations of critical slip values identified from these curves.

The effects of independent variables on peak and sliding coefficients of braking friction were very consistent. An increase of pavement skid number resulted in an increase of both coefficients, f_{xp} and f_{xs}, in all models except the f_{xp} model for the bias-ply rib tire. Increased speed as well as increased vertical load each resulted in decreased peak and sliding coefficients of friction.

The regression models for tire traction parameters in combined braking and cornering are summarized in table 3. All models pass the 0.05 p-value test of statistical significance. However, it should be noted that the coefficient of correlation is quite low in some models. This applies in particular to models of the peak coefficient of cornering friction. The curves of f_{yp} are very flat for slip angle--between 4 and 15 degrees--and as a result, the R^2 values for the f_{yp} models are the lowest among R^2 values for all models for four of the six test tires. The f_{yp} models also have highest values of standard deviation as a result of the flatness of the f_y versus longitudinal slip curves near critical slip values.

The effects of the independent variables--SN_{40}, speed, vertical load, and slip angle--on tire traction parameters were very consistent across the set of six test tires. An increasing pavement skid number led to an increase in peak and sliding values of coefficients of both braking and cornering friction. Critical slip, however, decreased when SN_{40} increased. When speed increased, all four coefficients of friction decreased, and so did the critical slip.

Table 3. Summary of regression models for tire traction in combined braking and cornering.

Tire Type	Dependent Variable	Regression Coefficients: Intercept	SN_{40}	Speed	Load	Slip Angle	R^2	Std. Dev.	p
Radial rib	f_{xp}	0.638	0.0116	-0.00525	-0.000076	-0.0137	75.4	0.10	0.000
	f_{xs}	0.462	0.0078	-0.00790	-0.000043	0.00195	70.1	0.08	0.000
	s_{crit}	0.465	-0.0015	-0.00405	-0.000036	0.01900	61.1	0.08	0.000
	f_{yp}	1.100	0.0103	-0.00721	-0.000084	-0.00696	42.7	0.17	0.000
	f_{ys}	0.048	0.0029	-0.00149	-0.000011	0.00900	55.3	0.05	0.000
Bias-ply rib	f_{xp}	0.779	0.0070	-0.00067	-0.000150	-0.0107	41.6	0.14	0.000
	f_{xs}	0.566	0.0059	-0.00521	-0.000093	0.00098	48.2	0.10	0.000
	s_{crit}	1.150	-0.0031	-0.01710	-0.000103	0.0300	66.7	0.12	0.000
	f_{yp}	0.685	0.0066	0.00742	-0.000137	0.00263	44.0	0.15	0.000
	f_{ys}	0.143	0.0029	-0.00057	-0.000056	0.00679	56.7	0.05	0.000
Bias-ply lug	f_{xp}	0.491	0.0101	-0.00637	-0.000034	-0.00810	57.2	0.09	0.000
	f_{xs}	0.298	0.0101	-0.00880	-0.000033	0.00500	68.5	0.08	0.000
	s_{crit}	0.631	-0.0006	-0.00709	-0.000057	0.0221	42.3	0.07	0.027
	f_{yp}	0.667	0.0034	-0.00243	-0.000029	0.03850	57.7	0.08	0.002
	f_{ys}	-0.011	0.0032	-0.00159	-0.000006	0.00988	53.2	0.04	0.004
Low-profile rib	f_{xp}	0.880	0.0097	-0.00850	-0.000113	-0.0118	66.7	0.12	0.000
	f_{xs}	0.739	0.0074	-0.01180	-0.000086	-0.00086	71.2	0.10	0.000
	s_{crit}	0.775	-0.00258	-0.00943	-0.000092	0.03280	81.1	0.09	0.000
	f_{yp}	0.853	0.00857	0.00082	-0.000147	0.00204	50.9	0.18	0.004
	f_{ys}	-0.015	0.0028	-0.00032	-0.000018	0.01150	75.3	0.04	0.000
Wide-base	f_{xp}	1.030	0.0086	-0.00306	-0.000185	-0.02260	59.0	0.15	0.000
	f_{xs}	0.531	0.0076	-0.00662	-0.000078	-0.00299	58.6	0.10	0.000
	s_{crit}	0.342	-0.0028	-0.00371	0.000017	0.0344	69.6	0.12	0.000
	f_{yp}	1.750	0.0048	-0.00746	-0.000239	-0.00700	31.1	0.20	0.008
	f_{ys}	0.372	0.0013	-0.00498	-0.000014	0.01020	45.7	0.08	0.000

Table 3. Summary of regression models for tire traction in combined braking and cornering (Continued).

Tire Type	Dependent Variable	Regression Coefficients							
		Intercept	SN_{40}	Speed	Load	Slip Angle	R^2	Std. Dev.	p
Radial lug	f_{xp}	0.651	0.0090	-0.00440	-0.000076	-0.0135	72.1	0.10	0.000
	f_{xs}	0.612	0.0063	-0.00869	-0.000052	-0.00359	79.1	0.07	0.000
	s_{crit}	0.270	-0.0034	0.00090	-0.000019	0.03830	81.8	0.09	0.000
	f_{yp}	0.852	0.0054	-0.00016	-0.000113	0.00687	31.3	0.18	0.006
	f_{ys}	-0.0176	0.0025	0.00095	-0.000013	0.01100	65.2	0.05	0.000

The same effect was observed when the tire vertical load was increased. The effect of the slip angle was not very consistent, but it was also rather small compared with the effects of SN_{40}, speed, and vertical load. In general, it appears that when the slip angle increased, the coefficients of cornering friction increased. The critical longitudinal slip increased with increasing slip angle for all types of tested tires.

The linear regression models of tire traction parameters presented here were derived from the field tests in which the independent test variables varied within certain limits. Table 4 shows the minimum, maximum, and mean values of the independent variables recorded in the field tests. It also shows the minimum, maximum and mean values of air temperature during the tests. The air temperature was not incorporated in any of the tire traction models. It is possible, however, that variations of air temperature influenced tire performance in some of the tests. Slip angle is not included in table 4 since it was equal to 0 in all "braking only" tests and varied from 4 to 15 degrees in all tests involving cornering.

Table 4. Variability of independent test variables.

Tire Type	Variable	Braking Only			Braking and Cornering		
		Min	Max	Mean	Min	Max	Mean
Radial rib	SN_{40}	36.6	74.7	53.6	31.9	67.3	49.1
	Speed, mi/h	25.5	46.8	34.2	22.0	46.4	33.1
	Load, lb	1,130	6,230	4,101	1,370	4,020	2,638
	Temp., °F	66	92	80	67	82	76
Bias-ply rib	SN_{40}	29.1	69.7	57.4	29.1	72.6	52.9
	Speed, mi/h	20.1	45.7	34.7	23.0	46.8	33.9
	Load, lb	2,030	4,230	3,148	1,060	3,370	2,362
	Temp., °F	74	88	80	69	88	78
Bias-ply lug	SN_{40}	45.8	59.8	52.7	40.9	67.7	53.2
	Speed, mi/h	25.5	37.8	31.5	24.1	38.2	30.9
	Load, lb	2,930	5,140	4,537	2,000	3,380	2,599
	Temp., °F	72	74	73	80	81	80
Low-profile rib	SN_{40}	28.7	60.0	51.9	31.6	76.6	50.2
	Speed, mi/h	24.0	41.4	32.5	22.9	47.0	34.4
	Load, lb	2,770	5,450	4,118	1,680	3,120	2,069
	Temp., °F	78	80	79	73	89	83
Wide-base	SN_{40}	32.2	78.7	55.9	31.6	69.7	50.2
	Speed, mi/h	24.7	44.7	33.1	21.6	45.6	34.7
	Load, lb	1,900	3,920	3,267	1,710	4,180	2,783
	Temp., °F	73	97	78	65	90	80
Radial lug	SN_{40}	27.2	68.7	47.7	27.2	74.0	50.7
	Speed, mi/h	24.8	44.8	36.0	23.1	45.5	35.6
	Load, lb	2,860	5,650	4,431	1,160	3,800	2,579
	Temp., °F	76	87	83	73	98	84

1 mi = 1.6 km
1 lb = 4.444 N

3. WORK PLAN FOR FIELD TESTS TO DETERMINE EFFECTS OF SUSPENSION CHARACTERISTICS

The main objective of the research outlined in this workplan was to determine the effects of truck suspension characteristics on the braking and cornering performance of truck tires tested on a variety of pavements.

In the following section, the test variables and their levels are described. The test variables were divided into two groups, primary variables and secondary variables, based on their significance to the main objective of the study. An experimental design consisting of three parts was proposed for the testing program. This three-part format offers the flexibility that may be necessary to tailor the testing program to particular needs and the resources available when the tests are conducted. Additional tests, including passenger car tests, roughness measurements, and skid resistance tests, are summarized. Testing procedures are described and discussion of data storage, retrieval, and analysis is included. The proposed methods of data analysis should be considered preliminary. These methods can be modified and new methods may be added when the test results become available. The major pieces of equipment needed to perform the testing program are briefly described. Finally, the level of effort necessary for successful completion of the proposed testing program is estimated.

TEST VARIABLES

The independent test variables are identified together with the levels at which these variables will be applied in the testing program.

SUSPENSION

The primary test variable is the suspension type. Two types of tandem-axle suspension will be used:

- Four-spring suspension (S1).
- Walking beam suspension (S2).

The two suspensions will be mounted on tandem axles of two separate trailers. The trailers should be of the same type and both in good technical condition. Schematics of the four-spring and walking beam suspensions are shown in figures 32 and 33. The stiffness and damping coefficients of each suspension are expected to remain unchanged during the entire testing program.

PAVEMENT

Four pavement sections will be selected:

- Tangent section, low roughness (P1).
- Tangent section, high roughness (P2).
- Nontangent section, low roughness (P3).
- Nontangent section, high roughness (P4).

The smooth sections, P1 and P3, should have a roughness index of approximately 50 IPM. The roughness index of sections P2 and P4 should be at least 150 IPM. The length of each pavement section should be greater than the stopping distance of the tractor-trailer used in the tests. The average stopping distances for tractor-semitrailers at 55 mi/h (88 km/h) reported in several studies are between 250 and 350 ft (75 and 106 m).[9,10] Therefore, the pavement test sections should be 350 ft (106 m) long.

The curvature of the two nontangent sections, P3 and P4, should allow for safe cornering at 55 mi/h (88 km/h), which is the highest speed in the tests. It is also desirable that both nontangent sections have the same radius of curvature. This can be accomplished by driving on the same road in and outside the wheel paths. The specific curvature of the nontangent pavement sections is of minor importance for this testing program, but, as a general selection guideline, the radius of curvature should be between 500 and 800 ft (152 and 244 m).

Each pair of pavement sections, P1-P2 and P3-P4, should include the same type of pavement material and similar texture characteristics in order to make roughness the dominant variable.

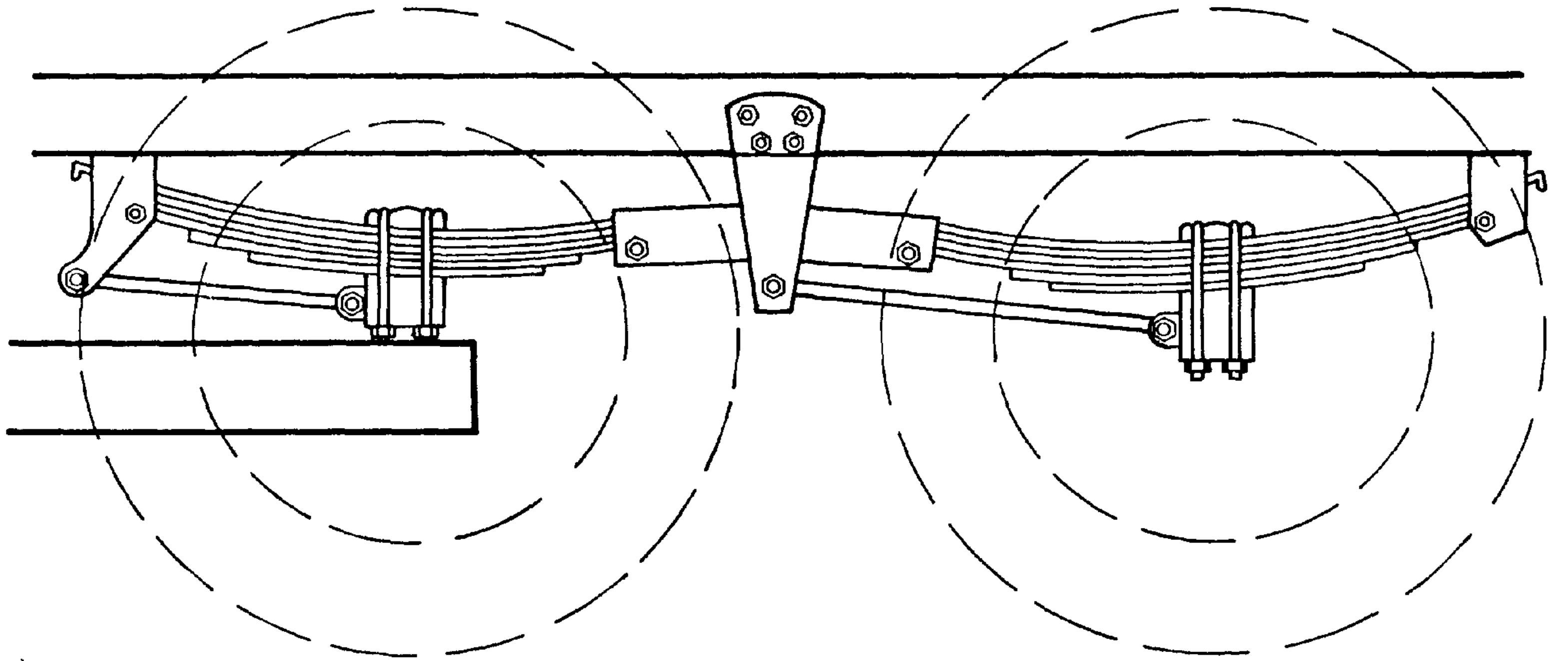

Figure 32. Diagram of four-spring suspension.

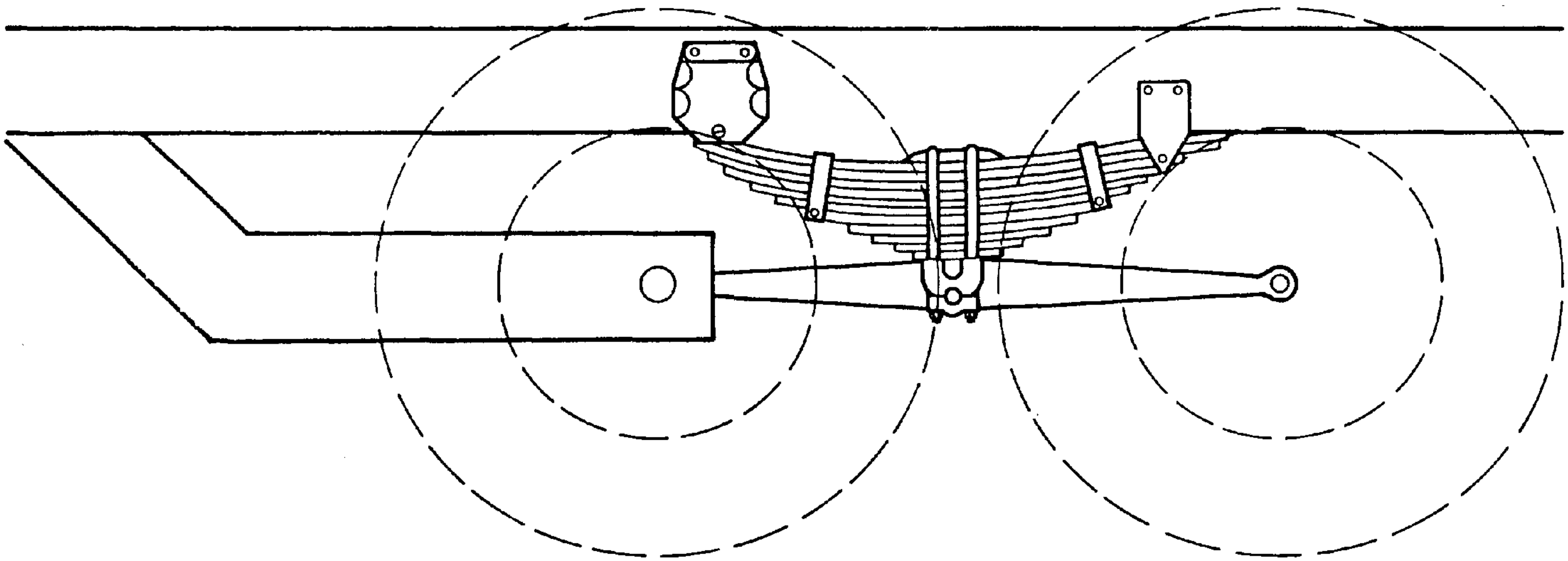

Figure 33. Diagram of walking beam suspension.

Each of the four surfaces will be tested under both dry and wet conditions, so there will be eight levels for the pavement variables in total: P1W, P2W, P3W, P4W, P1D, P2D, P3D, and P4D, where W denotes wet and D denotes dry pavement.

TIRE TYPE

Three types of tires will be tested:

- Radial--rib tread (T1).
- Bias-ply--rib tread (T2).
- Low-profile (T3).

These tire types were selected for the following reasons. First, all three types are widely used--the bias rib and the radial rib probably represent the majority of truck tires in use today, and the metric low-profile radial is becoming increasingly popular. The low profile radial will probably continue to increase in popularity because it is more compact than conventional tires and will allow future trucks either more cargo space or larger brakes while remaining within the present overall envelope. Also, these tires are normally used on all axles (i.e., steering, drive, and trailer), so installing them on a trailer for testing, as proposed, will yield a common configuration, whereas lug tires on a trailer would not yield a common configuration. Finally, the performance characteristics of these tires as measured in this project vary significantly, so the tires represent a range of mechanical properties. Of the six tires tested in Task 2, the bias rib had the lowest longitudinal friction, the radial rib had the second highest after the wide base, and the low profile was in between the two. Figure 34 shows the average longitudinal peak coefficients of friction measured in the tests conducted in Task 2. The same order also held for cornering stiffness, where the bias rib was near the low end, the radial rib was near the high end, and the low profile was in the middle, as illustrated in figure 35. If an additional or alternate tire were desired, the next choice would be the wide base tire, which will probably be growing in popularity and which exhibited the highest value of longitudinal friction.

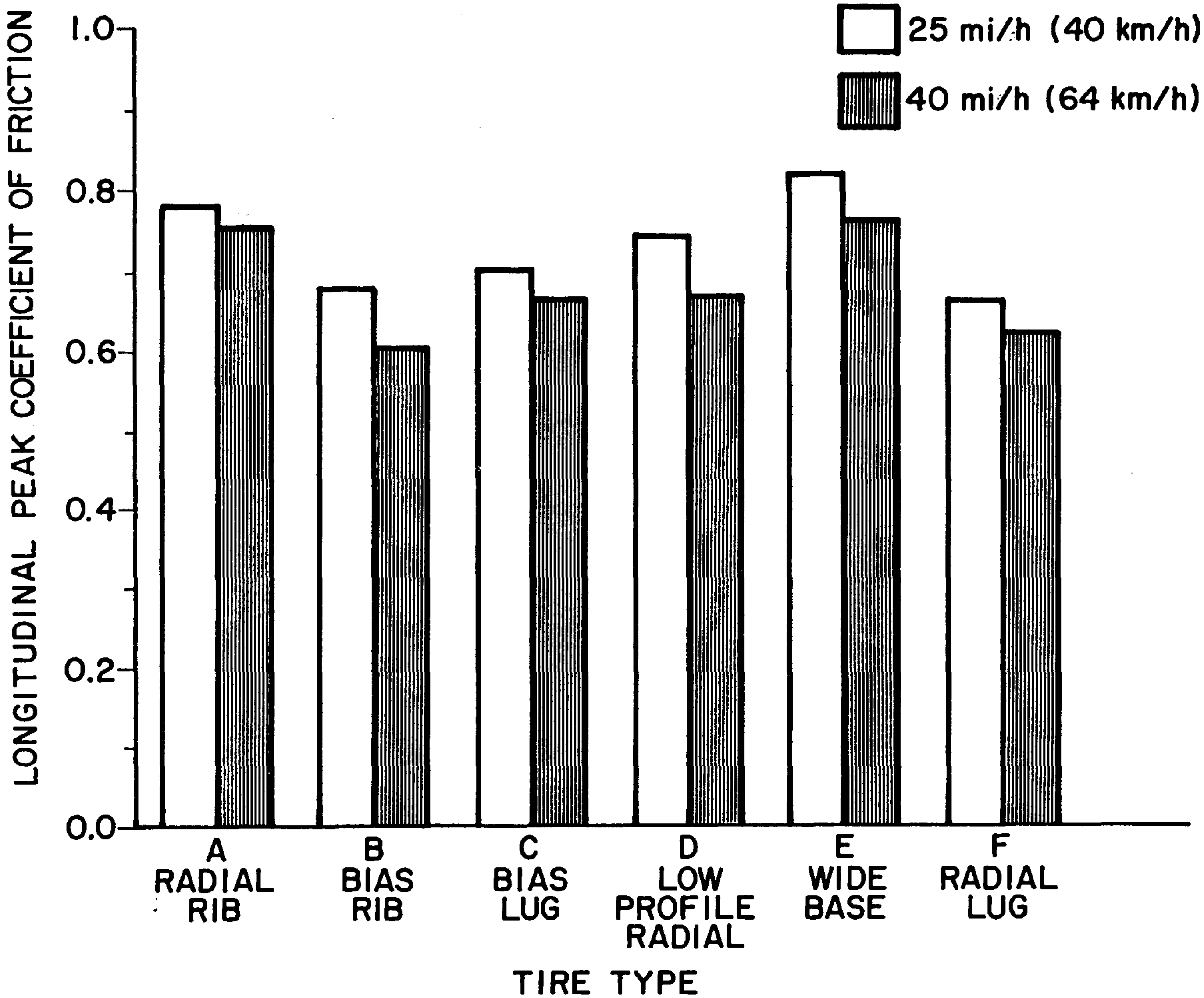

Figure 34. Longitudinal peak coefficients of friction for six tires at 25 and 40 mi/h (40 and 64 km/h).

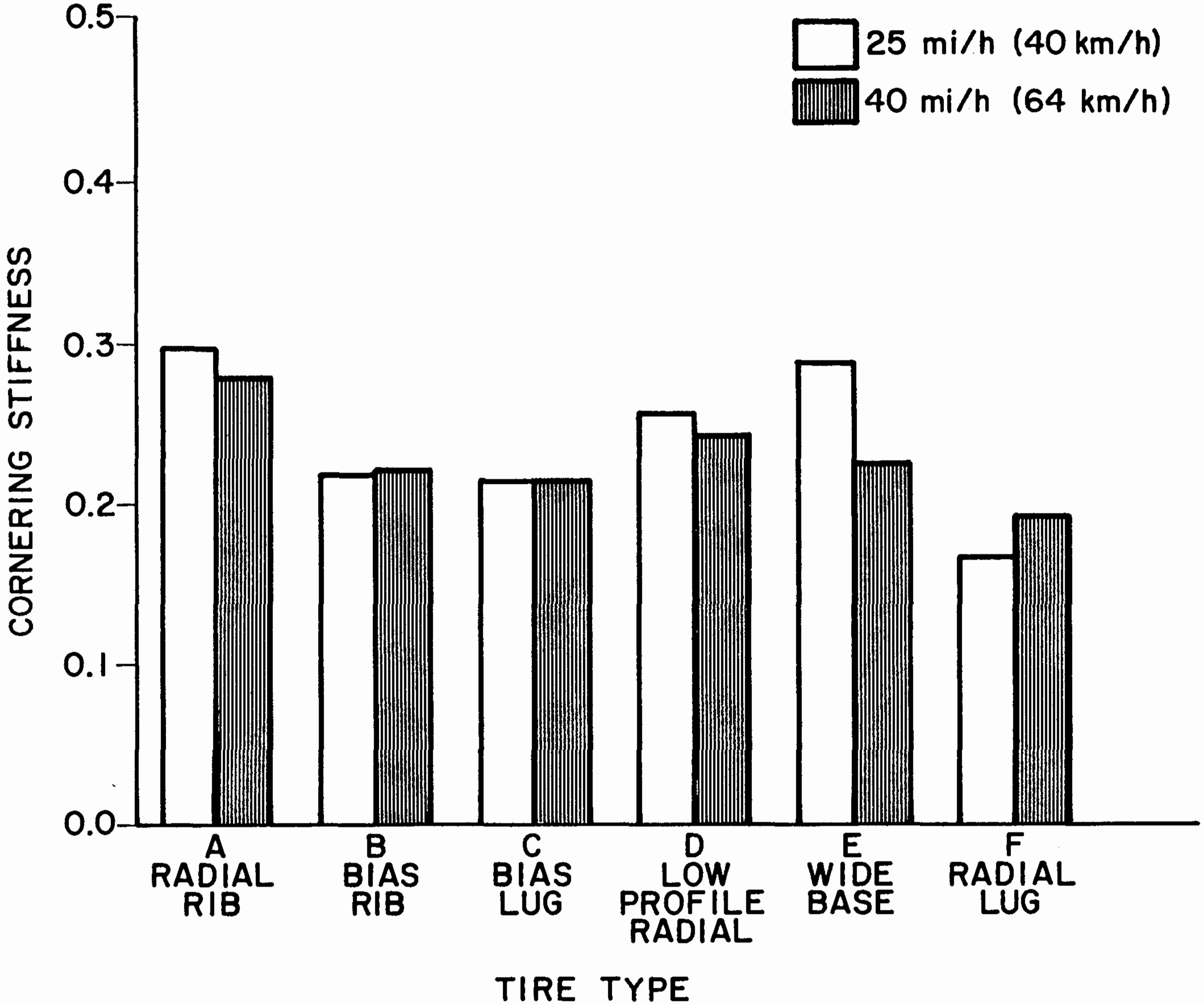

Figure 35. Cornering stiffness for six tires at 25 and 40 mi/h (40 and 64 km/h).

TIRE PRESSURE

Tire inflation pressure will be varied at three levels:

- Manufacturer's recommended pressure (TP1).
- Underinflated (TP2--approximately 20 psi below TP1).
- Overinflated (TP3--approximately 20 psi above TP1).

TIRE BALANCE

All tires will be tested while balanced and unbalanced. The tests with balanced tires will be performed first because testing unbalanced tires may cause serious tire damage. All balanced tires will then be made unbalanced by attaching the same weight (approximately 8 oz [20 g]) to each tire rim. Therefore, this variable will be varied at two levels:

- Balanced tires (TB1).
- Unbalanced tires (TB2).

It should be noted that a truck tire-wheel unit is dynamically balanced on a truck. This is usually done only for the two front tires of a tractor. Some drivers have the tandem-axle wheels balanced also, but this is a very time-consuming operation.

SPEED

The tests will be conducted at three speeds:

- 25 mi/h (40 km/h) (V1).
- 40 mi/h (64 km/h) (V2).
- 55 mi/h (88 km/h) (V3).

In cornering tests, a speed lower than 55 mi/h (88 km/h) may be used as V3 if it is necessary for safety.

LOAD AND LOAD DISTRIBUTION

Four different load situations will be used in the tests:

- Nominal load on trailer, uniformly distributed (L1).
- Trailer unloaded (L2).
- Front of trailer loaded, rear of trailer (tandem axle) unloaded (L3).
- Front of trailer unloaded, rear of trailer loaded (L4).

ANTILOCK BRAKE SYSTEM (ABS)

This variable may occur at two levels only:

- Tractor-semitrailer with ABS (ABS1).
- Tractor-semitrailer without ABS (ABS0). The ABS0 will be achieved by disconnecting the ABS control unit.

BRAKING DISTRIBUTION AMONG AXLES

Distribution of braking force between a vehicle's axles is a significant factor for the vehicle's braking performance if wheel lockup is prohibited.[9] The best braking performance is achieved when braking force distribution is the same as the distribution of maximum tire-pavement friction forces. If the coefficient of friction of all of the vehicle's tires is the same, the distribution of the braking force should match the distribution of the load on the axles. Since this testing program focuses on only one of the axles, the trailer tandem axle, the variable representing braking distribution among axles is not really meaningful. The effect of braking distribution on forces generated by the wheels on the tandem axle can be evaluated relatively from the results of tests including varied load. In conclusion, it is proposed that braking distribution among axles remains the same in all tests.

EXPERIMENTAL DESIGN

In order to design an effective testing program, especially one with a large number of independent test variables, it is necessary to keep in mind the main goals of the research. Implementing a full factorial experimental design, including all possible combinations of the eight test variables, each at their respective number of levels shown in table 5, is not feasible. More importantly, the full factorial design is not necessary to accomplish the objectives of the study. A fractional experimental design consisting of three independent parts is proposed.

The test variables and the levels at which they are to be tested are listed in table 5.

Table 5. Test variables and their levels.

No.	Variable	No. of Levels
1	Suspension Type	2
2	Tire Type	3
3	Pavement	8
4	Tire Pressure	3
5	Tire Balance	2
6	Antilock Brake System	2
7	Speed	3
8	Load	4

PART 1

In accordance with the statement of work for this project, the main objective of the field testing program should be "...to determine the effects of vehicles' suspensions on the braking/cornering performance of the tires being tested for a variety of pavements." The three variables mentioned in this statement, vehicles' suspension, tire type, and pavement type, were considered to be of primary importance to the outcome of this study. Therefore, in part 1 of the testing program, all combinations of the primary variables at their respective numbers of levels should be included in the testing program. The other test variables, which will be considered secondary, will be kept at their baseline levels in part 1. The secondary variables are: tire inflation pressure, tire balance, antilock brake system, speed, load, and load distribution among axles. The baseline values of the secondary variables, which represent typical or average operating conditions, are:

- Tire Pressure: TP1 (manufacturer's recommended pressure).
- Tire Balance: TB1 (balanced).
- Antilock Brake System: ABS0 (conventional brake system).
- Speed: V3 (55 mi/h (88 km/h)).
- Load: L1 (nominal load).

PART 2

In part 2 of the testing program, the effects of the secondary variables on the relationships among the primary variables, suspension, tire, and pavement, will be tested. In order to clearly see these effects, only one secondary variable will be varied in any test run while the other secondary variables will be kept at their baseline values. Table 6 shows the combinations of the secondary variables that will be included in part 2 of the testing program. No interactions among any of the secondary variables will be allowed in this part.

PART 3

In part 3, the effects of interactions among the secondary variables will be evaluated. The results of the tests conducted in this part are of considerably smaller significance for the main goals of the study, and therefore this part may be considered optional. The following combinations of secondary variables are expected to have a more significant effect on the braking and cornering performance of truck tires.

<u>Antilock Brake System and Speed</u>

The effectiveness of the ABS usually increases when tire-pavement friction decreases. When speed increases, friction between tires and pavement decreases, especially when the pavement surface is wet. The performance of the ABS will therefore be tested for truck speed equal to V1 and V2 (in addition to combination no. 5 in table 6).

Table 6. Combinations of tire inflation pressure, speed, and load to be tested in part 2 of the testing program.

No.	TP	TB	ABS	V	L
1*	TP1	TB1	ABS0	V3	L1
2	TP2	TB1	ABS0	V3	L1
3	TP3	TB1	ABS0	V3	L1
4	TP1	TB2	ABS0	V3	L1
5	TP1	TB1	ABS1	V3	L1
6	TP1	TB1	ABS0	V1	L1
7	TP1	TB1	ABS0	V2	L1
8	TP1	TB1	ABS0	V3	L2
9	TP1	TB1	ABS0	V3	L3
10	TP1	TB1	ABS0	V3	L4

*Baseline combination

Tire Balance and Speed

The effect of tire imbalance is typically more pronounced at high speed. To examine this effect more completely, the interaction of tire balance (TB), at two levels, and speed (V), at 3 levels, will be added to the testing program.

Tire Balance and Tire Pressure

There is no doubt that these two variables do interact. However, how significant this interaction is for the role of suspension in truck braking performance, is not clear. By conducting tests in which both TB and tire pressure (TP) are varied, the missing information will be acquired.

Table 7 lists the additional combinations of the secondary variables to be tested in part 3 of the testing program.

Table 7. Combinations of tire inflation pressure, speed, and load to be tested in part 3 of the testing program.

No.	TP	TB	ABS	V	L
1	TP1	TB1	ABS1	V1	L1
2	TP1	TB1	ABS1	V2	L1
3	TP1	TB2	ABS0	V1	L1
4	TP1	TB2	ABS0	V2	L1
5	TP2	TB2	ABS0	V3	L1
6	TP3	TB2	ABS0	V3	L1

The number of all possible combinations of the primary variables is:

$$N_1 = 2 \times 3 \times 8 = 48$$

Forty-eight tests should thus be conducted in part 1. The number of tests for part 2 is:

$$N_2 = (10-1) \times 48 = 432$$

and for part 3:

$$N_3 = 6 \times 48 = 288$$

The number of tests for parts 1 and 2 is:

$$N_{12} = 48 + 432 = 480$$

The total number of combinations for all three parts of the testing program is:

$$N_{123} = 48 + 432 + 288 = 768$$

It is proposed, in order to reduce the total number of tests, that the tests in part 3 be conducted on wet pavements only. Pavement dryness would not constitute a relevant variable in these tests. The number of tests in part 3 would then be reduced to:

$$N_3^* = 6 \times 24 = 144$$

and the total number of tests in parts 1, 2, and 3 would be:

$$N_{123}^* = 48 + 432 + 144 = 624$$

In each testing program, a certain number (usually about 10 percent of the total number of tests) of randomly selected tests should be repeated to validate the results. In this work plan, it is proposed that all tests planned for part 1 involving all combinations of the primary variables be repeated twice, because of the particular importance of these tests. The number of replicate tests would then be:

$$N_r = 2 \times 48 = 96$$

and the total number of tests:

$$\hat{N}_\Sigma = 624 + 96 = 720$$

ADDITIONAL TESTS

PASSENGER CAR TESTS

Passenger car braking distance tests will be conducted on all pavement sections under both wet and dry conditions.

ROUGHNESS MEASUREMENTS

The profile of each pavement test section will be measured and the roughness index calculated at the beginning of the testing program, before the first test, and after the last test on each day of testing.

SKID RESISTANCE TESTS

Standard ASTM E 274 skid resistance tests will be performed before the first test and after the last test on each day of testing, in order to monitor variations of skid resistance of the test surfaces.

TESTING PROCEDURES

Test tires are to be mounted on both the leading and trailing axles of the tandem trailer suspension, so that all of the tires on the test suspension are the same type. All test tires should be broken in by running for a distance of 50 mi (80 km) at a speed of 55 mi/h (88 km/h) and load level L1.

The roughness of the test section will be measured at the beginning and the end of each testing day. Roughness will be measured according to "Standard Practice for Simulating Vehicular Traveled Surface."[11] Likewise, skid resistance will also be measured at the beginning and end of each testing day using an ASTM E 274 skid resistance tester. Skid resistance will only be measured twice a day because it is measured on wet pavement, and since many of the tests will be run on dry pavement, a great deal of time would be wasted allowing the pavement to dry between tests if skid resistance were measured in between tests.

The following is a general procedure which would be used for each test:

1. At the start of each testing sequence, the instrumentation and data acquisition system should be checked to ensure that everything is functioning properly.
2. Make sure all test variables are at the proper values.

3. Before each test sequence, the tires should be warmed up by running 6 mi (10 km) at 50 mi/h (80 km/h) at the test load and inflation pressure. Following the warm-up, tire inflation pressure should be checked and adjusted to the proper value if necessary. Tires should also be checked for damage.

4. Also before each test sequence, make one stop from test speed to warm up the brakes. This will help maintain a constant brake temperature for all runs.

5. Run the test by bringing the truck to the required speed ahead of the test section. Apply the brakes at the beginning of the test section, which should be clearly marked with traffic cones on both sides of the pavement or by lines painted across the pavement, and bring the truck to a rapid controlled stop, that is, as quickly as possible without losing lateral stability or locking any of the wheels.

6. Record the braking distance.

7. Check that all test data have been recorded and stored by the computer data acquisition system.

Specific details of the testing procedure should be established by the research group performing the testing program according to the approved plan of tests. Important practical and theoretical aspects of truck tire testing are discussed in "Measurements of the Longitudinal and Lateral Traction Properties of Truck Tires" and "An Evaluation of Methods to Investigate Truck Tire Wet Traction."[5,12] Also, an NHTSA Tire Task Force is currently active in developing a standard tire testing procedure. The results of the Task Force work should be carefully reviewed when establishing the final testing procedure.

DATA STORAGE, RETRIEVAL, AND ANALYSIS

The test variables to be measured and recorded during the test runs are listed in table 8. The tire forces will be measured by wheel force transducers mounted on the four outside wheels of the trailer tandem axle. It is assumed that the wheel force transducers have encoders for measuring rotational velocity of the tire.

The measurements should be performed with a computer data acquisition system. There are numerous personal computer-based data acquisition systems with proper process interface boards that can be selected for this application.[13] The range of frequency over which significant harmonic components of tire forces are generated is approximately from 0 to 20 Hz.[14] It is therefore recommended that the sampling frequency of 100 Hz be used in collecting the data. The data should be stored on floppy disks for further processing.

Table 8. Basic measurements.

Variable	Measuring Device	Number of Signals
Tire braking force	Wheel force transducer	4
Tire cornering force	Wheel force transducer	4
Tire load	Wheel force transducer	4
Wheel rotational velocity	Encoder	4
Vehicle speed	Fifth wheel	1
	Total number of measuring speeds	17

The first step in processing the data will be filtering. A low pass digital filter can be used to eliminate high frequency noise, which is likely to contaminate the measuring data. The break frequency of the filter should be 20 Hz. A listing of a Finite Impulse Response (FIR) filter subroutine that can be used here is included in the appendix of this report.

The main objective in the data analysis will be a comparison of tire forces generated under a variety of test conditions. Specific methods to be employed in data analysis will be developed during the initial stages of the testing program. Some of the tire performance parameters that should be considered are:

- Average braking force:

$$\bar{F}_x=(\sum_{i=1}^{N} F_{xi})/N \tag{8}$$

where

N = the number of measurements of the tire braking force covering the braking distance

- Average cornering force:

$$\overline{F}_y = \left(\sum_{i=1}^{N} F_{yi}\right)/N \qquad (9)$$

- Braking distance:

$$BD = \sum_{i=1}^{N} v_i \Delta t \qquad (10)$$

where

v_i = truck speed at time $i\Delta t$

Δt = sampling period

- Dynamic force factor (for braking, cornering, and vertical load forces):[15]

$$DIF = \sqrt{\sum_{i=1}^{N} (F_i - \overline{F}^2/(N-1)\ \overline{F}^2} \qquad (11)$$

Additional methods for data analysis can be applied when initial sets of measurements become available. It is also expected that new, more efficient algorithms of data processing will be developed in a computer simulation study that will be performed in Task 4 of this project.

EQUIPMENT

Two trailers with tandem axles will be used in the testing program. One trailer will have a four-spring suspension and the other will have a walking beam suspension. Four-wheel force transducers will be available for measuring longitudinal, vertical, and lateral tire forces on both ends of each axle in the tandem axle of each trailer. Both trailers shall be equipped with an antilock brake system.

It should be possible to disconnect the ABS and run the trailers with conventional brake systems.

The tractor would be needed for 10 months. The trailers would be needed for 6 months each, assuming that they will be used sequentially, that is, all tests would be conducted on one trailer first and then on the second trailer. It would be better to conduct the tests with both trailers in parallel (rather than in sequence), that is, changing trailers after every series of several tests involving variation of one test variable. However, that would require frequent (as often as once a day) mounting and dismounting of the wheel force transducers, which may be impractical.

For the number of tests proposed in parts 1 and 2, two complete sets of eight tires for a tandem axle, one for each trailer, will be needed. If three types of tires are used, the total number of tires will be 48.

A computer data acquisition system will be used to collect measurement data. The following variables will be measured during each test:

- Tire vertical force (F_z).
- Tire longitudinal force (F_x).
- Tire lateral force (F_y).
- Test tire speed (V_w).
- Truck speed (V_o).

The total number of signals to be measured in each test is 17 (12 tire forces + 4 wheel speeds + 1 truck speed). Typical process interface boards in computer data acquisition systems have 16 input channels. Interface boards with a greater number of input channels are also available but are considerably more expensive. In order to reduce the number of measuring signals, one could consider measuring rotational speeds of only two wheels, one on the leading axle and one on the trailing axle, instead of four wheels. That would reduce the number of input channels needed in the computer data acquisition system to 15.

LEVEL OF EFFORT

It is believed that the successful completion of the proposed testing program would require the following personnel at the estimated level of effort in staff months:

• Mechanical engineer with vehicle suspension and tire-pavement interaction experience	5.0
• Statistician/data analyst	1.0
• Research assistant (mechanical engineering)	6.0
• Technician	5.0
• Truck driver	7.0
• Technical editor	1.0

The estimated period of performance is 13 months, assuming that parts 1, 2, and 3 of the testing program will be conducted. If only parts 1 and 2 were to be conducted, the estimated period of performance would be 11 months and the levels of effort given above would be reduced by approximately 20 percent. The proposed scheduled of work is shown in table 9.

Table 9. Work schedule.

		1	2	3	4	5	6	7	8	9	10	11	12	13
1.	Equipment Preparation	X	X											
2.	Preliminary Tests			X	X									
3.	Part 1 of Testing Program				X	X								
4.	Part 2 of Testing Program					X	X	X	X	X				
5.	Part 3 of Testing Program									X	X	X		
6.	Data Analysis					X	X	X	X	X	X	X	X	
7.	Report										X	X	X	X

4. EFFECTS OF TRUCK SUSPENSION CHARACTERISTICS

This chapter describes the computer simulation phase of the study. The objective of this phase was to investigate the dynamic interactions among the tires, the truck, and the road by running a series of computer simulations in which tire properties, truck properties, and the road surface roughness were varied.

COMPUTER SIMULATION PROGRAM

The computer program used for all of the simulation runs is a slightly modified version of the T3DRS, Phase 4 truck handling and braking simulation program, which is a three-dimensional dynamic simulation program written expressly for truck handling and braking studies.[16] The equations of motion were derived using Newtonian mechanics, and these equations are numerically integrated within the T3DRS, Phase 4 program.

The program can simulate various heavy truck configurations including straight trucks, bobtail tractors, and tractors with one, two, or three trailers. The simulation model is very detailed and includes tire models, axle and suspension models, both conventional and antilock brake system models, torsional frame stiffness, and payload placement and weight. Linear or nonlinear tire, spring, and brake models may be used. Steering may be directly controlled by an input table containing steering wheel angle versus time, or a driver model in the program may be used to follow a path defined by an input table of x,y coordinates.

The University of Michigan Transportation Research Institute conducted tests that verified the results obtained with T3DRS, Phase 4. Several maneuvers were simulated using T3DRS, Phase 4 and the results compared to actual test data. A complete discussion and presentation of the verification study can be found in the technical report Truck and Tractor Trailer Dynamic Response Simulation.[17] Another verification of the program is contained in A Comparison of Various Computer Simulation Models for Predicting the Directional Response of Articulated Vehicles.[18]

Preceding page blank

A computer subroutine was used to define the road surface for the T3DRS, Phase 4 program. The subroutine used for this project was a look-up routine that uses a road profile table to calculate the profile of the road at any desired point. The profile table consists of two columns of numbers, one for the left tire track and one for the right tire track, that are the elevations of the road surface at 6-in (0.15-m) intervals. A quadratic interpolation routine provides a continuous profile between points and is used to calculate the longitudinal slope of the road at any point.

The T3DRS, Phase 4 program was also modified to include unbalanced tire effects. An unbalanced tire term was added to the equations of motion to simulate an unbalanced weight added to the front left trailer wheel. The term illustrated by equation 12 is added to the vertical and roll axle equations:

$$F = mr\omega^2 \sin \theta \tag{12}$$

The term illustrated by equation 13 is added to the trailer body longitudinal and yaw equations:

$$F = mr\omega^2 \cos \theta \tag{13}$$

where

- m - unbalanced mass
- r - radius to the unbalanced mass (the wheel radius)
- ω - wheel angular velocity
- θ - wheel rotational angle with 0° forward

WORK PLAN

Following the general work plan described in chapter 3, this phase of the study was separated into two parts. In part 1, researchers investigated the primary test variables: suspension type, tire type, and pavement type. All combinations of the primary variables were simulated in part 1, with the secondary variables held constant at their baseline values. Part 2 involved determining the effects of the secondary variables. In this part, the primary variables were held constant at baseline values while the secondary variables were changed one at a time.

PRIMARY VARIABLES

- Two types of tandem suspensions:

  - Four spring.
  - Walking beam.

- Three types of tires from the group tested in the tire traction field tests:

  - Bias-ply rib.
  - Radial rib.
  - Low-profile radial.

  These tires were chosen because (1) they are widely used; (2) they are commonly used on all axles; and (3) they exhibited a significant range of performance characteristics in the traction measurements.

- Four pavement types:

  - Tangent section, low roughness.
  - Tangent section, high roughness.
  - Nontangent section, low roughness.
  - Nontangent section, high roughness.

  These sections were simulated both wet and dry for a total of eight road surfaces.

SECONDARY VARIABLES

- Three levels of tire pressure:

  - Manufacturer's recommended pressure (baseline value).
  - 20 psi below recommended pressure.
  - 20 psi above recommended pressure.

- Two levels of tire balance:

  - Balanced tires (baseline level).
  - One unbalanced tire.

- Three truck speeds:

  - 25 mi/h (40 km/h).
  - 40 mi/h (64 km/h).
  - 55 mi/h (88 km/h) (baseline speed).

- Four different load configurations:

  - Balanced, uniformly distributed load (baseline level).
  - Trailer unloaded.
  - Front of trailer loaded, rear unloaded.
  - Front of trailer unloaded, rear loaded.

- Two types of braking systems:

  - Conventional brakes (baseline braking system).
  - Antilock brakes.

INPUT DATA

Table 10 is the T3DRS, Phase 4 input data listing for one run. The basic truck used is a three-axle conventional highway tractor with a 48-ft (14.5-m), 2-axle trailer. The parameters are not for a specific model but are a

Table 10. T3DRS, Phase 4 input data listing.

HSRI/MVMA BRAKING AND HANDLING SIMULATION OF TRUCKS, TRACTOR-SEMITRAILERS, DOUBLES, AND TRIPLES - PHASE 4.   INPUT PAGE NO. 2

RUN IA1 INPUT DATA LIST

TRACTOR PARAMETERS

WHEELBASE - DISTANCE FROM FRONT AXLE TO CENTER OF REAR SUSPENSION	240.00
BASE VEHICLE CURB WEIGHT ON FRONT SUSPENSION (LB)	6959.00
BASE VEHICLE CURB WEIGHT ON REAR SUSPENSION (LB)	6879.00
SPRUNG MASS CG HEIGHT (IN. ABOVE GROUND)	40.00
SPRUNG MASS ROLL MOMENT OF INERTIA (IN-LB-SEC**2)	30139.00
SPRUNG MASS PITCH MOMENT OF INERTIA (IN-LB-SEC**2)	400980.00
SPRUNG MASS YAW MOMENT OF INERTIA (IN-LB-SEC**2)	400980.00
PAYLOAD WEIGHT (LB)	0.00
*** ZERO ENTRY INDICATES NO PAYLOAD ***	
*** FIVE PAYLOAD DESCRIPTION PARAMETERS ARE NOT ENTERED ***	
FIFTH WHEEL LOCATION (IN. AHEAD OF REAR SUSP. CENTER)	0.00
FIFTH WHEEL HEIGHT ABOVE GROUND (IN)	48.00
TRACTOR FRAME STIFFNESS (IN-LB/DEG)	50000.00
TRACTOR FRAME TORSIONAL AXIS HEIGHT ABOVE GROUND (IN)	36.00

TRACTOR FRONT SUSPENSION AND AXLE PARAMETERS	LEFT SIDE	RIGHT SIDE
SUSPENSION SPRING RATE (LB/IN/SIDE/AXLE)	1132.00	1132.00
SUSPENSION VISCOUS DAMPING (LB-SEC/IN/SIDE/AXLE)	15.00	15.00
COULOMB FRICTION (LB/SIDE/AXLE)	150.00	150.00

AXLE ROLL MOMENT OF INERTIA (IN-LB-SEC**2)	3719.00
ROLL CENTER HEIGHT (IN. ABOVE GROUND)	23.00
ROLL STEER COEFFICIENT (DEG. STEER/DEG. ROLL)	0.00
AUXILIARY ROLL STIFFNESS (IN-LB/DEG/AXLE)	1500.00
LATERAL DISTANCE BETWEEN SUSPENSION SPRINGS (IN)	32.00
TRACK WIDTH (IN)	80.00
UNSPRUNG WEIGHT (LB)	1200.00
STEERING GEAR RATIO (DEG STEERING WHEEL/DEG ROAD WHEEL)	0.00
*** NEGATIVE OR ZERO ENTRY INDICATES NO STEERING SYSTEM ***	
*** STEERING SYSTEM PARAMETERS NOT TO BE ENTERED ***	

TRACTOR FRONT TIRES AND WHEELS	LEFT SIDE	RIGHT SIDE
CORNERING STIFFNESS (LB/DEG/TIRE)	695.00	695.00
LONGITUDINAL STIFFNESS (LB/SLIP/TIRE)	-1.00	-1.00
*** NEGATIVE ENTRY INDICATES TABLE ENTERED ***		
*** ECHO WILL APPEAR ON TABLE INDEX PAGE ***		
CAMBER STIFFNESS (LB/DEG/TIRE)	0.00	0.00
ALIGNING MOMENT (IN-LB/DEG/TIRE)	1200.00	1200.00
TIRE SPRING RATE (LB/IN/TIRE)	4520.00	4520.00
TIRE LOADED RADIUS (IN)	19.50	19.50
POLAR MOMENT OF INERTIA (IN-LB-SEC**2/WHEEL)	103.00	103.00

Table 10. T3DRS, Phase 4 input data listing (Continued).

HSRI/MVMA BRAKING AND HANDLING SIMULATION OF TRUCKS, TRACTOR-SEMITRAILERS, DOUBLES, AND TRIPLES - PHASE 4. INPUT PAGE NO. 3

RUN 1A1 INPUT DATA LIST

TRACTOR REAR SUSPENSION AND AXLE PARAMETERS	LEADING TANDEM AXLE			TRAILING TANDEM AXLE	
	LEFT SIDE	RIGHT SIDE		LEFT SIDE	RIGHT SIDE
SUSPENSION KEY - 0 INDICATES SINGLE AXLE, 1 INDICATES FOUR SPRING, 2 WALKING BEAM			2		
TANDEM AXLE SEPARATION (IN BETWEEN LEADING AND TRAILING AXLES)			51.10		
STATIC LOAD TRANSFER (PERCENT LOAD ON LEAD AXLE)			50.00		
DYNAMIC LOAD TRANSFER (% BRAKE TORQUE REACTED AS TANDEM AXLE LOAD TRANSFER)			0.00		
SUSPENSION SPRING RATE (LB/IN/SIDE/AXLE)	7200.00	7200.00		7200.00	7200.00
SUSPENSION VISCOUS DAMPING (LB-SEC/IN/SIDE/AXLE)	15.00	15.00		15.00	15.00
COULOMB FRICTION (LB/SIDE/AXLE)	500.00	500.00		500.00	500.00
AXLE ROLL MOMENT OF INERTIA (IN-LB-SEC**2)	4458.00				4458.00
ROLL CENTER HEIGHT (IN. ABOVE GROUND)	29.00				29.00
ROLL STEER COEFFICIENT (DEG. STEER/DEG. ROLL)	0.00				0.00
AUXILIARY ROLL STIFFNESS (IN-LB/DEG/AXLE)	6000.00				6000.00
LATERAL DISTANCE BETWEEN SUSPENSION SPRINGS (IN)	38.00				38.00
TRACK WIDTH (IN)	72.63				72.63
UNSPRUNG WEIGHT (LB)	2300.00				2300.00

TRACTOR REAR TIRES AND WHEELS	LEFT SIDE	RIGHT SIDE
DUAL TIRE SEPARATION (IN)	13.00	13.00
CORNERING STIFFNESS (LB/DEG/TIRE)	695.00	695.00
LONGITUDINAL STIFFNESS (LB/SLIP/TIRE)	-2.00	-2.00
*** NEGATIVE ENTRY INDICATES TABLE ENTERED ***		
*** ECHO WILL APPEAR ON TABLE INDEX PAGE ***		
CAMBER STIFFNESS (LB/DEG/TIRE)	0.00	0.00
ALIGNING MOMENT (IN-LB/DEG/TIRE)	1200.00	1200.00
TIRE SPRING RATE (LB/IN/TIRE)	4520.00	4520.00
TIRE LOADED RADIUS (IN)	19.50	19.50
POLAR MOMENT OF INERTIA (IN-LB-SEC**2/WHEEL)	103.00	103.00

TRACTOR FRONT BRAKES	LEFT SIDE	RIGHT SIDE
TIME LAG (SEC)	0.0500	0.0500
RISE TIME (SEC)	0.2500	0.2500
BRAKE TORQUE (IN-LB/PSI/BRAKE)	800.0000	800.0000
BRAKE HYSTERESIS KEY: 0 ENTRY INDICATES BRAKE HYSTERESIS OPTION NOT IN USE ON VEHICLE TRAIN		0
BRAKE PROPORTIONING KEY: 0 ENTRY INDICATES BRAKE PROPORTIONING OPTION NOT IN USE ON VEHICLE TRAIN		0

TRACTOR REAR BRAKES	LEADING TANDEM AXLE		TRAILING TANDEM AXLE	
	LEFT SIDE	RIGHT SIDE	LEFT SIDE	RIGHT SIDE
TIME LAG (SEC)	0.0750	0.0750	0.0750	0.0750
RISE TIME (SEC)	0.2500	0.2500	0.2500	0.2500
BRAKE TORQUE (IN-LB/PSI/BRAKE)	1500.0000	1500.0000	1500.0000	1500.0000

Table 10. T3DRS, Phase 4 input data listing (Continued).

HSRI/MVMA BRAKING AND HANDLING SIMULATION OF TRUCKS, TRACTOR-SEMITRAILERS, DOUBLES, AND TRIPLES - PHASE 4. INPUT PAGE NO. 4

RUN 1A1 INPUT DATA LIST

TRAILER NO. 1 PARAMETERS

WHEELBASE - DISTANCE FROM KINGPIN TO CENTER OF REAR SUSPENSION (IN)	486.00
BASE VEHICLE KINGPIN STATIC LOAD (LB)	5237.00
BASE VEHICLE CURB WEIGHT ON REAR SUSPENSION (LB)	8562.00
SPRUNG MASS CG HEIGHT (IN. ABOVE GROUND)	71.00
SPRUNG MASS ROLL MOMENT OF INERTIA (IN-LB-SEC**2)	80000.00
SPRUNG MASS PITCH MOMENT OF INERTIA (IN-LB-SEC**2)	1328867.00
SPRUNG MASS YAW MOMENT OF INERTIA (IN-LB-SEC**2)	1328867.00
PAYLOAD WEIGHT (LB)	52363.00
PAYLOAD DISTANCE AHEAD OF REAR SUSPENSION CENTER(IN)	246.82
PAYLOAD CG HEIGHT (IN. ABOVE GROUND)	90.00
PAYLOAD ROLL MOMENT OF INERTIA(IN-LB-SEC**2)	151074.00
PAYLOAD PITCH MOMENT OF INERTIA(IN-LB-SEC**2)	3425480.00
PAYLOAD YAW MOMENT OF INERTIA(IN-LB-SEC**2)	3465907.00

TRAILER NO. 1 REAR SUSPENSION AND AXLE PARAMETERS

	LEADING TANDEM AXLE			TRAILING TANDEM AXLE	
	LEFT SIDE	RIGHT SIDE		LEFT SIDE	RIGHT SIDE
SUSPENSION KEY - 0 INDICATES SINGLE AXLE, 1 INDICATES FOUR SPRING, 2 WALKING BEAM			1		
TANDEM AXLE SEPARATION (IN BETWEEN LEADING AND TRAILING AXLES)			48.00		
STATIC LOAD TRANSFER (PERCENT LOAD ON LEAD AXLE)			50.00		
DYNAMIC LOAD TRANSFER (% BRAKE TORQUE REACTED AS TANDEM AXLE LOAD TRANSFER)			-13.00		
SUSPENSION SPRING RATE (LB/IN/SIDE/AXLE)	7500.00	7500.00		7500.00	7500.00
SUSPENSION VISCOUS DAMPING (LB-SEC/IN/SIDE/AXLE)	15.00	15.00		15.00	15.00
COULOMB FRICTION (LB/SIDE/AXLE)	1000.00	1000.00		1000.00	1000.00
AXLE ROLL MOMENT OF INERTIA (IN-LB-SEC**2)	4100.00			4100.00	
ROLL CENTER HEIGHT (IN. ABOVE GROUND)	29.00			29.00	
ROLL STEER COEFFICIENT (DEG. STEER/DEG. ROLL)	0.00			0.00	
AUXILIARY ROLL STIFFNESS (IN-LB/DEG/AXLE)	10000.00			10000.00	
LATERAL DISTANCE BETWEEN SUSPENSION SPRINGS (IN)	44.00			44.00	
TRACK WIDTH (IN)	78.00			78.00	
UNSPRUNG WEIGHT (LB)	1500.00			1500.00	

TRAILER NO. 1 REAR TIRES AND WHEELS

	LEADING TANDEM AXLE		TRAILING TANDEM AXLE	
	LEFT SIDE	RIGHT SIDE	LEFT SIDE	RIGHT SIDE
DUAL TIRE SEPARATION (IN)	13.00	13.00	13.00	13.00
CORNERING STIFFNESS (LB/DEG/TIRE)	695.00	695.00	695.00	695.00
LONGITUDINAL STIFFNESS (LB/SLIP/TIRE)	-4.00	-4.00	-5.00	-5.00
*** NEGATIVE ENTRY INDICATES TABLE ENTERED ***				
*** ECHO WILL APPEAR ON TABLE INDEX PAGE ***				
CAMBER STIFFNESS (LB/DEG/TIRE)	0.00	0.00	0.00	0.00
ALIGNING MOMENT (IN-LB/DEG/TIRE)	1200.00	1200.00	1200.00	1200.00
TIRE SPRING RATE (LB/IN/TIRE)	4520.00	4520.00	4520.00	4520.00
TIRE LOADED RADIUS (IN)	19.50	19.50	19.50	19.50
POLAR MOMENT OF INERTIA (IN-LB-SEC**2/WHEEL)	103.00	103.00	103.00	103.00

Table 10. T3DRS, Phase 4 input data listing (Continued).

RUN 1A1 INPUT DATA LIST

TRAILER NO. 1 REAR BRAKES

	LEADING TANDEM AXLE		TRAILING TANDEM AXLE	
	LEFT SIDE	RIGHT SIDE	LEFT SIDE	RIGHT SIDE
TIME LAG (SEC)	0.1750	0.1750	0.1750	0.1750
RISE TIME (SEC)	0.2500	0.2500	0.2500	0.2500
BRAKE TORQUE (IN-LB/PSI/BRAKE)	1500.0000	1500.0000	1500.0000	1500.0000

ANTILOCK KEY: 1 INDICATES ANTILOCK WILL BE USED 0 ollection of typical parameters compiled for previous projects. The truck, therefore, represents an average truck that could commonly be found on U.S. highways. The test variables for this project were chosen as described below.

TIRE MODEL

The longitudinal friction data measured earlier in this project were used in look-up table form in the simulation program for the longitudinal tire models. The experimental results are for wet pavement. The dry pavement tables were obtained by assuming equal peak friction values for both wet and dry, and equal peak and slide friction values for dry pavement. Inflation pressures were assumed to have no effect on longitudinal friction for the operating ranges used in this study.[5] Plots of the coefficient of braking friction versus slip are shown in figures 36 through 47.

A linear vertical tire stiffness model was used in the simulation program. The spring stiffnesses were determined from Goodyear experimental data for an 11-22.5 G bias-ply tire and an 11R22.5 G radial tire. The conventional and low-profile radial tires were assumed to have equal vertical stiffnesses. The vertical tire stiffnesses were changed to simulate underinflation and overinflation based on the Goodyear data, which include results for recommended inflation pressure, 25 psi overinflation, and 25 psi underinflation. The Goodyear data were proportioned to obtain stiffnesses for 20 psi overinflation and underinflation.

The lateral tire model was also linear. Cornering stiffnesses are typical values obtained from A Factbook of the Mechanical Properties of the Components for Single-Unit and Articulated Heavy Trucks for average bias-ply and radial tires.[19] The conventional and low-profile radial tires were assumed to have equal cornering stiffnesses. Inflation pressure was assumed to have no effect on cornering stiffness for the operating ranges reported in the "Factbook."[19]

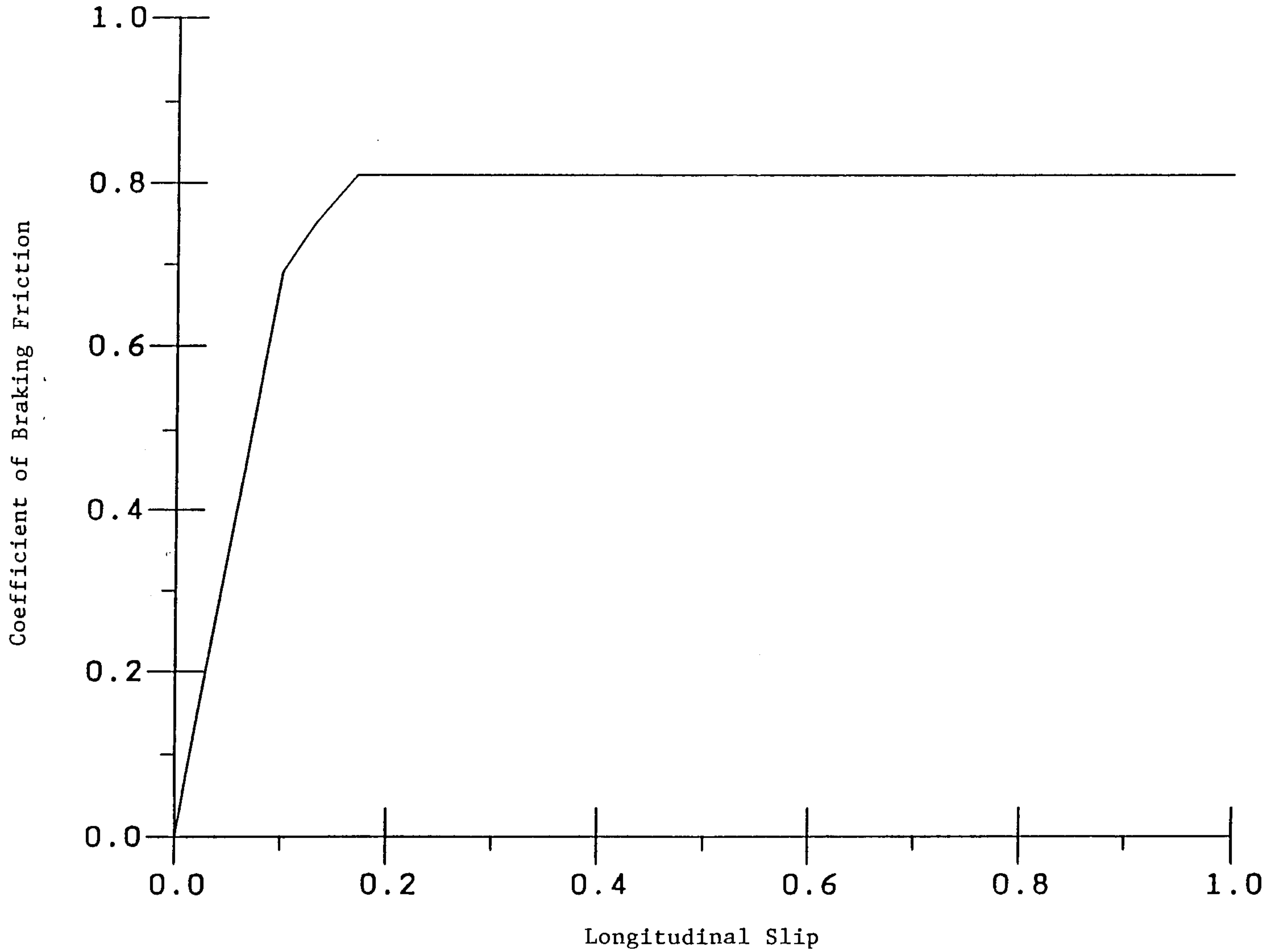

Figure 36. Coefficient of braking friction versus longitudinal slip for the radial rib tire on dry pavement at 25 mi/h (40 km/h).

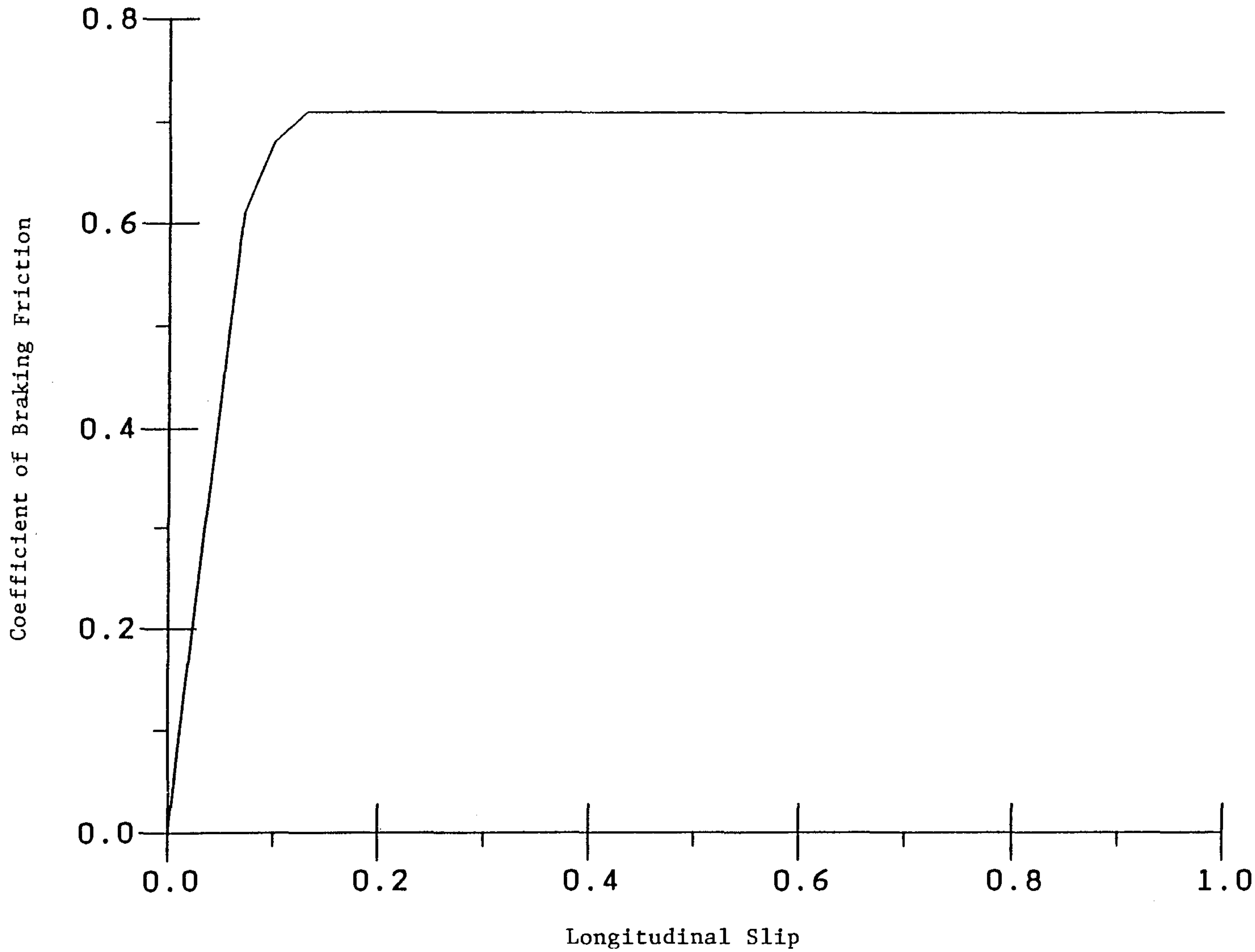

Figure 37. Coefficient of braking friction versus longitudinal slip for the bias rib tire on dry pavement at 25 mi/h (40 km/h).

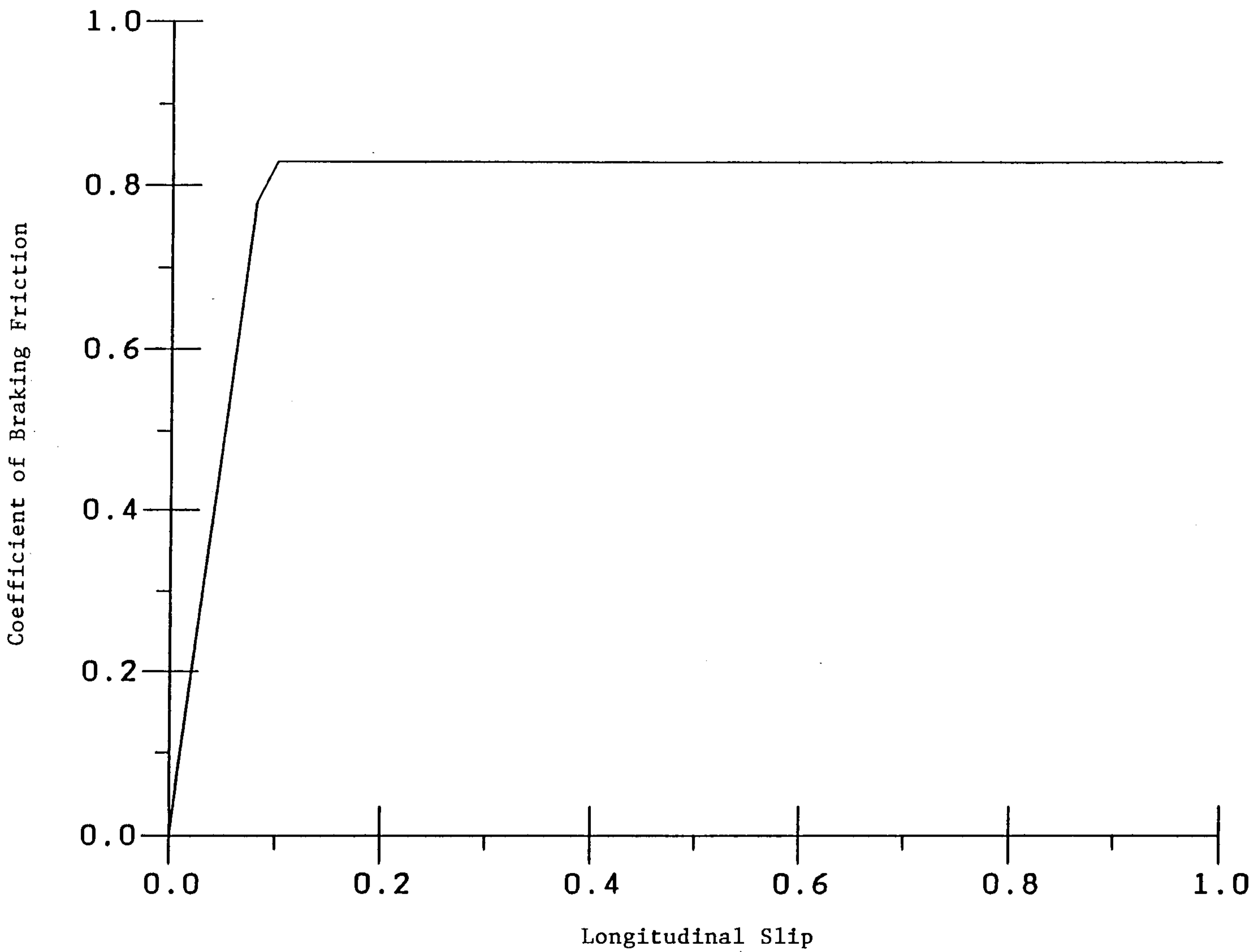

Figure 38. Coefficient of braking friction versus longitudinal slip for the low-profile radial tire on dry pavement at 25 mi/h (40 km/h).

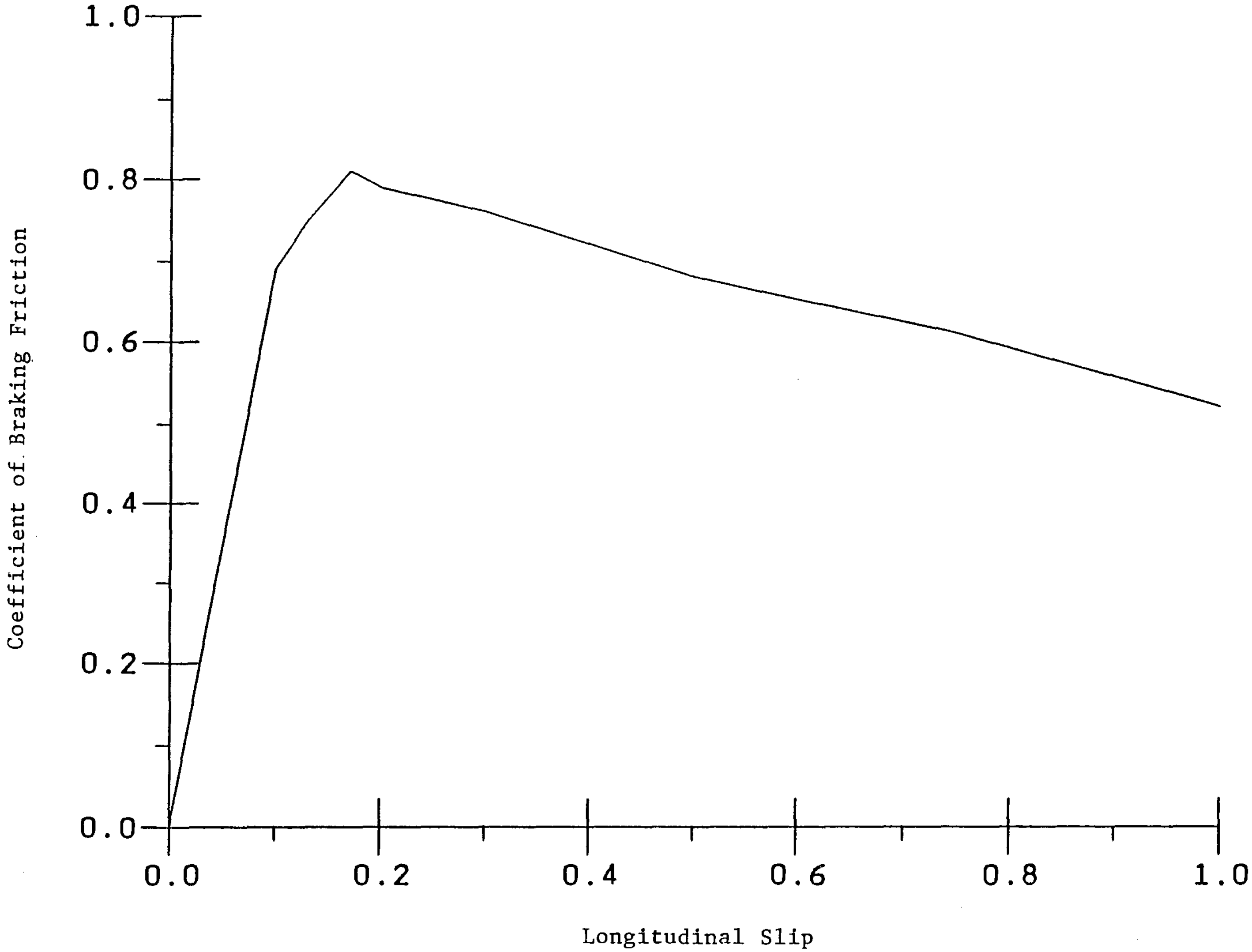

Figure 39. Coefficient of braking friction versus longitudinal slip for the radial rib tire on wet pavement at 25 mi/h (40 km/h).

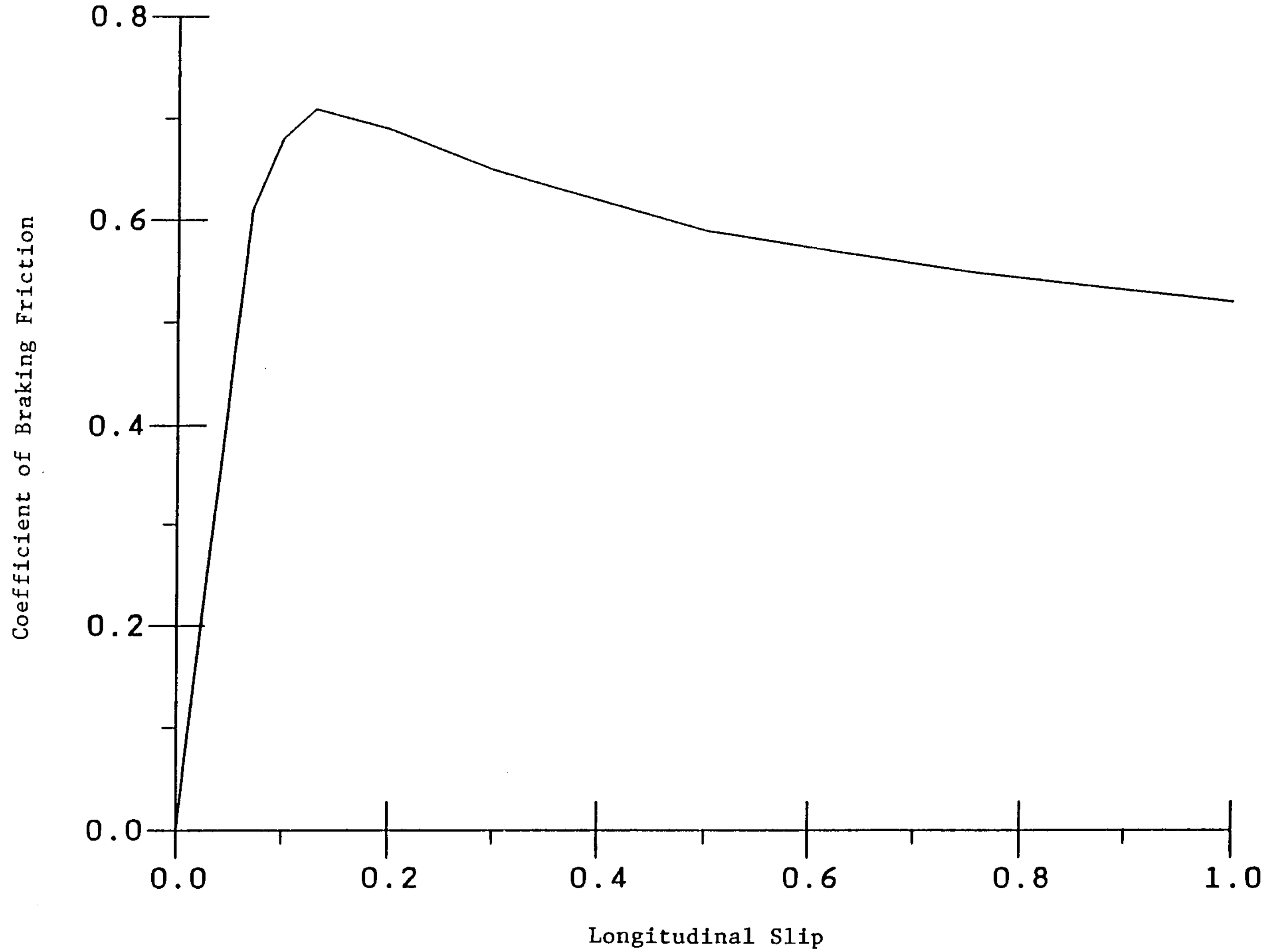

Figure 40. Coefficient of braking friction versus longitudinal slip for the bias rib tire on wet pavement at 25 mi/h (40 km/h).

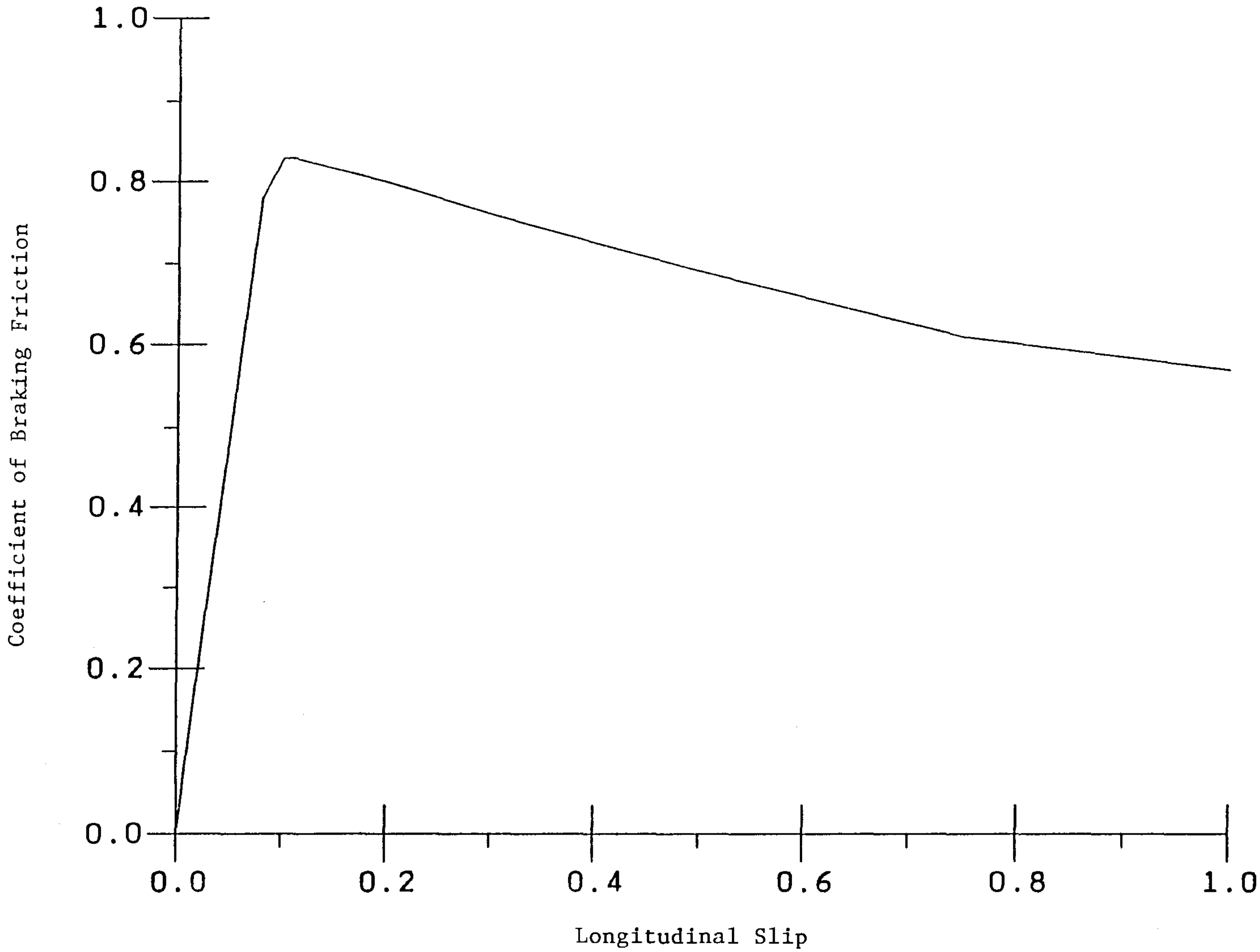

Figure 41. Coefficient of braking friction versus longitudinal slip for the low-profile radial tire on wet pavement at 25 mi/h (40 km/h).

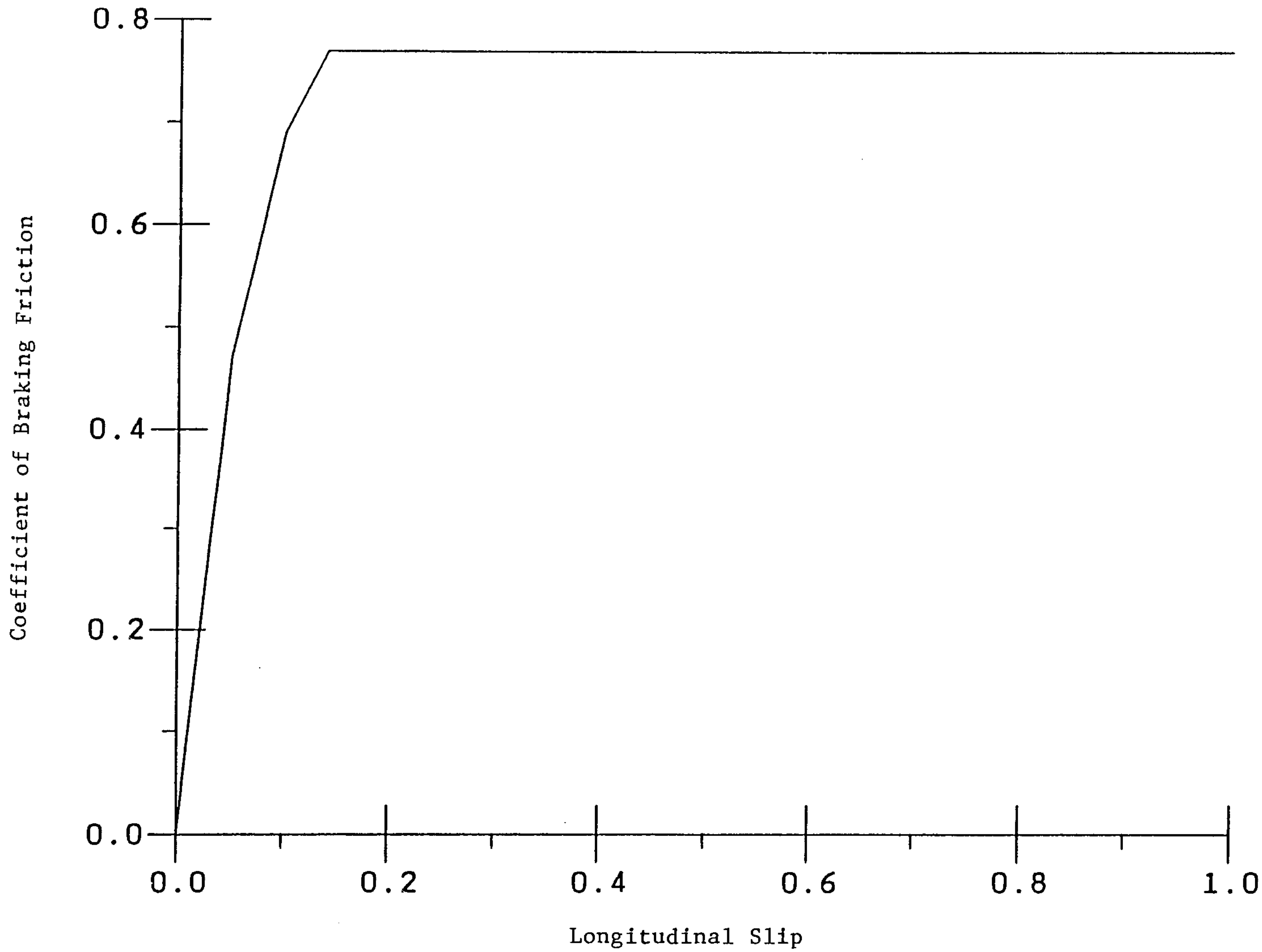

Figure 42. Coefficient of braking friction versus longitudinal slip for the radial rib tire on dry pavement at 40 mi/h (64 km/h).

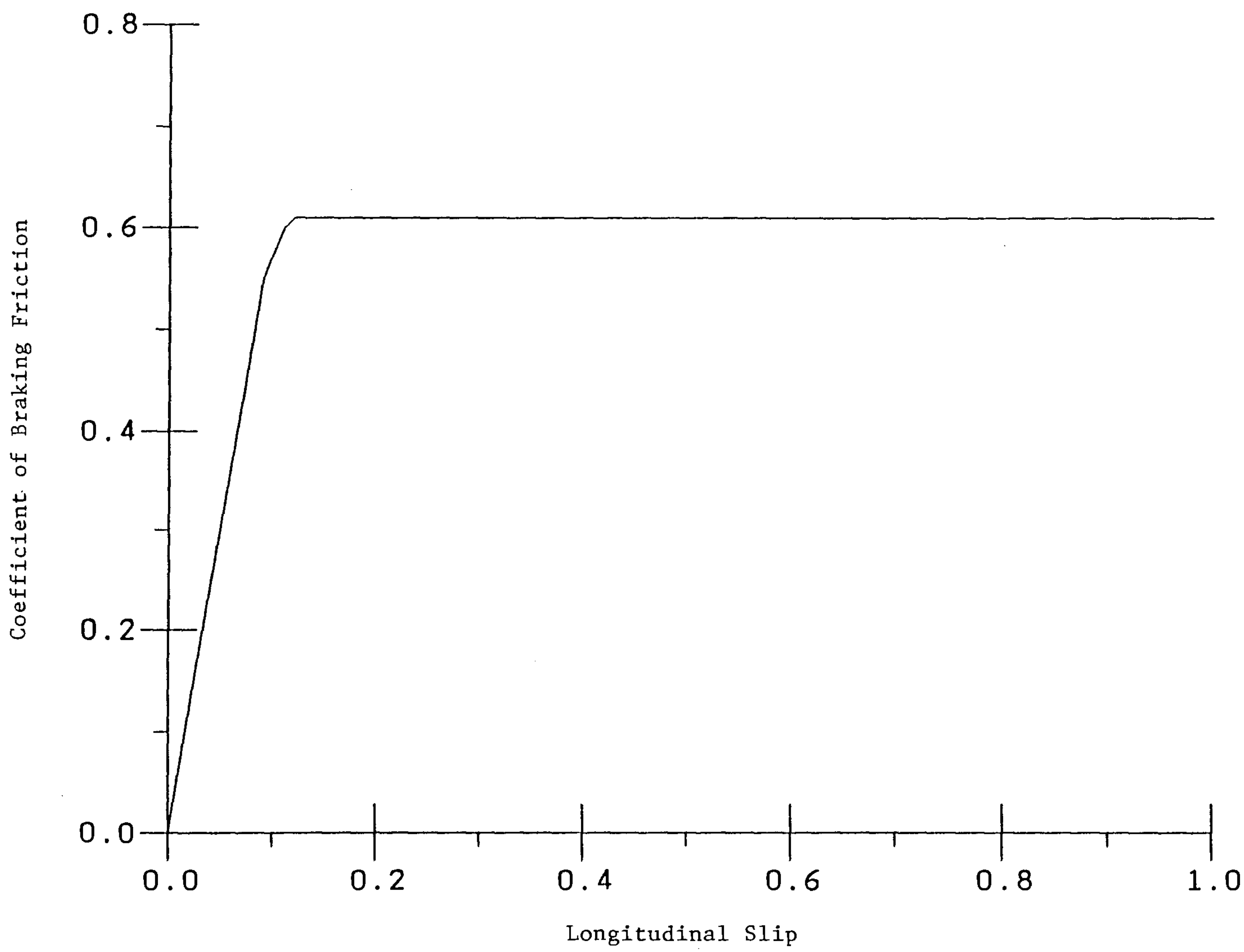

Figure 43. Coefficient of braking friction versus longitudinal slip for the bias rib tire on dry pavement at 40 mi/h (64 km/h).

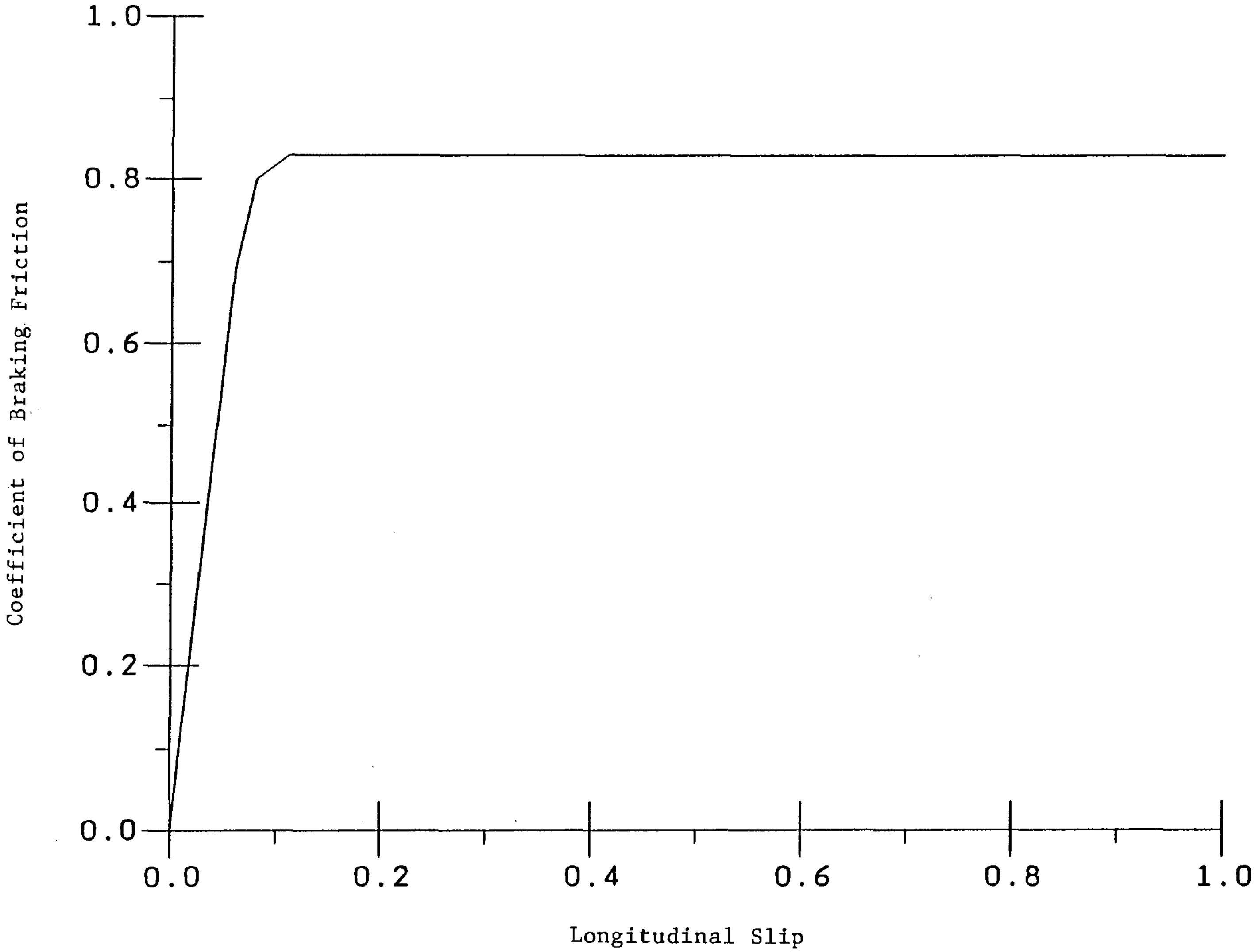

Figure 44. Coefficient of braking friction versus longitudinal slip for the low-profile radial tire on dry pavement at 40 mi/h (64 km/h).

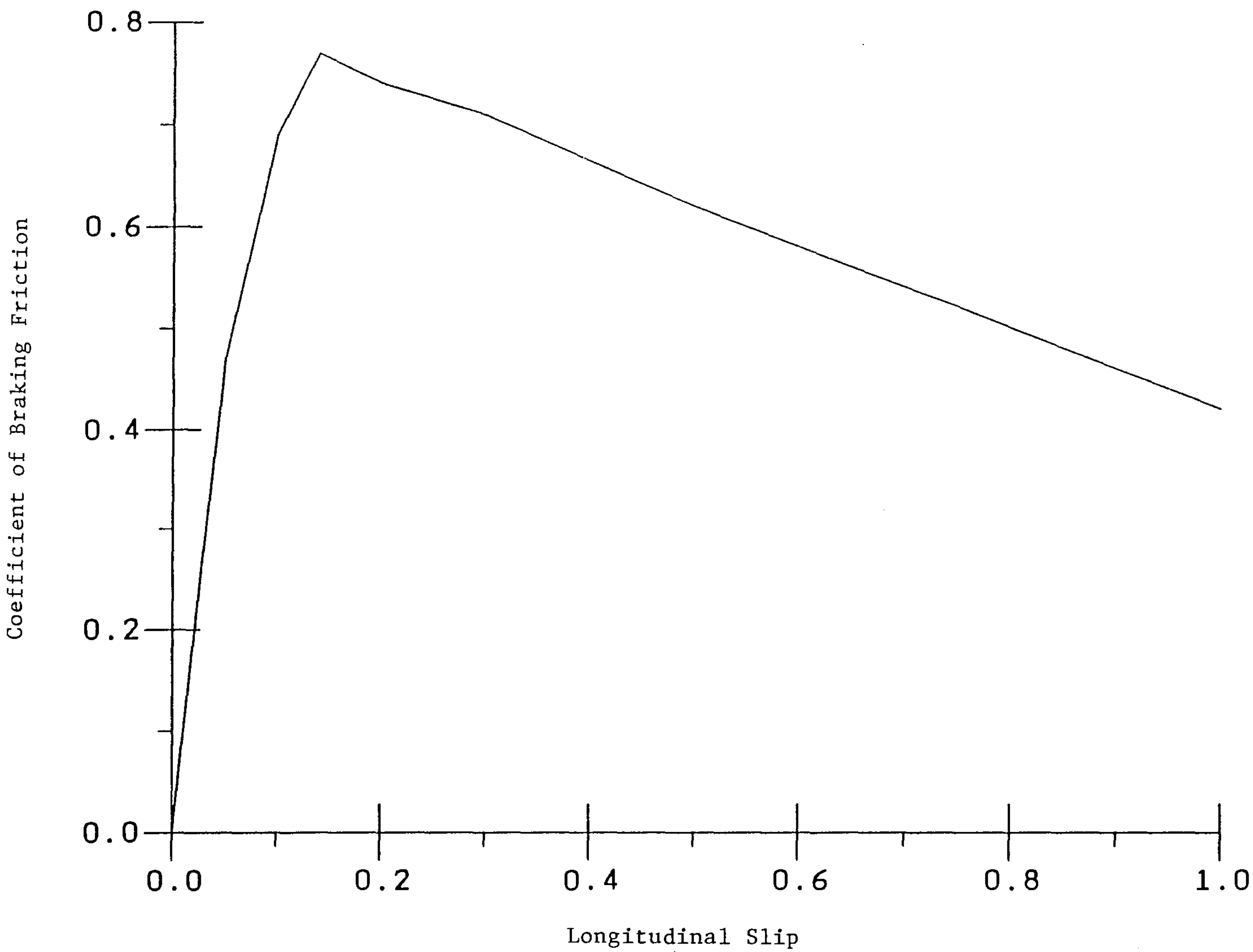

Figure 45. Coefficient of braking friction versus longitudinal slip for the radial rib tire on wet pavement at 40 mi/h (64 km/h).

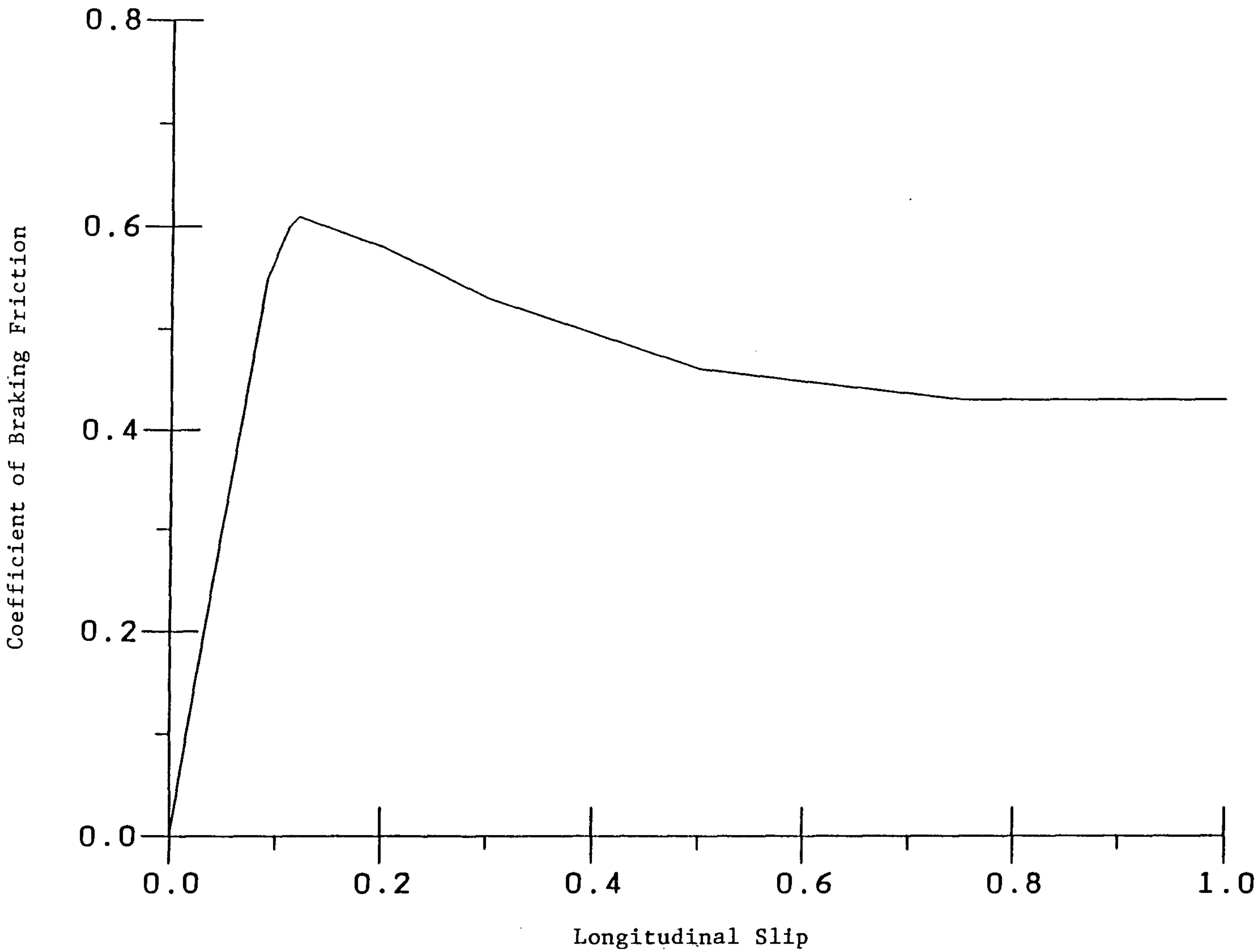

Figure 46. Coefficient of braking friction versus longitudinal slip for the bias rib tire on wet pavement at 40 mi/h (64 km/h).

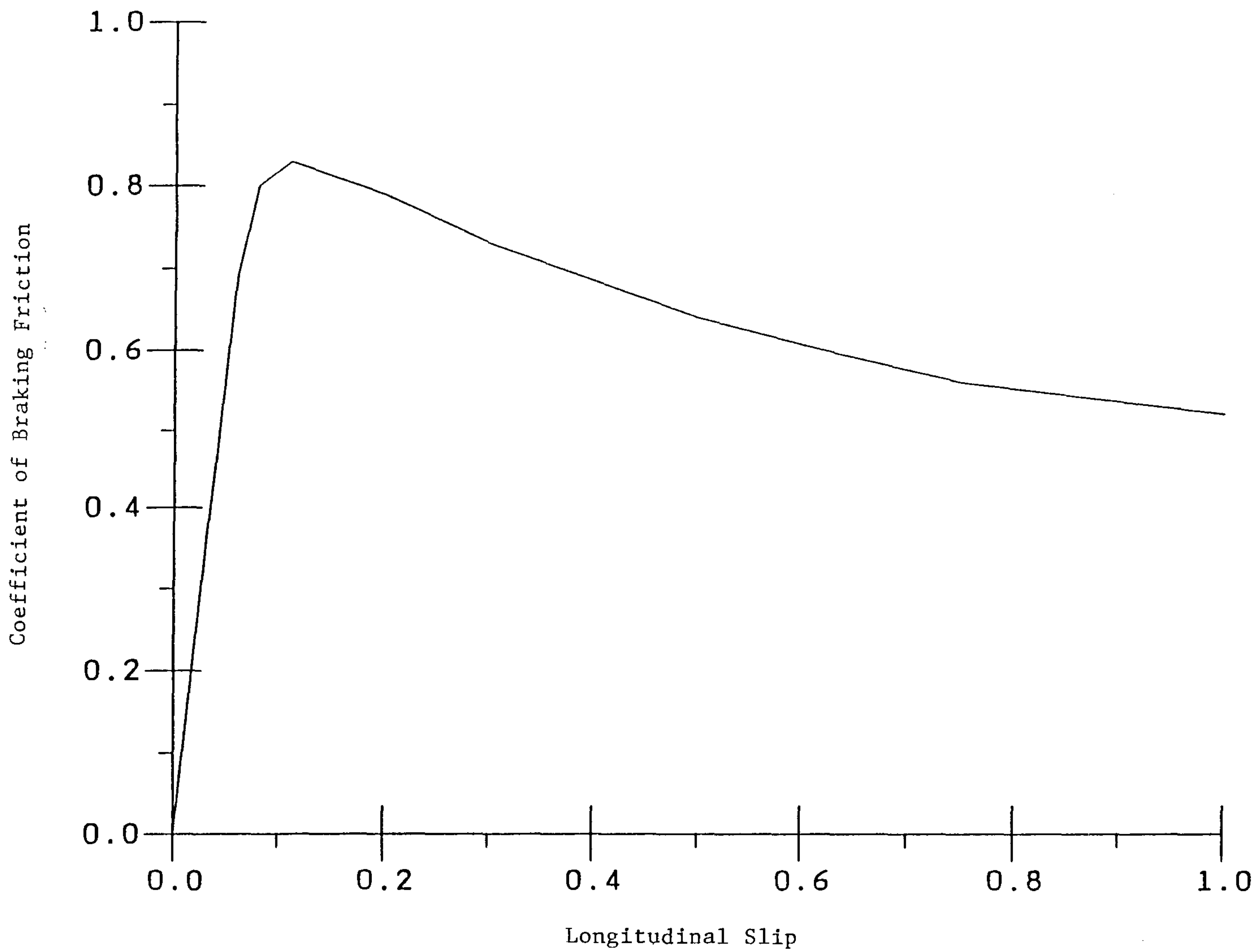

Figure 47. Coefficient of braking friction versus longitudinal slip for the low-profile radial tire on wet pavement at 40 mi/h (64 km/h).

ROAD ROUGHNESS

Experimentally measured road profiles from the researcher's files--a low roughness profile and a high roughness profile--were used in look-up table form to model the road surface. These two profiles were used for both tangent and nontangent sections. The roughness indices for the two profiles as determined by a quarter-car simulation model were 105 IPM for the low roughness profile and 212 IPM for the high roughness profile. These values were obtained for 0.1-mi-long (0.16-km-long) sections of roads.

WHEEL UNBALANCE

An unbalanced force was added to the front left trailer tire by simulating a 8-oz (2.2-N) weight attached to the wheel. This weight was chosen as the largest commonly used balancing weight based on a conversation with a mechanic at a heavy-duty truck alignment garage.

LOAD AND LOAD DISTRIBUTION

The baseline load (L1) was a 52,363-lb (232 932-N) solid block 546 in (13.9 m) long, 92 in (2.4 m) wide, and 70 in (1.8 m) high. This represents a uniformly distributed load with center of gravity located 247 in (6.3 m) in front of the rear suspension and 90 in (2.3 m) above the ground. This loading results in a gross vehicle weight of 80,000 lb (355 871 N).

The no load (L2) was a tractor with an unloaded trailer. The forward load (L3) was the same block positioned to represent a uniformly distributed load with center of gravity located 36 in (0.9 m) behind the kingpin and 90 in (2.3 m) above the ground, resulting in a heavily loaded tractor rear suspension and a lightly loaded trailer suspension.

The rear load (L4) used the same block positioned so that the center of gravity was located 36 in (0.9 m) in front of the rear suspension and 90 in (2.3 m) above the ground, resulting in a lightly loaded tractor rear suspension and a heavily loaded trailer suspension.

SUSPENSION TYPE

The walking beam and four-spring tandem suspension models are both included in the T3DRS, Phase 4 simulation program. Equal static axle load distribution was chosen for both tandem suspensions. The interaxle load transfer coefficient for the walking beam suspension was chosen to be 0.0 (no load transfer due to braking torque), while the coefficient for the four-spring suspension was chosen to be -0.13 (13 percent of braking force reacted as load transfer to the rear axle). These values were chosen as typical values from Truck and Tractor Trailer Dynamic Response Simulation.[17]

BRAKE SYSTEM

Two types of braking systems were used in this study: conventional and antilock brakes. The conventional system is a model of common pneumatic brakes with a time lag, a rise time (the time required for the brake chamber pressure to reach 63 percent of the treadle pressure), and a torque coefficient that defines the brake torque for a certain brake chamber pressure.

The antilock system includes a 10-ms wheel sensor delay and a 20-ms delay in computing wheel acceleration from the sensor signal. The wheel acceleration (α) is defined as the acceleration of the wheel at the tire-road interface expressed as an equivalent translational acceleration. The control logic generates an OFF signal (no brake pressure) for wheel acceleration below -50.0 ft/s^2 (-15.3 m/s^2) and an ON signal (full brake pressure applied) for wheel acceleration greater than -10.0 ft/s^2 (-3.0 m/s^2). There is a 40-ms pressure modulator time for OFF signals and a 60-ms delay for ON signals. The chamber pressure rate of change is an exponential function of wheel acceleration. The pressure fall rates are 10.0 for $\alpha \leq$ -100 ft/s^2 (-30.5 m/s^2) and 5.0 for $\alpha >$ -100 ft/s^2 (-30.5 m/s^2). The pressure rise rates are 5.0 for $\alpha \leq$ 50 ft/s^2 (15.3m/s^2) and 10.0 for $\alpha >$ 50 ft/s^2 (15.3 m/s^2).

The truck traveled at a constant speed for the first 1.5 s of each run to allow all wheels of the truck to travel past the starting point of the road profile. The brakes were then applied at the 1.5-s point. A constant 40-psi treadle pressure was applied for all runs except for the runs with an unloaded trailer and a forward loaded trailer. The treadle pressure had to be reduced on these runs to maintain control of the truck.

OUTPUT DATA

The standard output from T3DRS, Phase 4 is a single large output file that contains all of the output data such as sprung and unsprung mass position, velocity and acceleration, tire forces, and brake data. The researchers modified the program output slightly to obtain an additional file that contains the distance traveled for the truck. A postprocessing program was also created for this project to extract the relevant data from the T3DRS, Phase 4 output and to create more convenient plotting files. These plotting files represent the measurements that would be used in an experimental test program and include longitudinal, lateral, and vertical tire forces for all four dual tire assemblies, slip for all four dual tire assemblies, and a plot of truck speed versus position that can be used to obtain the stopping distance. Figures 48 through 51 are output data plots for one sample run. The high frequency components present in these plots are caused by wheel bouncing on a rough road. When the wheel bounces off the surface, the tire forces become zero and, if brakes are applied, the wheel is locked up. When the tire regains contact with the road surface, the forces increase rapidly whereas the longitudinal slip decreases. As a result, tire forces undergo continuous rapid changes, even on a low-roughness road.

METHODS OF DATA REDUCTION

Initial data reduction is performed by another postprocessing program that uses the previously mentioned plotting files and calculates average tire forces, dynamic force factors for the tire forces, stopping distance, and stopping time. Average forces are calculated using the following equation:

$$\overline{F} = \frac{1}{N} \sum_{i=1}^{N} F_i \qquad (14)$$

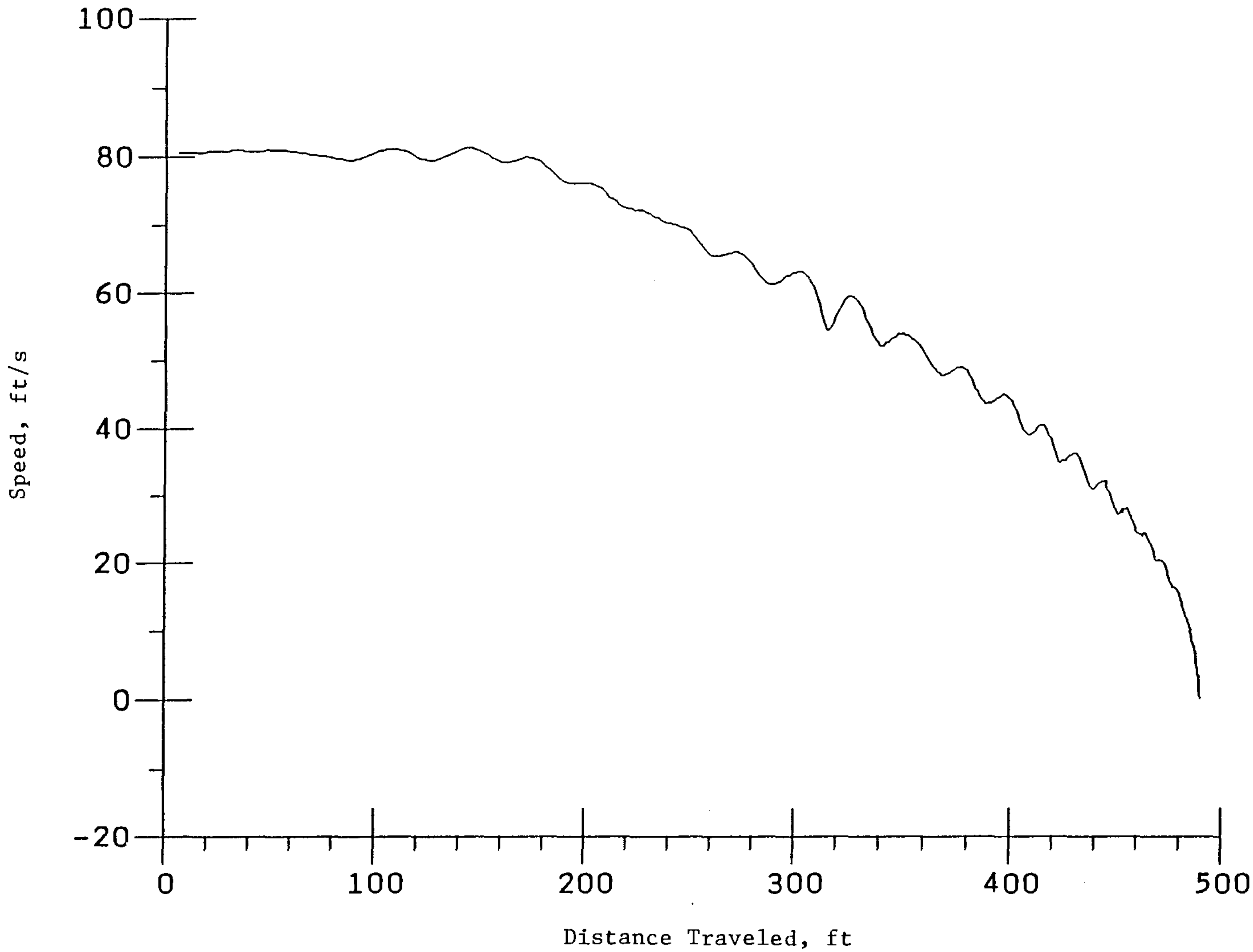

Figure 48. Truck speed versus distance traveled for a truck with four-spring suspension and radial rib tires on wet, low roughness tangent section (Run 1A1).

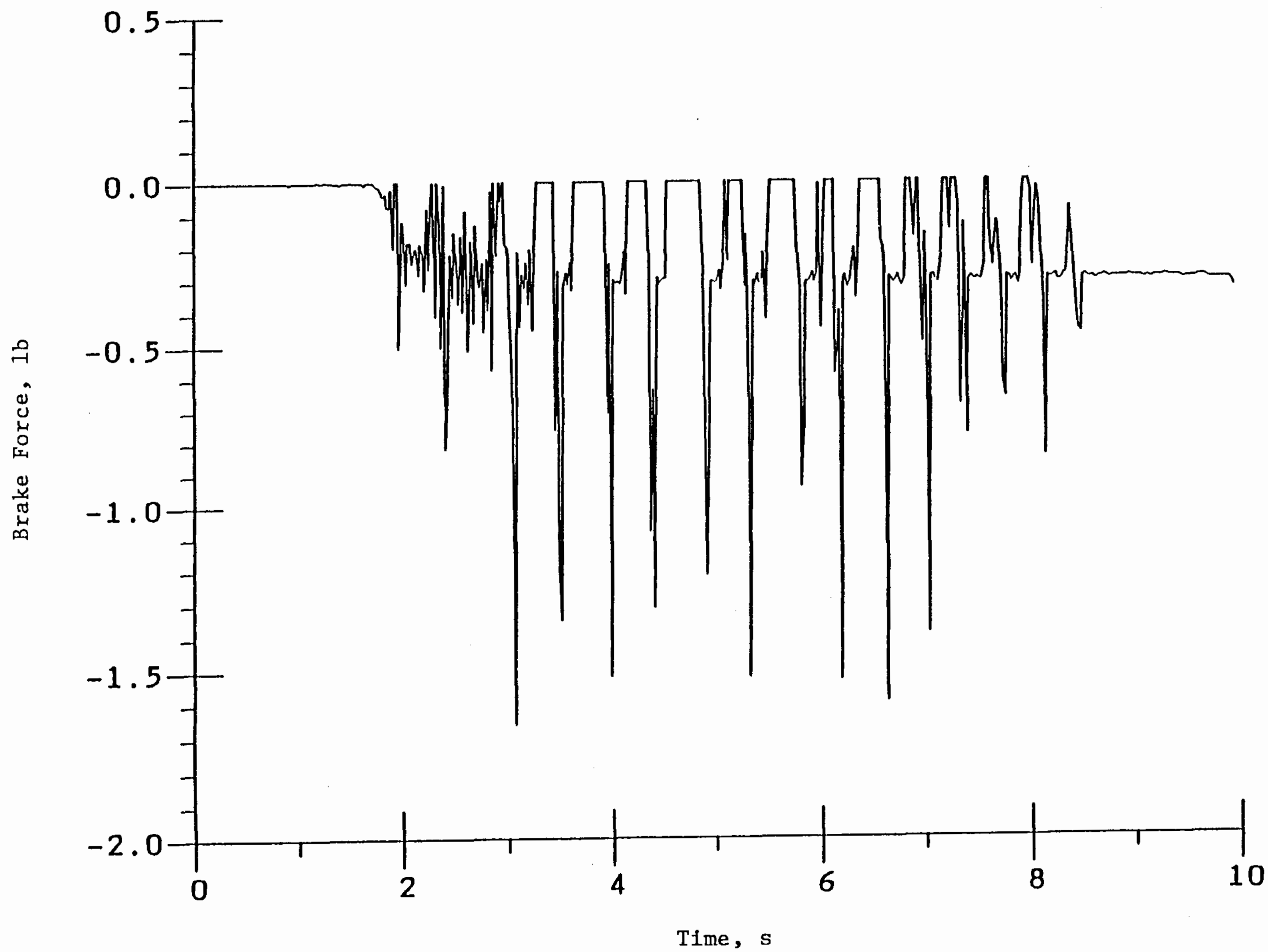

Figure 49. Brake force for front left trailer tires for a truck with four-spring suspension and radial rib tires on wet, low roughness tangent section (Run 1A1).

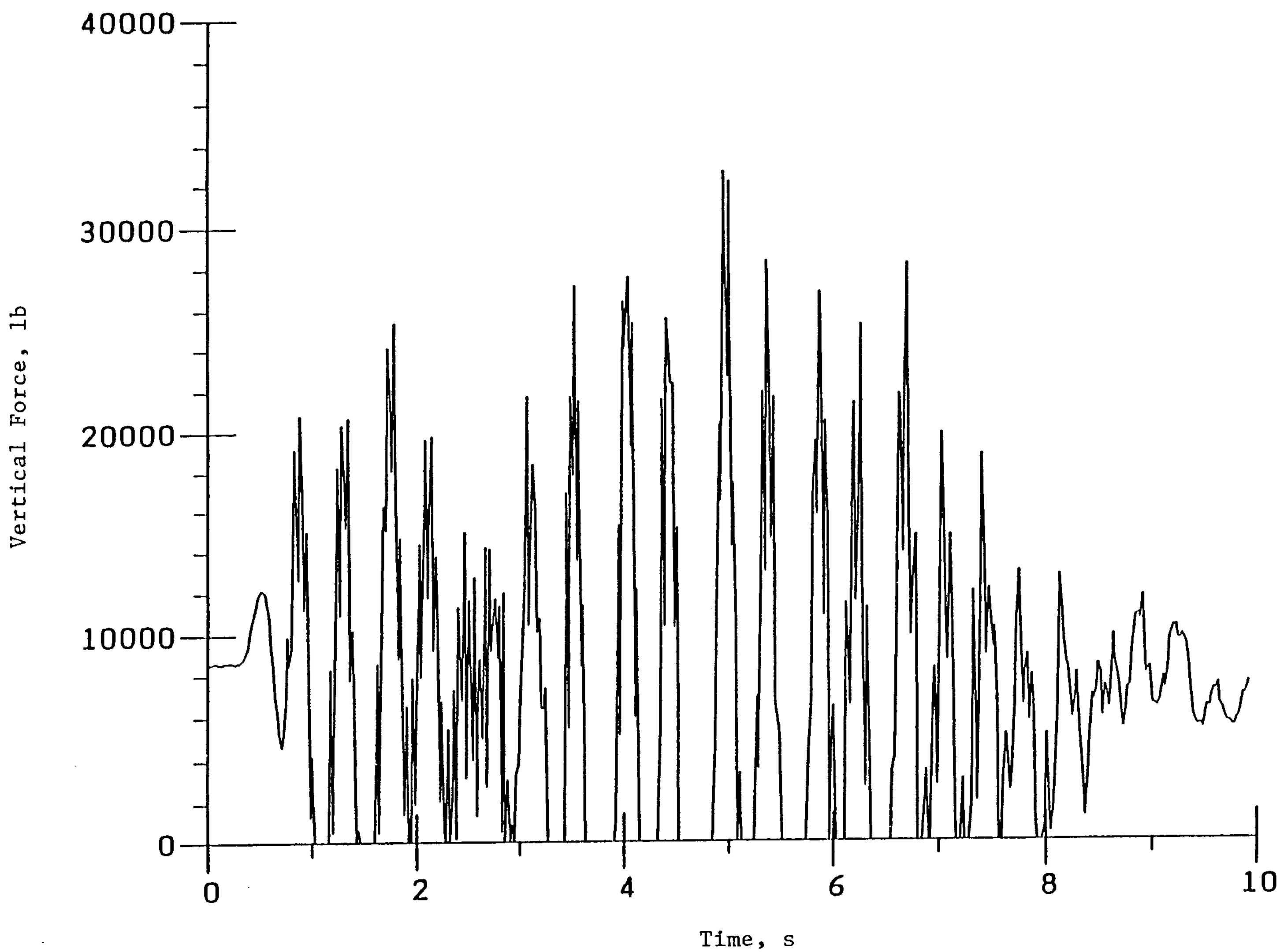

Figure 50. Vertical force for front left trailer tires for a truck with four-spring suspension and radial rib tires on wet, low roughness tangent section (Run 1A1).

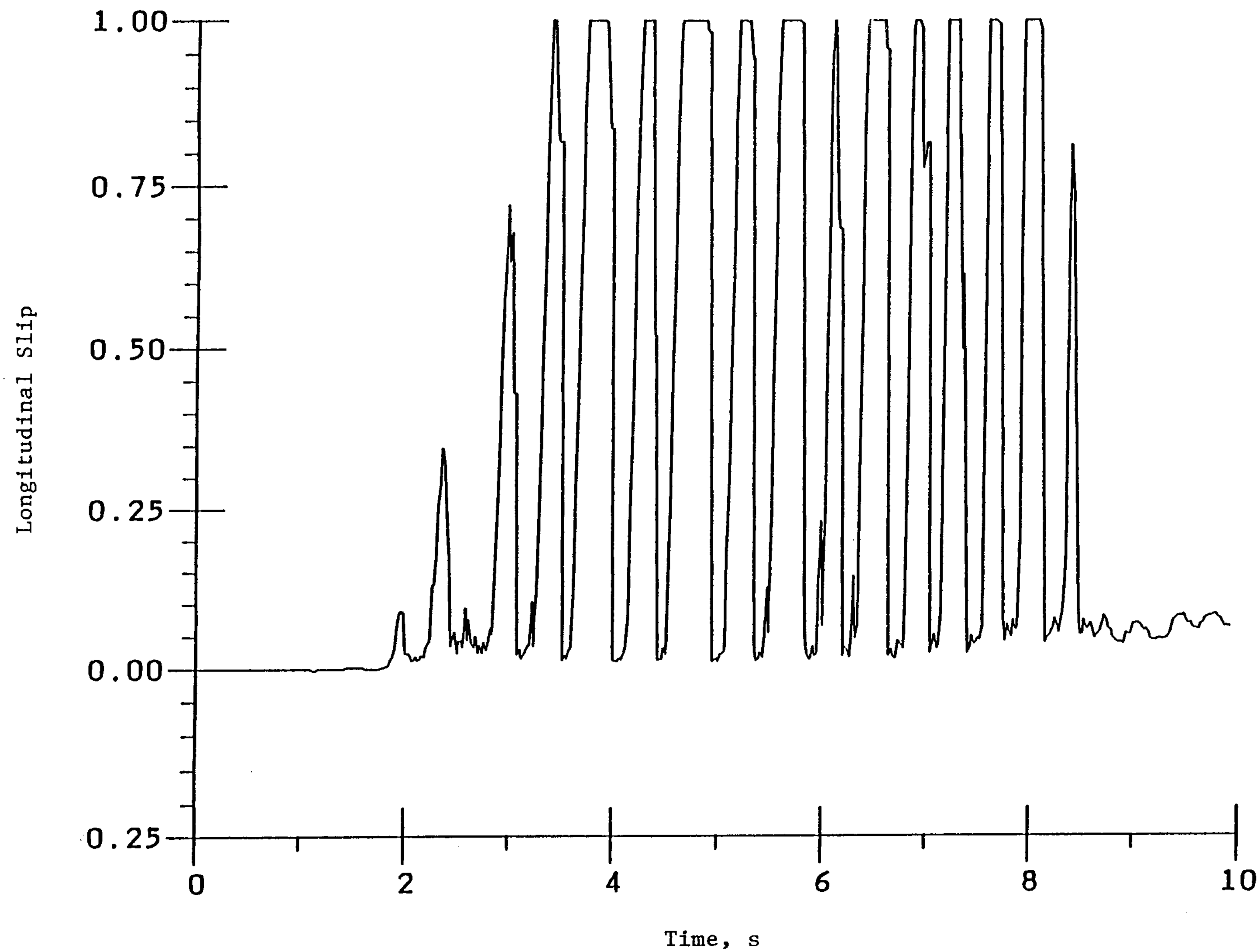

Figure 51. Longitudinal slip for front left trailer tires for a truck with four-spring suspension and radial rib tires on wet, low roughness tangent section (Run 1A1).

where N is the number of force measurements. Longitudinal, lateral, and vertical forces are individually averaged. Dynamic force factors are also calculated for longitudinal, lateral, and vertical forces using this equation:

$$DIF = \sqrt{\frac{1}{(N-1)\overline{F}^2}\sum_{i=1}^{N}(F_i-\overline{F})^2} \tag{15}$$

The stopping distance is determined simply by calculating the distance traveled at the 1.5-s point when the brakes are applied and subtracting this value from the distance traveled when the truck comes to rest. Additional data reduction is described in chapter 5.

RESULTS OF SIMULATION

PRIMARY VARIABLES

The effects of the primary variables--suspension type, pavement type, and tire type--on truck stopping distance and tire braking and vertical forces are summarized below.

Stopping Distance

The walking beam suspension produced slightly shorter stopping distances for all the runs except for two nontangent roads. The differences in stopping distance between the two suspensions for one nontangent section are small and mixed, while for the other section of road, the four-spring suspension resulted in slightly shorter distances. The rougher profile resulted in longer stopping distances for all cases.

For most of the runs, the low-profile radial tire produced the shortest stopping distance, followed by the conventional radial rib tire, and then the bias rib tire.

The stopping distances were shorter for dry roads than wet roads in all cases, although the differences were often small. For the tangent roads, the differences were within 6 ft (1.8 m) for most runs; the differences were slightly higher for the nontangent roads. The highest differences were for the walking beam suspension on a nontangent road: the differences between wet and dry stopping distances were as high as 24 ft (7.3 m).

The differences in stopping distance between a tangent and nontangent road varied between almost 0 to around 40 ft (12.2 m). The nontangent road always resulted in longer stopping distances, but the differences varied depending on the other variables. Walking beam suspensions tended to have greater differences between tangent and nontangent roads, and wet roads seemed to result in greater differences. In some cases, the bias tire had much larger differences than the radials.

Braking Forces

The overall average braking forces are directly represented by the stopping distances. Thus, the average braking forces are, in general, higher for the walking beam suspensions than for four-spring suspensions and higher for the smooth profile than for the rough. In most cases, the average braking force is higher on the rear axle of the four-spring suspension, but this is significant only for the rougher profile.

Vertical Tire Forces

Suspension type, axle load, road profile, and tire type had the most significant impact on the vertical tire force. The average vertical forces are higher on the rear axle of the four-spring suspension due to the brake torque load transfer. Brake torque does not cause interaxle load transfer on the walking beam suspension used in this study. The four-spring suspension had slightly lower dynamic loading on the tangent roads with the smooth profile, but the walking beam suspension had higher dynamic loading on nontangent roads and on roads with the rougher profile.

The two test road sections had different surface profiles in the left and right wheel paths. The different levels of roughness together with the specific geometry of the two roads resulted in different vertical loads. The smoother road profile increased the average vertical loads on the left-side tires, while the right-side tires had higher average vertical loads for the rougher profile. The walking beam suspension had higher interaxle load transfer for the rough profile than for the smooth, especially for the tangent runs in which more load was transferred to the rear axle. The rougher profile also caused more load transfer to the rear axle of the four-spring suspension on tangent roads.

Different tire types produced small, mixed differences in average vertical load, but the bias rib tire had significantly higher dynamic loading than the radials.

The differences in vertical tire load for wet and dry roads were small and mixed.

The nontangent roads naturally produced higher vertical tire loads on the outside tires.

SECONDARY VARIABLES

The effects of the secondary variables--tire inflation pressure, tire balance, antilock brakes, speed, and load and load distribution--are summarized below.

Tire Inflation Pressure

Reducing the tire inflation pressure reduced the stopping distance slightly; increasing the pressure increased the stopping distance. The dynamic loading also increased with inflation pressure.

Tire Balance

Adding an 8-oz (2.2-N) unbalanced weight to the front left wheel had very little effect on the measured variables. The stopping distance increased an insignificant amount, and the average vertical loads increased very slightly. The changes are probably very small because of the relative magnitude of the unbalanced force (< 40 lb [178 N]) to the average tire loads (≈ 7,500 lb [33 363 N]).

Antilock Brakes

The antilock brake system used for this study resulted in a higher stopping distance for one case, but the wheel slip was greatly reduced. The antilock system also significantly reduced the vertical and longitudinal dynamic load factors. The antilock brake system becomes effective on low-friction pavements whereas the pavements included in the T3DRS, Phase 4 model have relatively high friction surfaces.

Initial Speed

The stopping distance increases substantially for each 15-mi/h (24-km/h) increment in initial speed. The average braking forces are the highest for the 40 mi/h (64 km/h) initial speed, but the dynamic loading, both vertical and longitudinal, increases greatly with initial speed.

Load and Load Distribution

Trailer loading significantly affected braking performance. The unloaded truck stopped very quickly and the average brake forces and vertical loads were very small because of the low weight of the truck, but the dynamic load factors were very high.

The truck with a full load placed on the front of the trailer could not stop within the available road length (profile length) before the trailer began to swing out, causing the truck to go out of control. This happens because the truck is very heavy and requires high braking loads, but the trailer tires have very small loading and lock up at low brake pressure.

Placing a full load on the rear of the trailer degraded braking performance slightly, increasing the stopping distance by 19 ft (5.8 m). The trailer wheels were heavily loaded for this run, resulting in high average braking forces and low dynamic load factors.

STATISTICAL ANALYSIS OF BRAKING DISTANCE DATA

Data on the distances required for trucks to brake to a stop were obtained with the T3DRS, Phase 4 simulation model. These distances are referred to as braking distances rather than stopping distances, because the term stopping distance typically includes the driver's perception-reaction time in addition to the distance required to brake to a stop.

The objective of the braking distance analysis was to determine the effects of five factors and their interactions on braking distance. The five factors and the level considered for each factor are listed in table 11.

Table 11. Factors affecting braking distance.

Factor	Number of Levels	Description of Levels
Vehicle suspension type	2	Four spring/walking beam
Roadway alignment	2	Tangent/nontangent
Pavement surface roughness	2	High/low
Pavement surface condition	2	Dry/wet
Tire type	3	Bias rib/low profile/radial rib

An experimental design that considered all (2 x 2 x 2 x 2 x 3 = 48) combinations of these factors was used. One T3DRS, Phase 4 run was made for each of these combinations. (Replicate runs were not needed because the model is deterministic; thus, any replicate runs would provide the same results.) A full-factorial design based on these 48 runs enabled the evaluation of the main effects of each of the 5 factors and all their two-way interactions.

Each T3DRS, Phase 4 run involved controlled braking to a complete stop from an initial speed of 55 mi/h (88 km/h). Table 12 shows the assumed values of the tire-pavement friction coefficient for each tire type under both wet and dry conditions. The braking control algorithm for each run of the T3DRS, Phase 4 model was adjusted to provide controlled braking without locking any of the wheels. This was achieved in most cases, although a few lockups for very short time periods were observed for some wheels. The braking distances for the 48 T3DRS, Phase 4 runs ranged from 350.9 to 421.2 ft (107.0 to 128.5 m), with an overall mean of 381.81 ft (116.45 m).

Table 12. Tire-pavement friction coefficients used as input to the T3DRS, Phase 4 model.

		Pavement Surface			
		Wet		Dry	
Tire Type	Friction Coefficient Type	25 mi/h	40 mi/h	25 mi/h	40 mi/h
Radial rib	Peak	0.81	0.77	0.81	0.77
	Sliding	0.52	0.42	0.81	0.77
Bias rib	Peak	0.71	0.61	0.71	0.61
	Sliding	0.52	0.43	0.71	0.61
Low profile	Peak	0.83	0.83	0.83	0.83
	Sliding	0.57	0.52	0.83	0.83

1 mi = 1.6 km

An analysis of variance of the braking distance data found that the main effects of all 5 factors and 6 of the 10 two-way interactions were statistically significant at the 90 percent confidence level. Table 13 summarizes the results of this analysis of variance. The table indicates that the analysis of variance model fits the data very well; the model explains 97 percent of the variation in braking distance (i.e., $R^2 = 0.97$). The main effects show a strong relationship between braking distance and each of the five factors. The six two-way interactions (i.e., interactions between pairs of variables) that display significant relationships to braking distance at the 90 percent confidence level are:

- Suspension/alignment.
- Suspension/surface condition.
- Alignment/roughness.
- Alignment/surface condition.
- Alignment/tire type.
- Roughness/surface condition.

The four two-way interactions that were not statistically significant are:

- Suspension/roughness.
- Suspension/tire type.
- Roughness/tire type.
- Surface condition/tire type.

It is worth noting that only one of the tire type interactions (i.e., alignment/tire type) is statistically significant. Thus, the main effect of tire type together with this one interaction is sufficient to explain the effect of tire type on braking distance.

To accurately quantify the magnitude of these effects on braking distance, the analysis of the variance model was reevaluated excluding the four nonsignificant interaction terms. The revised analysis of variance results, including the five main effects and only those two-way interactions that were statistically significant, are summarized in table 14. The table shows that this revised model explains 96 percent of the variation in braking distance (i.e., $R^2 = 0.96$) and, thus, the model in table 14 provides

Table 13. Analysis of variance of truck distance for all main effects and two-way interactions.

Source of Variation	Degrees of Freedom	Sum of Squares	Mean Square	F-value	Significance Level	Significant at 10% Level?
MODEL	20	11,855.06	592.75	42.57	≤0.0001	Yes
ERROR	27	375.99	13.93			(R^2 = 0.97)
CORRECTED TOTAL	47	12,231.05				
<u>Main Effects</u>						
Suspension	1	971.26	971.26	69.75	≤0.0001	Yes
Alignment	1	2,849.41	2,849.41	204.62	≤0.0001	Yes
Roughness	1	4,530.87	4,530.87	325.36	≤0.0001	Yes
Surface condition	1	805.86	805.86	57.87	≤0.0001	Yes
Tire type	2	973.23	486.62	34.94	≤0.0001	Yes
<u>Two-Way Interactions</u>						
Suspension/alignment	1	811.48	811.48	58.27	≤0.0001	Yes
Suspension/roughness	1	31.94	31.94	2.29	0.1415	No
Suspension/surface condition	1	58.08	58.08	4.17	0.0510	Yes
Suspension/tire type	2	42.60	23.30	1.53	0.2348	No
Alignment/roughness	1	148.64	148.64	10.67	0.0030	Yes
Alignment/surface condition	1	251.49	251.49	18.06	0.0002	Yes
Alignment/tire type	2	264.27	132.14	9.49	0.0008	Yes
Roughness/surface condition	1	92.75	92.75	6.66	0.0156	Yes
Roughness/tire type	2	5.94	2.97	0.21	0.8092	No
Surface condition/tire type	2	17.22	8.61	0.62	0.5463	No

Table 14. Analysis of variance of truck distance for significant main effects and two-way interactions only.

Source of Variation	Degrees of Freedom	Sum of Squares	Mean Square	F-value	Significance Level	Significant at 10% Level?
MODEL	13	11,757.35	904.41	64.92	≤0.0001	Yes
ERROR	34	473.69	13.93			(R^2 = 0.96)
CORRECTED TOTAL	47	12,231.05				
<u>Main Effects</u>						
Suspension	1	971.26	971.26	69.75	≤0.0001	Yes
Alignment	1	2,849.41	2,849.41	204.62	≤0.0001	Yes
Roughness	1	4,530.87	4,530.87	325.36	≤0.0001	Yes
Surface condition	1	805.86	805.86	57.87	≤0.0001	Yes
Tire type	2	973.23	486.62	34.94	≤0.0001	Yes
<u>Two-Way Interactions</u>						
Suspension/alignment	1	811.48	811.48	58.27	≤0.0001	Yes
Suspension/surface condition	1	58.08	58.08	4.17	0.0510	Yes
Alignment/roughness	1	148.64	148.64	10.67	0.0030	Yes
Alignment/surface condition	1	251.49	251.49	18.06	0.0002	Yes
Alignment/tire type	2	264.27	132.14	9.49	0.0008	Yes
Roughness/surface condition	1	92.75	92.75	6.66	0.0156	Yes

essentially just as good a prediction of braking distance as the model in table 10.

Table 15 presents the magnitude of the main effects and interaction effects on braking distance using the analysis of variance model shown in table 14. Table 15 can be used to determine the controlled braking distance from 55 mi/h (88 km/h) for any combination of the variables and interactions. The positive and negative terms for specific levels (or combinations of levels) of each factor can be added to the overall mean braking distance (381.81 ft [116.45 m]) to estimate the braking distance for that condition. For example, the controlled braking distance from 55 mi/h (88 km/h) to a stop for a truck with a walking beam suspension and bias rib tires on a tangent alignment on a high roughness pavement under wet conditions would be calculated as:

$$\begin{aligned} \text{Braking Distance} &= 381.81 - 4.5 - 7.70 + 9.72 + 4.10 + 6.24 - 4.11 \\ &\quad + 1.10 + 1.76 - 2.29 - 3.15 + 1.39 \\ &= 384.37 \text{ ft } (117.23 \text{ m}) \end{aligned} \tag{16}$$

Each of the main effects shown in table 15 is in a direction that would be expected from existing knowledge of truck braking distance. In other words, it is to be expected that braking distances are shorter for tangent than for nontangent alignments, shorter for low than for high roughness pavement surfaces, shorter for dry than for wet pavement surfaces, and shorter for radial and low-profile tires than for bias rib tires. The shorter braking distance obtained with the walking beam suspension as compared with the four-spring suspension is somewhat unexpected. In general, four-spring suspensions are ranked higher than walking beam suspensions in terms of dynamic tire forces [20,21] and thus should provide a better isolation from the pavement roughness. Since roughness increases braking distance, a truck with a four-spring suspension was expected to have a shorter braking distance than a truck with a walking beam suspension. This ranking order, however, depends on the particular suspension parameters and test conditions. Indeed, when all two-way interaction terms are included, the braking distance for a truck with walking beam suspension may become greater than the distance required by a

Table 15. Magnitude of factor effects on truck braking distance.

	Braking Distance (ft)
Overall Mean	381.81
MAIN EFFECTS	
Suspension	
Four spring	4.50
Walking beam	-4.50
Alignment	
Nontangent	7.70
Tangent	-7.70
Roughness	
High	9.72
Low	-9.72
Pavement Surface Condition	
Dry	-4.10
Wet	4.10
Tire Type	
Bias rib	6.24
Radial rib	-2.04
Low profile	-4.20
TWO-WAY INTERACTIONS	
Suspension/Alignment Interaction	
Four spring/nontangent	-4.11
Four spring/tangent	4.11
Walking beam/nontangent	4.11
Walking beam/tangent	-4.11
Suspension/Pavement Surface Condition Interaction	
Four spring/dry	1.10
Four spring/wet	-1.10
Walking beam/dry	-1.10
Walking beam/wet	1.10

Table 15. Magnitude of factor effects on truck braking distance (Continued).

	Braking Distance (ft)
Overall Mean	381.81
Alignment/Roughness Interaction	
Nontangent/high	-1.76
Nontangent/low	1.76
Tangent/high	1.76
Tangent/low	-1.76
Alignment/Pavement Surface Condition Interaction	
Nontangent/dry	-2.29
Nontangent/wet	2.29
Tangent/dry	2.29
Tangent/wet	-2.29
Alignment/Tire Type Interaction	
Nontangent/bias rib	3.15
Nontangent/radial rib	-0.66
Nontangent/low profile	-2.49
Tangent/bias rib	-3.15
Tangent/radial rib	0.66
Tangent/low profile	2.49
Roughness/Pavement Surface Condition Interaction	
High/dry	-1.39
High/wet	1.39
Low/dry	1.30
Low/wet	-1.39

1 ft = 0.305 m

Note: Truck braking distance for a controlled stop from 55 mi/h (88 km/h) can be computed by adding the effects shown for the appropriate combination of factors and interactions to the overall mean of 381.81 ft (116.45 m).

truck with a four-spring suspension, depending on the road alignment and surface conditions.

The model given in table 15 can be used to determine the controlled braking distance for a truck traveling at 55 mi/h (88 km/h) for any particular combination of factors. Table 16 shows the braking distances for each tire type for the least favorable and most favorable combinations of the other factors. Under the most favorable combination of conditions, the maximum difference in braking distance caused by truck tire type is 4.80 ft (1.46 m). The braking distances for a radial rib tire and a low-profile tire are very close, and the braking distance for a bias rib tire exceeds the braking distance of a low-profile tire by only about 1.4 percent. Thus, in this situation, tire type has very little effect on braking distance.

However, tire type has a much more important effect on braking distance under the least favorable combination of conditions. The maximum difference in braking distance caused by truck tire type is 16.08 ft (4.90 m), which represents a difference in braking distance of 4.0 percent. Thus, the effect of tire type on braking distance is about three times as large under unfavorable conditions than under favorable conditions.

Table 17 shows a similar comparison of the effect of suspension type on braking distance for one particular tire type. The bias rib tire was selected for use in table 17 for illustrative purposes. The table shows that, in contrast to the observed effect for tire type, the effect of suspension type is greater under the most favorable combination of conditions than under the least favorable combination. Under the most favorable conditions, the maximum difference in braking distance caused by suspension type is 19.42 ft (5.92 m), or nearly 5.5 percent. Under the least favorable combination of conditions (i.e., the longest braking distances), the maximum difference in braking distance caused by suspension type is only 1.42 ft (0.43 m), or 0.3 percent. Furthermore, under these unfavorable conditions, the four-spring suspension results in a shorter braking distance than the walking beam suspension. This result illustrates the importance of the interaction terms in assessing the effects of the five factors on braking distance.

Table 16. Variation of braking distance as a function of tire type.

	Estimated Braking Distance (ft)	
Tire Type	Shortest[1]	Longest[2]
Bias rib	355.59	397.85
Radial rib	351.12	401.84
Low profile	350.79	413.93

1 ft = 0.305 m

[1] Under most favorable combination of conditions (walking beam suspension, tangent alignment, low roughness, dry pavement).

[2] Under least favorable combination of conditions (four-spring suspension, nontangent alignment, high roughness, wet pavement).

Table 17. Variation of braking distance as a function of suspension type.

	Estimated Braking Distance (ft)	
Tire Type	Shortest[1]	Longest[2]
Four spring	375.01	413.93
Walking beam	355.59	415.35

1 ft = 0.305 m

[1] Under most favorable combination of conditions (tangent alignment, low roughness, dry pavement).

[2] Under least favorable combination of conditions (nontangent alignment, high roughness, wet pavement).

Note: These values are applicable only to trucks with bias rib tires.

5. SAFETY IMPLICATIONS OF BRAKING DISTANCE RESULTS

Safety implications of the braking distance results obtained from T3DRS, Phase 4 computer simulation must be assessed in comparison to the established criteria for stopping sight distance. Sight distance is the length of the roadway ahead that is visible to the driver. The minimum sight distance available on the roadway should be sufficient to enable a vehicle traveling at or near the design speed to stop before reaching a stationary object in its path. This minimum sight distance, known as stopping sight distance, is the basis for design criteria for crest vertical curves and minimum offsets to horizontal sight obstructions.

Table 18 summarizes the American Association of State Highway Officials (AASHTO) criteria for stopping sight distance.[22] As shown in table 18, stopping sight distance is the sum of two components: brake reaction distance and braking distance. Braking distance is determined from the following relationship:

$$d = \frac{v^2}{30f} \qquad (17)$$

where

d = braking distance (ft)
v = initial speed (mi/h)
f = coefficient of friction

The braking distances used in the AASHTO criteria are based on locked-wheel braking by a passenger car on a level surface. The pavement surface is assumed to have a coefficient of sliding friction of 0.32 under wet conditions at 40 mi/h (64 km/h). Trucks cannot stop safely in the locked-wheel mode, which can lead to loss of steering control and jackknifing. Controlled stops by trucks, made without locking their wheels, require greater braking distances.

Table 18. AASHTO stopping sight distance criteria.[22]

Design Speed (mi/h)	Assumed Speed for Condition (mi/h)	Brake Reaction		Coefficient of Friction f	Braking Distance on Level (ft)	Stopping Sight Distance	
		Time (s)	Distance (ft)			Computed (ft)	Rounded for Design (ft)
20	20-20	2.5	73.3-73.3	0.40	33.3-33.3	106.7-106.7	125-125
25	24-25	2.5	88.0-91.7	0.38	50.5-54.8	138.5-146.5	150-150
30	28-30	2.5	102.7-110.0	0.35	74.7-85.7	177.3-195.7	200-200
35	32-35	2.5	117.3-128.3	0.34	100.4-120.1	217.7-248.4	225-250
40	36-40	2.5	132.0-146.7	0.32	135.0-166.7	267.0-313.3	275-325
45	40-45	2.5	146.7-165.0	0.31	172.0-217.7	318.7-382.7	325-400
50	44-50	2.5	161.3-183.3	0.30	215.1-277.8	376.4-461.1	400-475
55	48-55	2.5	176.0-201.7	0.30	256.0-336.1	432.0-537.8	450-550
60	52-60	2.5	190.7-220.0	0.29	310.8-413.8	501.5-633.8	525-650
65	55-65	2.5	201.7-238.3	0.29	347.7-485.6	549.4-724.0	550-725
70	58-70	2.5	212.7-256.7	0.28	400.5-583.3	613.1-840.0	625-850

Table 18 shows that the locked-wheel braking distance of a passenger car at 55 mi/h (88 km/h) is assumed to be 336.1 ft (102.5 m). This is shorter than the shortest truck braking distance found with the T3DRS, Phase 4 model. However, the surface represented by the friction coefficients in table 11 has substantially higher skid resistance than the pavement surface assumed by AASHTO. Table 11 shows that the coefficient of friction assumed for radial rib and bias rib tires is approximately 0.425 under wet conditions at 40 mi/h (64 km/h). A comparison between the established stopping sight distance criteria for passenger cars and the truck braking distance results obtained in this study must be made for comparable pavement surfaces. An adjustment for this difference in pavement surfaces is derived below.

Researchers have shown that truck tires have coefficients of friction that are approximately 70 percent of those of passenger car tires.[23] Furthermore, passenger cars generally have coefficients of friction that are about 120 percent of those for the standard tires used in skid testing. Therefore, the pavement surface used in the T3DRS, Phase 4 model runs can be estimated to have the following coefficient of friction at 40 mi/h (64 km/h) under standard skid test conditions:

$$\frac{0.425}{(1.2)(0.7)} = 0.51 \qquad (18)$$

Thus, the T3DRS, Phase 4 model was run on a pavement surface with a coefficient of sliding friction approximately 59 percent higher than the coefficient of sliding friction assumed by AASHTO (0.51 versus 0.32). If a skid number-speed gradient proportional to that used by AASHTO is assumed, the coefficient of sliding friction at 55 mi/h (88 km/h) for the pavement surface used in the T3DRS, Phase 4 model is:

$$0.51 \times \frac{0.30}{0.32} = 0.48 \qquad (19)$$

The locked-wheel braking distance from 55 mi/h (88 km/h) to a stop on a pavement with a coefficient of friction of sliding friction of 0.48 is:

$$d = \frac{(55)^2}{(30)(0.48)} = 210.1 \text{ ft} \tag{20}$$

These results imply that, on the surface used in the T3DRS, Phase 4 model, a passenger car can make a locked-wheel stop in 210 ft (64 m), while a truck making a controlled stop would require at least 351 ft (107 m). These results also suggest that trucks can require braking distances for controlled stops at least 67 percent longer than those required for locked-wheel stops by passenger cars, as assumed in stopping sight distance design criteria.

One objective of this study was to develop recommendations for improving pavement roughness and surface texture characteristics to obtain equal and acceptable levels of braking for trucks, buses, and passenger cars. The study findings discussed above have documented that there are substantial differences in braking distances between passenger cars and trucks. However, only a portion of this difference is due to tire design, very little may be attributable to pavement roughness, and none is attributable to the friction characteristics of the pavement itself (which are the same whether a passenger car or a truck is traveling on it). In fact, most of the difference in braking distances is due to differences in vehicle design and braking system design.

The results of previous research, which appear to be consistent with the data obtained in this study, have shown that the tire-pavement friction coefficients of truck tires are about 70 percent of those for passenger car tires.[24] These results, together with equation 17, suggest that truck braking distances would be about 1.43 times longer than passenger car braking distances if trucks could safely brake to a stop in the locked-wheel braking mode. In other words, the inherent differences in tire design are responsible for about two-thirds of the difference between passenger car and truck braking distances.

In fact, trucks cannot use locked-wheel braking to stop safely because trucks, unlike passenger cars, risk complete loss of control if one or more wheels lock up. Locking of the rear wheels of the truck tractor can result in a jackknifing accident, while locking of the rear wheels of the trailer can result in trailer swing. Therefore, truck drivers are trained to modulate the brake pedal to prevent wheel lockup and loss of control. There is great variability in driver braking performance in controlled braking, because drivers who are not experienced in emergency braking maneuvers may--in trying to avoid locking their wheels--be quite timid about using the full braking ability of the vehicle. On the other hand, truck drivers who are experienced in emergency braking maneuvers can utilize nearly all of the vehicle braking capability. This difference between braking distances using locked-wheel braking and controlled braking is responsible for the other one-third of the difference between passenger car and truck braking distances.

These findings illustrate that there is no method of providing equal levels of braking for trucks, buses, and passenger cars without radical changes in tire design or vehicle design. Therefore, efforts should be directed toward assuring that acceptable levels of braking are available for all vehicle types. Improvements in pavement surface friction and reduction in pavement roughness have the potential to reduce braking distances for both passenger cars and trucks and are, therefore, highly desirable.

Another truck braking consideration involves ascertaining that, where appropriate, the highway system is designed to accommodate the longer braking distances of trucks. A thorough review of stopping sight distance requirements for trucks was recently undertaken in the FHWA-sponsored study "Truck Characteristics for Use in Highway Design and Operation."[25] In this study, researchers examined the stopping sight distance requirements to accommodate controlled stops by trucks rather than locked-wheel stops by passenger cars. Researchers found that trucks with conventional brake systems and poor performance drivers may require longer stopping sight distances than those shown in table 18. Table 19 shows that the braking distance recommendations for controlled stops by trucks from the FHWA-sponsored truck characteristics study are approximately equal to the lower end of the range of the results obtained from the T3DRS, Phase 4 model (353.1 ft versus 356.6 ft [107.7 m versus 108.8 m]).

Note that driver behavior--a key variable in modeling stopping distances for controlled stops by trucks--was difficult to account for realistically in

Table 19. Braking distances from 55 mi/h (88 km/h) to a complete stop under wet-pavement conditions.

Condition	Braking Distance (ft)
Locked-wheel stop by a passenger car[1]	210.9
Controlled stop by a truck from PHASE 4 model results[2]	356.6 to 413.9
Controlled stop by a truck from FHWA-sponsored truck characteristics study[1,3]	353.1

1 mi = 1.6 km

1 ft = 0.305 m

[1]Adjusted to a pavement surface with a coefficient of sliding friction of 0.48 at 55 mi/h (88 km/h).

[2]Range of estimate from table 10 for wet pavement surfaces only.

[3]For 70 percent driver control efficiency.

both the FHWA-sponsored truck characteristics study and the T3DRS, Phase 4 model. The FHWA-sponsored truck characteristics study assumed for design purposes that drivers had a 70 percent efficiency in controlled braking (i.e., they used only 70 percent of the vehicle capability).

In the T3DRS, Phase 4 program, braking is controlled by an input table of treadle pressure versus time. A constant treadle pressure of 40 psi was used for most of the runs, as described in the input data section. This treadle pressure was selected after running a number of simulations at different pressures with the aim of selecting a constant pressure that would most closely simulate an emergency stop. Simulations with 40 psi treadle pressure resulted in fairly short stopping distances and tire slip low enough to maintain directional control, the slip normally reaching 100 percent only instantaneously while passing over bumps. The lack of real-world data on the braking performance of drivers makes it difficult to determine braking performance precisely.

Shorter braking distances can be achieved by equipping trucks with antilock brake systems.[26] The main objectives of antilock brake systems are (in order of importance):

- Improvement of vehicle stability during braking.
- Improvement of steering performance during braking.
- Reduction of braking distance.

The purpose of antilock brake systems is to take advantage of the available tire-pavement friction capabilities without locking wheels and losing vehicle control. Antilock brake systems use microcomputer control to monitor each wheel for impending lockup. When wheel lockup is anticipated, the system releases brake pressure on the wheel. When the wheel begins to roll freely again, the system reapplies brake pressure. The system constantly monitors each wheel and readjusts the brake pressure until the wheel torque is no longer sufficient to lock the wheel. Antilock brake systems eliminate the concern about driver control efficiency associated with conventional brake systems because the driver merely applies the brakes and the microprocessor ensures that wheel lockup does not occur. The braking effectiveness of a particular antilock system depends on the hardware and the control algorithm implemented in the system, and it is also affected by road surface conditions. Figure 52 shows the braking effectiveness of two different antilock systems on dry, wet, and icy roads.[27] The braking effectiveness is defined here as the ratio of the locked wheel stopping distance and the stopping distance with antilock control system. Figure 52 shows that the stopping distance with an antilock brake system is longer on dry road, about the same on wet road, and shorter on icy road, as compared with the locked wheel stopping distance. Similar results have been reported elsewhere.[28] In tests conducted in an NHTSA study, a commercially available antilock brake system reduced the braking distance of a two-axle truck in a straight line stop from 60 mi/h (97 km/h) on a wet polished concrete pavement, with an approximate skid number of 30, by 15 percent.[29] The braking effectiveness of the antilock control algorithm depends primarily on the length of the brake release period, which is often unnecessarily long.

The T3DRS, Phase 4 model results suggest the possibility that the truck braking distances assumed in the FHWA-sponsored truck characteristics study should be up to 70 ft (21 m) longer at 55 mi/h (88 km/h). However, the T3DRS, Phase 4 model results alone do not provide a case for changing the conclusions of the FHWA-sponsored truck characteristics study or for modifying the AASHTO stopping sight distance criteria. Field braking tests on a surface similar to that assumed in the AASHTO criteria would be necessary to resolve this issue.

In conclusion, the results of the truck braking data obtained from the T3DRS, Phase 4 model do not provide sufficient basis for modifying the conclusions and recommendations of the FHWA-sponsored truck characteristics study:[25]

- Current AASHTO stopping sight distance criteria are adequate for trucks with antilock brake systems.
- Current AASHTO criteria are adequate at vertical sight restrictions for trucks with conventional brake systems and the best performance driver. At horizontal sight restrictions, a truck with the best performance driver needs approximately 50 ft (15 m) of additional stopping sight distance.

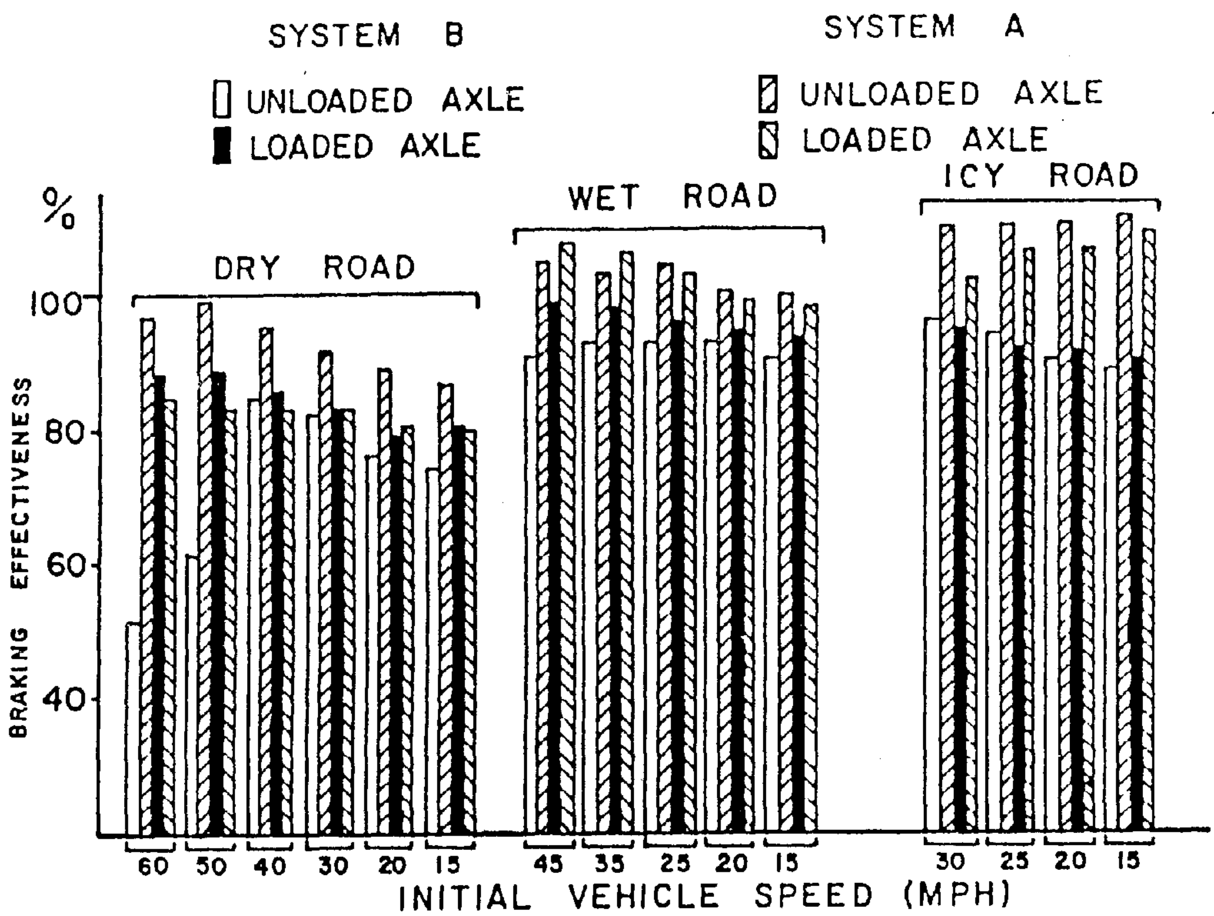

Figure 52. Braking effectiveness for various operating conditions.[27]

- Current AASHTO criteria are not adequate to accommodate trucks with conventional braking systems and poor performance drivers. Many drivers have minimal experience with the proper procedures for controlled braking in emergency situations because emergency situations on the road are rare events and very few drivers have had the opportunity to practice emergency stops on a test track. A driver with 70 percent control efficiency (a poor but not extreme value) requires 25 to 425 ft (8 to 130 m) of additional stopping sight distance, depending on speed. The higher driver eye height for trucks offsets some but not all of this difference at vertical sight restrictions.

- Revised stopping sight distance criteria to accommodate trucks with conventional brake systems would be cost effective only for new construction or major reconstruction projects on rural, two-lane roadways that carry more than 800 trucks/day and rural freeways that carry more than 4,000 trucks/day. Revised criteria would not be cost effective for rehabilitation projects and would not be needed if antilock brake systems for trucks are required by Government regulations or come into widespread use.

The complete explanation of and justification for these conclusions and recommendations are presented in the final report of the FHWA-sponsored truck characteristics study.[25]

The effects of selected truck and roadway parameters on truck braking distance derived from the T3DRS, Phase 4 simulation data were presented in chapter 4 in "Statistical Analysis of Braking Distance Data." These results would also have to be validated by experimental data, collected in field tests conducted according to the testing program described in chapter 4 in "Work Plan," to provide the basis for possible modifications of the current roadway design criteria.

6. CONCLUSIONS AND RECOMMENDATIONS

The large amount of tire traction data collected in the field testing program represents the most significant result of this study. A new truck tire tester proved to be a useful tool in measuring tire forces in braking and cornering under various speed, vertical load, and slip angle conditions and on different pavement surfaces. Six most common truck and bus tires were tested: radial rib, bias-ply rib, bias-ply lug, radial lug, low-profile rib, and wide-base. In general, rib tires performed better than lug tires. The superiority of rib tires over lug tires was more pronounced in braking and less significant in cornering coefficients of friction. Previous studies also showed that lug tires produce more noise than rib tires.[7] Another general observation made from the tire traction data is that radial tires perform better than bias-ply tires. Overall, the radial rib tire performed best, both in braking and in cornering, among the six test tires. The advantage of the radial rib tire over other types of tires is particularly large in peak values of the coefficient of braking friction, which will be even more significant when antilock braking systems become commonly used.

All of the four other independent test variables besides tire type--pavement type, speed, vertical load, and slip angle--have a significant effect on tire traction performance. Pavement skid number, SN_{40}, correlates strongly with tire coefficients of friction. An increase of SN_{40} always improves tire braking and cornering traction. The quantitative effects of SN_{40} on tire coefficients of friction are determined by the corresponding coefficients of the regression models summarized in tables 2 and 3. For example, an increase of the pavement skid number by 10 increases the sliding coefficient of braking friction by 0.05 to 0.10, which is considered very significant. Two other variables that have a significant effect on tire traction performance are speed and vertical load. Increasing speed by 10 mi/h (16 km/h) has about the same effect on sliding coefficient of braking friction as decreasing pavement skid number by 10. Also, a similar reduction of the sliding coefficient of braking friction occurs when tire vertical load is increased by 1000 lb (4440 N). It is not uncommon to see trucks traveling on interstate highways at speeds very close to or exceeding the speed limit. Some of those trucks carry heavy loads. The combination of high speed and heavy load is particularly hazardous for traffic safety.

The tire traction data were processed to derive 48 regression models relating peak and sliding coefficients of friction and critical slip in braking and combined braking and cornering maneuvers. Most of the measuring signals recorded in the field tests were heavily contaminated by noise. In spite of the elaborate digital filtering procedure that was applied to the raw data, the level of noise contamination remained significant, which caused a considerable scatter of data around the regression models. As a result, low values of R^2 and high values of standard deviations obtained with some models require that the models be interpreted with care. Remember, however, that even though the values of R^2 and standard deviations obtained for the models developed in this study are not as impressive as those usually reported in computer simulation and laboratory studies, the results of the field tests have a much greater significance because they reflect all elements of the actual system and its environment, some of which may not be present in laboratory and computer simulation studies.

In the computer simulation study described in chapter 4, the effects of suspension type, tire type, roadway alignment, pavement roughness, and surface wetness were investigated using the T3DRS, Phase 4 program. The results show that all of these variables have a statistically significant effect on truck braking distance. Moreover, the direction in which each variable influences the braking distance is in agreement with current knowledge in this area. The results of the T3DRS, Phase 4 simulations show that trucks can require braking distances for controlled stops at least 67 percent longer than those required for locked-wheel stops by passenger cars. Unfortunately, no field tests could be conducted to validate the computer results and therefore all conclusions drawn from these results must be considered tentative at this time.

In summary, based on the field tests and computer simulation results obtained in this study, the following recommendations can be made:

- Recommendation 1: The radial rib tire has the best overall traction performance on a range of pavement surfaces and should be used whenever possible.
- Recommendation 2: Rib tires are recommended over lug tires because of their better traction characteristics.

- Recommendation 3: High speeds and heavy loads combine to significantly reduce tire traction in braking and cornering and represent particularly hazardous conditions for traffic safety.

- Recommendation 4: Conduct a field testing program outlined by the Work Plan presented in chapter 4 to validate and extend the results obtained from computer simulation of truck braking performance.

APPENDIX: FIR FILTER SUBROUTINE

```
      SUBROUTINE FILTER(FIR,IWP,IWS)
C------------------------------------------------------------------
C            This is a 1024 points FIR subroutine used to process
C            data files obtained from PTI dynamometer PC based
C            data acqusition system
C------------------------------------------------------------------
C            FIR(1024): Low pass filter on frequency domain
C            IWP      : Pass frequency (Hz) * 10
C            IWS      : Stop frequency (Hz) * 10
C------------------------------------------------------------------
      COMPLEX FIR(1024), W(512)
      PI=2.0*ACOS(0.0)
      X1= 0.003                    ! DELTA1
      X2= 0.005                    ! DELTA2
      RP1=1.5                      ! NUMBER OF RIPPLE AT PASS BAND
      RP2=2.                       ! NUMBER OF RIPPLE AT STOP BAND
      FACTOR=2.
      W1= RP1*2.*PI/FLOAT(IWP)
      W2= RP2*2.*PI/FLOAT(1024-IWS-1)
      DO I=1,IWP
        VALUE=1.+X1*COS(W1*FLOAT(I))
        VALUE=VALUE
        FIR(I)=CMPLX(VALUE,0.0)
      END DO
      DO I=IWP+1,IWS
        VALUE=(1.-X1)-(1.-X1-X2)*FLOAT(I-IWP)/FLOAT(IWS-IWP)
        VALUE=VALUE
        FIR(I)=CMPLX(VALUE,0.0)
      END DO
      DO I=IWS+1,1204
        VALUE=0.+X2*COS(W2*FLOAT(I))
        FIR(I)=CMPLX(VALUE,0.0)
      END DO
      CALL IFFT(FIR,W,1024,2)
      DO I=1,1024
        VALUE= FACTOR*REAL(FIR(I))
        FIR(I)= CMPLX(VALUE,0.0)
      END DO
      CALL FFT(FIR,W,1024,2)
      FIR(1)=CMPLX(1.0,0.0)
      FIR(1024)=CMPLX(1.0,0.0)
      CALL IFFT(FIR,W,1024,2)
      DO I=1,1024
        FIR(I)=CMPLX(REAL(FIR(I)),0.0)
      END DO
      CALL FFT(FIR,W,1024,2)
      RETURN
      END
```

REFERENCES

1. Williams, T., and J. K. Meades, 1975, Effects of Tread Pattern Depth and Tire Grooving on Lorry Tire Skidding Resistance, TRRL Report 687 (Crawthorne, U.K.: Transport and Road Research Laboratory).

2. Schloesser, L. H. M., 1976, "Tires on Road Surfaces," Transportation Research Record 624, pp. 15-26.

3. Dijks, A., 1977, "Influence of Tread Depth on Wet Skid Resistance of Tires," Transportation Research Record 621, pp. 126-47.

4. Hayhoe, G. F., and C. G. Shapley, 1982, "Factors Affecting the Skidding Performance of Trucks," Proceedings of ASME Winter Annual Meeting, Phoenix, Arizona, November 14-19, pp. 19-30.

5. Gusakov, I., R. Rice, S. Pugliese, and R. Galganski, 1984, An Evaluation of Methods to Investigate Truck Tire Wet Traction, Report No. DOT-HS-806-577 (Washington, DC: National Highway Traffic Safety Administration).

6. Ervin, R. D., C. B. Winkler, J. E. Bernard, and R. K. Gupta, 1976, Effects of Tire Properties on Truck and Bus Handling, Report No. DOT-HS-802142 (Washington, DC: National Highway Traffic Safety Administration).

7. Ervin, R. D., and R. E. Wild, 1976, The Noise and Traction Characteristics of Bias Ply Truck Tires, Report No. UM-HSRI-PF-76-2-1 (Ann Arbor, MI: University of Michigan, Highway Safety Research Institute).

8. Harwood, D. W., R. R. Blackburn, B. T. Kulakowski, and D. F. Kibler, 1987, Wet Weather Exposure Measures, Report No. FHWA/RD-87/105 (Washington, DC: Federal Highway Administration).

9. Radlinski, R. W., and S. F. Williams, 1985, NHTSA Heavy Duty Vehicle Brake Research Program--Stopping Capability of Air Braked Vehicles, Report Nos. 1 DOT HS 806738 and 739 (Washington, DC: National Highway Traffic Safety Administration).

10. Radlinski, R. W., S. F. Williams, and J. M. Machey, 1982, "The Importance of Maintaining Air Brake Adjustments," Paper No. 821263 (Warrendale, PA: Society of Automotive Engineers).

11. "Standard Practice for Simulating Vehicular Response to Longitudinal Profiles of a Vehicular Traveled Surface," 1989, Designation: E 1170, Annual Book of ASTM Standards, Vol. 04.03 (Philadelphia, PA: American Society of Testing Materials).

12. Ervin, R. D., 1976, Measurements of the Longitudinal and Lateral Traction Properties of Truck Tires (New York, NY: Mechanical Engineering Publications, 1976-5), pp. 93-100.

13. Schreirer, P. G., 1989, "Annual Review: Data Acquisition and Control," Personal Engineering and Instrumentation News (February), pp. 41-46.

14. Todd, K. B., and B. T. Kulakowski, 1989, "Simple Computer Models for Predicting Ride Quality and Pavement Loading for Heavy Trucks," paper presented at the 68th annual meeting of the Transportation Research Board, January 22-26, Washington, DC.

15. Sweatman, P., 1978, The Dynamic Loading Performance of Heavy Vehicle Performance, Vol. 9, Part 5 (Melbourne, Australia: Australian Road Research Board).

16. MacAdam, C. C., P. S. Fancher, G. T. Hu, and T. D. Gillespie, 1980, A Computerized Model for Simulating the Braking and Steering Dynamics of Trucks, Tractor Semi-Trailers, Doubles, and Triples Combinations: User's Manual - Phase 4, Report No. UM-HSRI-80-58 (Ann Arbor, MI: Highway Safety Research Institute).

17. Gillespie, T. D., C. C. MacAdam, G. T. Hu, J. Bernard, and C. Winkler, 1979, Truck and Tractor Trailer Dynamic Response Simulation Volume 2, Technical Report, Report No. UM-HSRI-79-85-2 (Ann Arbor, MI: Highway Safety Research Institute).

18. El-Gindy, M., and J. Y. Wong, 1987, "A Comparison of Various Computer Simulation Models for Predicting the Directional Response of Articulated Vehicles," Vehicle System Dynamics 16, No. 5-6, p. 249-68.

19. Fancher, P. S., R. D. Ervin, C. B. Winkler, and T. D. Gillespie, 1986, A Factbook of the Mechanical Properties of the Components for Single-Unit and Articulated Heavy Trucks, Report No. DOT HS 807 125 (Washington, DC: U.S. Department of Transportation).

20. Cebon, D. 1989, "Vehicle-Generated Road Damage: A Review," Vehicle System Dynamics, No. 18, pp. 107-150.

21. Mitchell, C. G. B., and L. Gyenes, 1989, "Dynamic Pavement Loads Measured for a Variety of Truck Suspensions," presented at the 2nd International Conference on Heavy Vehicle Weights and Dimensions, Kelowna, British Columbia.

22. American Association of State Highway and Transportation Officials, 1990, A Policy on Geometric Design of Highways and Streets (Washington, DC: AASHTO).

23. Olson, P. L., D. E. Cleveland, P. S. Fancher, L. P. Kostyniuk, and L. W. Schneider, 1984, Parameters Affecting Stopping Sight Distance, NCHRP Report 270 (Washington, DC: Transportation Research Board).

24. Fancher, P. S., 1986, "Sight Distance Problems Related to Large Trucks," Transportation Research Record 1052 (Washington, DC: Transportation Research Board).

25. Harwood, D. W., J. M. Mason, W. D. Glauz, B. T. Kulakowski, and K. Fitzpatrick, 1988, Truck Characteristics for Use in Highway Design and Operation, Report Nos. FHWA-RD-89-226 and -227 (Washington, DC: Federal Highway Administration).

26. Estmar, G., 1988, "Anti-Skid Brakes on Scania Trucks and Buses," in Trucks Technology International, P. M. Kennett ed. (Sterling Publications Limited, London), pp. 139-145.

27. Srinivasa, R., R. R. Guntur, and J. Y. Wong, 1980, "Evaluation of the Performance of Anti-Lock Brake Systems Using Laboratory Simulation Techniques," Int. J. of Vehicle Design 1, No. 5, pp. 467-468.

28. Niu, W. T., 1990, "Simulation of the Tractor-Semitrailer Antilock Braking System," M.S. thesis, Department of Mechanical Engineering, The Pennsylvania State University, University Park (February).

29. Radlinski, R. W., and S. C. Bell, 1986, NHTSA's Heavy Vehicle Brake Research Program--Report No. 6: Performance Evaluation of a Production Anti-Lock System Installed on a Two-Axle Straight Truck, DOT HS 807 046 (Washington, DC: National Highway Traffic Safety Administration).

★U.S. GOVERNMENT PRINTING OFFICE: 1992 -619 -537/41379